Air Force Institute of Technology

AFIT Scholar

3-2020

An Analytic Study of Pursuit Strategies

Mark E. Vlassakis

Recommended Citation

An Analytic Study of Pursuit Strategies

THESIS

Mark E Vlassakis, Second Lieutenant, USAF

AFIT/ENG/20M

DEPARTMENT OF THE AIR FORCE
AIR UNIVERSITY

AIR FORCE INSTITUTE OF TECHNOLOGY

Wright-Patterson Air Force Base, Ohio

AFIT/ENG/20M

An Analytic Study of Pursuit Strategies

THESIS

Presented to the Faculty

Department of Electrical and Computer Engineering

Graduate School of Engineering and Management

Air Force Institute of Technology

Air University

Air Education and Training Command

in Partial Fulfillment of the Requirements for the

Degree of Master of Science in Electrical Engineering

Mark E Vlassakis, B.S.A.E

Second Lieutenant, USAF

March 19, 2020

AFIT/ENG/20M

An Analytic Study of Pursuit Strategies

THESIS

Mark E Vlassakis, B.S.A.E
Second Lieutenant, USAF

Committee Membership:

Meir Pachter, Ph.D
Chair

Robert C. Leishman, Ph.D
Member

Maj Joshuah A. Hess, Ph.D
Member

AFIT/ENG/20M

Abstract

The Two-on-One pursuit-evasion differential game is revisited where the holonomic players have equal speed, and the two pursuers are endowed with a circular capture range $\ell > 0$. Then, the case where the pursuers' capture ranges are unequal, $\ell_1 > \ell_2 \geq 0$, is analyzed. In both cases, the state space region where capture is guaranteed is delineated and the optimal feedback strategies are synthesized. Next, pure pursuit is considered whereupon the terminal separation between a pursuer and an equal-speed evader less than the pursuer's capture range $\ell > 0$. The case with two pursuers employing pure pursuit is considered, and the conditions for capturability are presented. The pure pursuit strategy is applied to a target-defense scenario and conditions are given that determine if capture of the attacker before he reaches the target is possible. Lastly, three-on-one pursuit-evasion is considered where the three pursuers are initially positioned in a fully symmetric configuration. The evader, situated at the circumcenter of the three pursuers, is slower than the pursuers. We analyze collision course and pure pursuit guidance and provide evidence that conventional strategy for "optimal" evasive maneuver is incorrect.

Acknowledgments

The following work would not have been possible without my fellow students, advisor, instructors, friends, and family. I have had the pleasure of working with incredible people over the past 18 months, and I am forever grateful for the friendships and support from my time at AFIT.

<div align="right">Mark E. Vlassakis</div>

Contents

List of Figures

x

An Analytic Study of Pursuit Strategies

I. Introduction

1.1 Overview

The following document provides an analysis of pursuit-evasion games. We begin by analyzing the Two-on-One pursuit-evasion differential game *à* la Rufus Isaacs' "Two Cutter and Fugitive Ship" [1]. Isaacs' geometrically derived the optimal feedback strategies for the two Pursuers (P_1, P_2), who employ Collision Course (CC) guidance, and the Evader under the stipulation that their respective speeds, v_P and v_E, were such that the speed ratio $\mu \triangleq \frac{v_E}{v_P} < 1$ – that is, the Pursuers were faster than the Evader. It is often stipulated that the players have simple motion/are holonomic; this assumption is maintained throughout the proceeding chapters.

Wasz and Pachter [2] expanded upon Isaacs formulation by endowing the Pursuers with capture ranges of radius ℓ. They furthered the adaptation of the "Two Cutters and Fugitive Ship" game by equalizing the speeds of the three players – the speed ratio $\mu = 1$ [3]. Wasz and Pachter delineated the solution to the Game of Kind by determining the region in the reduced state space where isochronous capture of the Evader is guaranteed. Then, they determined the solution to the Game of Degree by deriving the optimal state feedback strategies for the three players.

This research picks up where [3] left off by first developing a streamlined derivation for the Game of Degree in the Two-on-One pursuit-evasion differential game when the speed ratio $\mu = 1$ and the two Pursuers are endowed with capture ranges of radius ℓ – see Chapter III. We continue to adapt the "Two Cutters and Fugitive

1

Ship" game by solving the Game of Kind for the case when the two Pursuers are endowed with unequal capture ranges, $\ell_1 > \ell_2 \geq 0$. As shown in Chapter IV, we conjecture that the state space region which guarantees isochronous capture of the Evader is delimited by the two tangents to the Pursuers' capture disks. The validity of the conjecture is confirmed through numerical simulation and exploration of special cases. The solution to the Game of Degree is then provided through the derivation of the players' optimal state feedback strategies. We complete the solution of the Two-on-One pursuit-evasion differential game by analyzing the reduced state space in 3-dimensions.

Next, we analyze games of Pure Pursuit (PP) in which a single Pursuer instantaneously heads toward an Evader's position. Pure pursuit games have been considered for centuries [4], [5], however, most research was limited by the assumptions that the Evader initially travels abeam the Pursuer, point capture is required, and the speed ratio $\mu \triangleq \frac{v_E}{v_P} < 1$. Fairly recently, Barton and Eliezer [6] provided a closed-form solution when the Evader's initial heading is unrestricted.

In this paper, we analyze the game in which a Pursuer, endowed with a circular capture disk of radius ℓ, gives chase to a course-holding Evader when the speed ratio $\mu = 1$. We analytically derive the Pursuer's PP curve and determine the necessary and sufficient conditions for capture. We then turn our attention to Two-on-One PP games – see Chapter V.

Next, we look at the application of Pure Pursuit in defense of a target. Isaacs [1] studied the Target Defense scenario under the assumptions that the speed ratio $\mu < 1$ and point capture was required. In this research, in Chapter VI, we analyze the defense of a stationary Target (T) under attack by a course-holding Evader/Attacker and defended by a Pursuer/Defender endowed with a capture range $\ell > 0$. We analyze the Target Defense game for both a slow Evader/Attacker ($\mu < 1$) and an equal speed

Evader/Attacker ($\mu = 1$). A "Winning Region" is developed in which the Attacker reaches the Target before being intercepted by the Defender.

Lastly, in Chapter VII, we consider a Three-on-One pursuit-evasion game. The inclusion of a third Pursuer greatly increases the complexity of the problem. Thus, we examine the Three-on-One game under the stipulation that the initial configuration is fully symmetric, that is, the three Pursuers' initial positions rest on the vertices of an equilateral triangle $\triangle P_1 P_2 P_3$. The slow Evader ($\mu < 1$), is initially positioned at the circumcenter of the equilateral triangle. In the work of Von Moll, Pachter, Garcia, Casbeer, and Milutinovic [7], it was determined the Pursuer's "optimal" strategy was to stay put. In Chapter VII, we challenge this notion by introducing a dithering Evader. We determined the "optimal" frequencies to increase the time-to-capture when compared to a stationary Evader.

1.2 Motivation

With the evolution of autonomous aircraft and drone technology, it is of interest to study air-to-air conflict. Drone swarming and other air-combat strategies regarding multiple players require special consideration. Previous research in this field focused on pursuit-evasion games with fast ($\mu > 1$) Pursuers. In this research, however, we analyze the operationally relevant case where all of the players have similar capabilities. Thus, we endow the Pursuer(s) with finite capture ranges to simulate an aircraft weapon system. It is also important to note that most of the research in this document was developed analytically. Deriving closed-form solutions expand the understanding of what occurs at the boundaries of the game.

1.3   Organization

The organization of this paper is as follows. Chapter I provides a brief background and introduction into the research described in later chapters. Chapter II summarizes the relevant sources used to develop this research and is broken down into two major sections: Section 2.1 outlines the relevant papers regarding pursuit-evasion games where the Pursuer(s) employ Collision Course (CC) guidance, and Section 2.3 describes the literature relevant to games of Pure Pursuit (PP). Chapters III-VII are individual papers. Chapters III and IV discuss the Two-on-One pursuit-evasion differential game in which the Pursuers employ CC guidance. Chapters V and VI discuss games of PP. Chapter VII discuss both CC and PP, but in the context of Three-on-One pursuit-evasion. Chapter VIII summarizes the findings in this research.

II. Background and Literature Review

The following literature review summarizes the sources pertaining to the research in the proceeding chapters. This chapter is broken down into two sections: the works concerning Collision Course (CC) guidance and the works concerning Pure Pursuit (PP) guidance. The research relevant to CC guidance, found in Section 2.1, is further broken down into subsections that regard the magnitude of the speed ratio $\mu = \frac{v_E}{v_P}$ as well as the number of pursuers. Section 2.3 discusses the literature pertaining to games of Pure Pursuit, which is then broken down to discuss the interesting case of the Target Defense Scenario.

2.1 Collision Course Guidance

2.1.1 The Speed Ratio $\mu < 1$

The basis of this research stems from the work of Rufus Isaacs [1], who in 1951 developed the concept of the differential game. A differential game is a subset of game theory which models and analyzes a dynamic system in conflict. In [1], Isaacs analyzed pursuit-evasion games and discussed their application in wartime. Relevant to the following research, Isaacs formulated the "Two Cutters and Fugitive Ship" differential game, which described the chase of two fast Pursuers (P) against a slow Evader (E). Isaacs stipulated that the Pursuers and Evader were holonomic, the speed ratio $\mu = \frac{v_E}{v_P} < 1$, the pursuers employed Collision Course (CC) guidance, and point capture was required. He derived a solution to the game geometrically with the use of Apollonius circles. Apollonius circles are generated from a set of points whose distances from two fixed points, the positions of the Pursuer(s) and the Evader, are a constant ratio, the speed ratio $\mu = \frac{v_E}{v_P}$. Isaacs determined that, under optimal play in the Two-on-One pursuit-evasion differential game, the Pursuers and Evader should

aim for the farthest vertex of the intersection of two Apollonius circles. This strategy is discussed and analyzed further in Chapter VII. Isaacs also discusses the "Cornered Rat" scenario in [1], where an evader is trapped between a wall and a pursuer. We analyze a variation of this scenario in Chapter IV.

The geometry-based strategies derived in [1] were verified in Pachter's work in [8]. Pachter showed the pursuit-evasion strategies from [1] were recovered from the solution of the Hamilton-Jacobi-Isaacs partial differential equation. His work was especially helpful in developing the costates for the 3-dimensional state space solution found in Chapter IV.

In a continuation to Isaacs' work, Pachter, Von Moll, and Garcia [9] delineated the solution to the Game of Kind for the Two-on-One pursuit-evasion differential game with the speed ratio $\mu < 1$. They determined the state space region in which the pursuers isochronously capture the evader.

Wasz and Pachter [2] expanded analysis of two-on-one differential games by endowing the pursuers with a capture range $\ell > 0$. With the inclusion of capture ranges, the Apollonius circles in [1] become Apollonius ovals. They geometrically derived the solution to the Game of Kind, then provided the players' optimal feedback strategies. In Chapter IV, we compare the state space region, derived in [2], where the Pursuers isochronously capture the Evader when endowed with a capture range $\ell > 0$ and the region where the Evader is isochronously captured by equal speed pursuers, $\mu = 1$, endowed with capture ranges $\ell > 0$.

2.1.1.1 Three-On-One

Von Moll, Pachter, Garcia, Casbeer, and Milutinovic [7] expanded the study of pursuit-evasion games by incorporating a third pursuer. The inclusion of a third pursuer in pursuit-evasion games greatly increases the complexity. In [7], they ana-

lyzed the Three-on-One pursuit-evasion scenario in which the configuration is fully symmetric, that is, the three Pursuers' positions exist on the vertices of an equilateral triangle and the Evader is positioned at the circumcenter. In the Two-on-One scenario, the vertices of the intersection of two Apollonius circles provide the optimal aimpoint to prolong the Evader's life given the Pursuers are employing "optimal" CC guidance. In the case with three pursuers, as pointed out by [7], the vertices of the intersection of three Apollonius circles provide an aimpoint that result in a faster time-to-capture than if the Evader remained stationary at the circumcenter of the equilateral triangle. Thus, they concluded the best course of action for the evader was to remain stationary. Chapter VII further discusses the implications of three pursuers in pursuit-evasion games.

Pachter, Von Moll, and Garcia [10] continued the study of the Three-on-One pursuit-evasion game where the pursuers employ Collision Course (CC) guidance. They analyzed the game in which the Evader runs away from one of the Pursuers. As pointed out in [10] and referenced in VII, it is best for the Evader to remain stationary at the circumcenter of the equilateral triangle in the initial configuration.

2.1.2 The Speed ratio $\mu = 1$

Same speed pursuit-evasion differential games, that is the speed ratio $\mu = \frac{v_E}{v_P} = 1$, require special consideration. In the seminal paper [11] discriminating pursuit strategies are employed, which, according to the survey paper [12], is common in many-on-one pursuit-evasion games. However, in this paper, we use state feedback strategies. The motivation for studying same speed pursuit-evasion games comes from Kang [13] and Horie [14], who discuss the operational relevance of studying opposing players with similar capabilities. Prior to [13] and [14], most research analyzed pursuit-evasion games with fast pursuers as in [15]. Chapters III, IV, V, and VI all analyze

pursuit games with equal speed players, $\mu = 1$.

In [3], Wasz and Pachter continued their research of two-on-one pursuit evasion with a non-zero capture range with the stipulation that the speed ratio $\mu = 1$. When the players have the same speed, the boundaries for capture are no longer defined by Apollonius ovals, but arcs of hyperbolae. They delineated the solution to the Game of Kind by determining the state space region where capture is guaranteed. The solution to the Game of Degree was found by deriving the optimal feedback strategies for the players. Chapter III is a derivative from [3], as we take the solution of the Game of Kind from Wasz and Pachter and generate a streamlined derivation of the solution to the Game of Degree.

2.2   Target Defense

Isaacs [1] analyzed a Target Defense game in which the Pursuer/Defender and Evader/Attacker have equal speed, $\mu = 1$, and point capture is required. In this case, the Defender employs CC pursuit, and the Target is an area in the state space.

2.3   Pure Pursuit

Pure Pursuit (PP) strategies in pursuit-evasion games have been studied for centuries. Traditionally, PP games were analyzed under the stipulation that the pursuer is faster than the evader and point capture is required. Until recently, closed-form solutions for games of PP only existed under the assumption that the pursuer is initially abeam the evader, as is the case in [4] and [5]. In the early 2000's, Barton and Eliezer [6] derived a closed form solution for the Pursuer's path when the Evader's heading is not restricted to being abeam the Pursuer's initial line of sight. These works provided the background necessary for the research developed in Chapters V, VI, and VII.

2.3.1 Target Defense

Another source that provided relevant information for this research includes the work of Garcia, Casbeer, Fuchs, and Pachter [16]. They looked at the 2-Dimensional differential game with a Target, a Pursuer, and a Defender, where the Defender acted to intercept the Pursuer before it reached the Target. Assuming equal and constant speeds, an analytical solution was determined using Isaacs' Methodology. Given the Defender had a positive capture radius, the analytical solutions provide the optimal interception point, thus providing the optimal headings for the players at each time step. Target Defense games are further discussed in Chapter VI.

III. Two-on-One Pursuit when the Pursuers Have the Same Speed as the Evader

3.1 Abstract

A two-on-one pursuit-evasion differential game is considered. The setup is akin to Isaacs' Two Cutters and Fugitive Ship differential game. In this paper it is however assumed that the three players have equal speeds and the two cutters/pursuers have a non-zero capture radius. The case where just one of the Pursuers is endowed with a circular capture set is also considered. The state space region where capture is guaranteed is delineated, thus providing the solution of the Game of Kind, and the players' optimal state feedback strategies and the attendant value function are synthesized, thus providing the solution of the Game of Degree.

3.2 Introduction

Isaacs' Two Cutters and Fugitive Ship differential game [1] is revisited – see Fig. 1 . In Isaacs' formulation, the cutters are faster than the fugitive ship and point capture
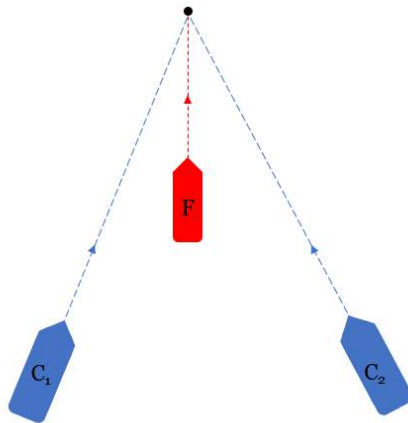
Figure 1: Two Cutters and Fugitive Ship

is required. The solution of the game was obtained using a geometric method, sans

a proof. In [8] the validity of Isaacs' geometric approach was proven. It was shown that the geometric method–provided strategies are recovered from the solution of the HJI PDE. In [1], [8], and [9], point capture was considered and the case where the two pursuers are endowed with circular capture sets of radius $\ell > 0$ was addressed in [2]. In references [1], [8], [9], and [2], the pursuers are faster than the evader.

In this paper it is assumed that all three players have the same speed. Many-on-one pursuit-evasion games where the players have simple motion and the pursuers and evader have the same speed require special consideration – see, e.g. the seminal paper [11], where discriminating/stroboscopic pursuit strategies are employed. This has become a standard feature in the many-on-one pursuit-evasion literature as documented in the recent survey paper [12]. Not so in this paper where the optimal strategies are state feedback strategies.

In this paper, the three players have equal speeds but, as in [2], the cutters have a non-zero capture radius; when the two pursuers have the same speed as the evader, point capture is not possible, and this even if the Evader would be obliged to pre-announce his course; thus the need for finite capture sets. This game, where all the players have the same speed and the pursuers have a non-zero capture range, was considered in our preliminary work [3]. The state space region where capture is guaranteed was delineated thus providing the solution of the Game of Kind and the closed form solution of the Game of Degree which yields the players optimal state feedback strategies was outlined. In this paper, a streamlined derivation of the main result – the pursuers' and the evader's optimal state feedback strategies, and the Value function, is presented. The novel approach lends itself to the consideration of additional interesting scenarios, e.g., the case where the pursuers have different capture ranges.

The motivation behind this research is directly tied to air-to-air operations [13],

11

[14]. Previous research into this field has focused on games with fast pursuers where the objective is point capture, as in [15], but we are expanding this to include operationally relevant instances where both the blue and red sides have similar capabilities and the pursuers are endowed with finite capture sets, to reflect the range of aircraft weapon systems. This allows for the considerations of bounded capture regions, which was not the case when fast pursuers and point capture only is considered.

3.3 Geometry

The Two Cutters and Fugitive Ship differential game is herein solved using a geometric method based on the solution of the max-min open-loop optimal control problem – as opposed to solving the HJI PDE – the validity of the geometric method in the case when the pursuers are faster than the evader having been proven in [8]. Now, when a pursuer and an evader; both with simple motion á la Isaacs, have the same speed and the pursuer is endowed with a circular capture set of radius ℓ, the locus of points in the Euclidean plane which they can reach at the same time is a hyperbola. Therefore, for any value of capture range $\ell > 0$ of the pursuer, what would have been a Cartesian oval had the pursuer been faster than the evader, as in [2], will now become a hyperbola. The Boundary of the Safe Region of the Evader (BSR) will now be delineated by an arc of the hyperbola

$$\frac{X^2}{a^2} - \frac{Y^2}{b^2} = 1$$

with the parameters

$$a = \frac{\ell}{2} , \quad b = \frac{1}{2}\sqrt{d^2 - \ell^2}$$

where d is the $P-E$ separation. Since there are two pursuers, there are two hyperbolae at play. The asymptotes of those hyperbolae are used to solve the Game of Kind,

12

and these are given by

$$Y = \pm \frac{b}{a} X$$

It will be useful to define the hyperbola's "eccentricity" $e \triangleq \frac{d}{\ell}$, and so the asympototes' slope is

$$\frac{b}{a} = \sqrt{e^2 - 1} \tag{1}$$

The hyperbola locus, whose foci are the instantaneous positions of the pursuer P and the Evader E, and it's asymptotes, is shown in Figure 2. We use the hyperbola construct to designate the Safe Region (SR) of E in the two-on-one differential game when the Pursuers have the same speed as the Evader. Figure 2 shows the Boundary of the Evader's Safe Region (BSR) in the realistic plane (X,Y) when the pursuer is at $(-\frac{d}{2}, 0)$ and the evader at $(\frac{d}{2}, 0)$. Because the Pursuer is not faster than the Evader, this BSR is open; in other words, the Evader can escape. Hence, we need at least one other pursuer to obtain a closed SR so that the Evader might be isochronously captured by the two cooperating pursuers.

In the version of the Two Cutters and Fugitive Ship Differential Game investigated herein we have two pursers with capture radius ℓ and one evader, with all three having the same speed. We use a rotating reference frame (x, y), with the x-axis running through the instantaneous positions of the Pursuers P_1 and P_2 and the y-axis is the orthogonal bisector of the segment $\overline{P_1 P_2}$. The state is specified by three variables: half of the separation of the pursuers, x_p, and the x and y position, (x_E, y_E), of the Evader in the rotation (x, y) frame. For example, the symmetric situation where E, P_1, and P_2 are collinear and the Evader is located halfway between P_1 and P_2 is illustrated in Figure 3. This Figure shows both the hyperbolae and their asymptotes, which intersect. The SR is therefore bounded and under optimal play the two pursuers will isochronously capture the Evader.
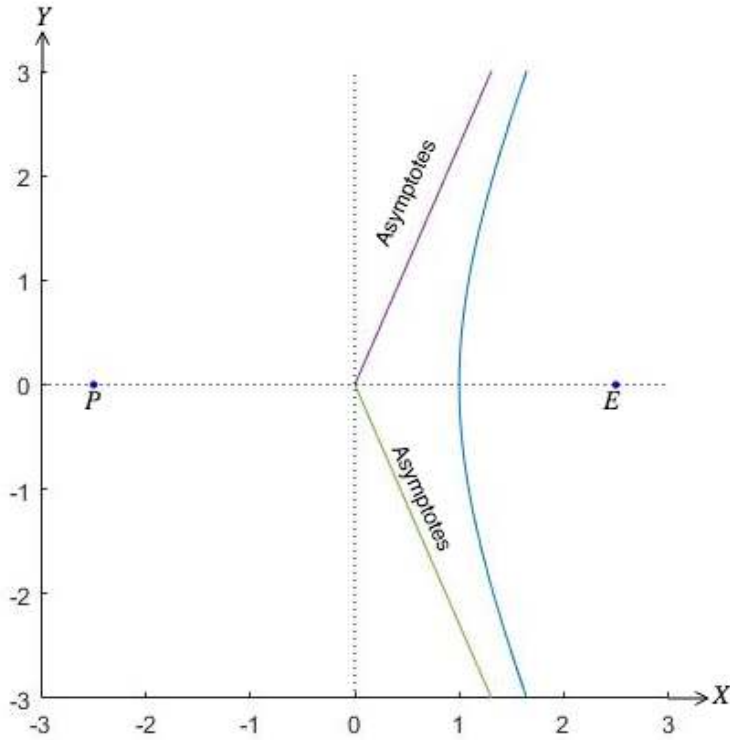
Figure 2: The Hyperbola is the BSR of E

If the asympototes don't intersect the evader can escape. But if the hyperbolae intersect and E is in the lens shaped region formed by the intersecting hyperbolae, if the pursuers play optimally, captures of the Evader is guaranteed. I_1 and I_2 are the points of intersection of the (P_1, E) and (P_2, E) based hyperbolae. Each of these points will be important in the sequel. Our immediate goal is to determine whether the SR is bounded, that is, the asymptotes intersect, which obviously is the case in the symmetric configuration illustrated in Figure 3 – when the evader is hemmed in by the pursuers, the asymptotes of the hyperbolae intersect at I' and I''.
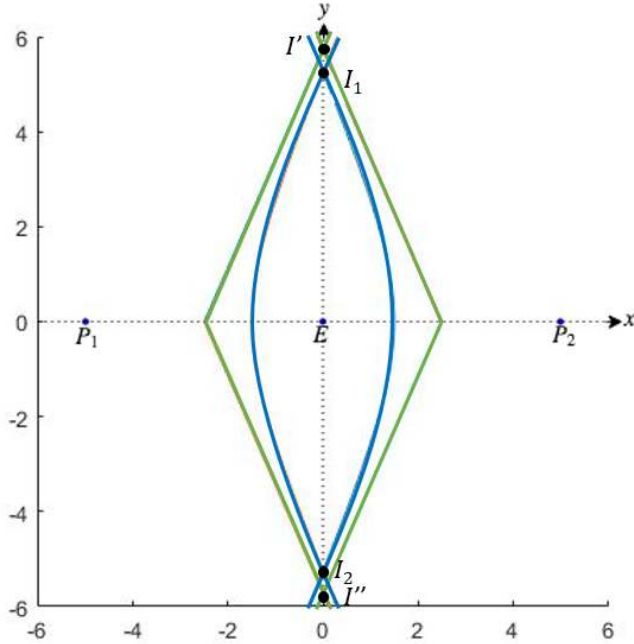
Figure 3: Symmetric State – Two Pursuer Action

3.4 Game of Kind

When the players are in general position, to find the solution to the Game of Kind, that is, whether under optimal pursuer play the Evader's capture is guaranteed, we need to determine whether the SR is bounded, which is the case if and only if the asymptotes of the hyperbolae intersect. Consider now the diagram in Figure 4. There are four points of interest, O_1, O_2, I', and I'' that are vertices of a quadrilateral. This quadrilateral contains the entirety of the evader's SR, so we can ensure capturability if we determine that this quadrilateral is indeed formed.

To this end, consider the angles θ, α_1, α_2 in Figure 4. Since a quadrilateral must have all internal angles sum to 360 degrees, we have the following

$$(360 - \theta) + \alpha_1 + \alpha_2 < 360$$

15
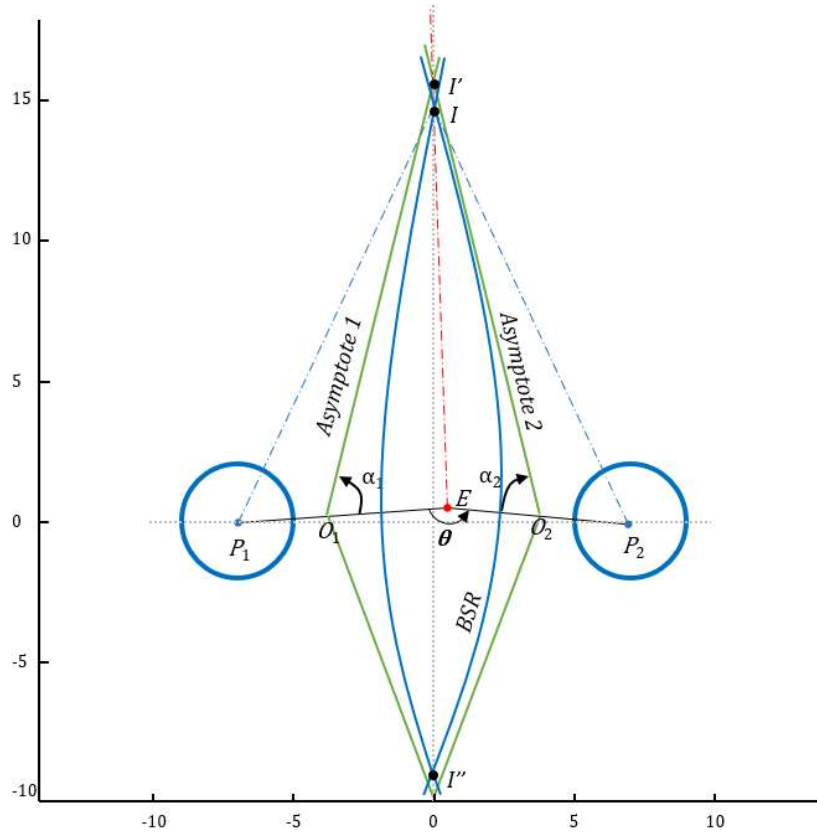
Figure 4: Quadrilateral Formed by Intersecting Asymptotes

This yields the condition for a closed SR, and consequently the capturability condition is

$$\theta > \alpha_1 + \alpha_2$$

Since the slope of the asymptotes in the realistic plane (X, Y) are specified by Equation 1, we know that $\alpha_1 = \arctan(\sqrt{e_1^2 - 1})$ and $\alpha_2 = \arctan(\sqrt{e_2^2 - 1})$, with $e_1 = \frac{r_1}{\ell}$ and $e_2 = \frac{r_2}{\ell}$. The angles α_1, α_2, and θ are exclusively determined by the game's state (x_P, x_E, y_E). This is shown in Figure 5 where P_1, P_2, and E are in a general position. In Figure 5 the points

$$O_1 = \frac{1}{2}(x_E - x_P, y_E), \quad O_2 = \frac{1}{2}(x_E + x_P, y_E)$$

16
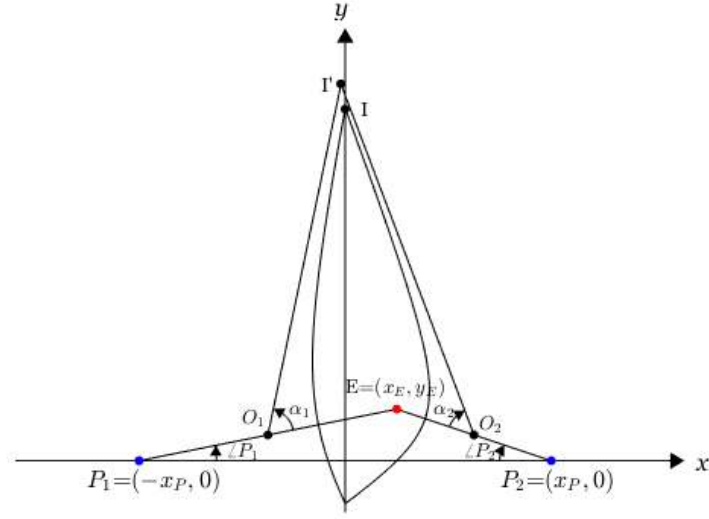
Figure 5: The State (x_P, x_E, y_E)

The angles

$$\tan \alpha_1 = \sqrt{e_1^2 - 1} \ , \quad \tan \alpha_2 = \sqrt{e_2^2 - 1}$$

and

$$\tan P_1 = \frac{y_E}{x_P + x_E} \ , \quad \tan P_2 = \frac{y_E}{x_P - x_E}$$

Therefore, summing those angles, we can characterize the captured zone in the reduced state space (x_P, x_E, y_E). Based on these arguments, in Ref. [3] it was shown that the SR is closed and capturability is guaranteed if and only if in the realistic plane (x, y) the evader is located in the gray zone shown in Figure 6. If the y-coordinate is greater than ℓ, the evader can escape along a straight line path; he might even pre-announce his course and he'll still get away. The broken line in Figure 6 is not part of the gray zone where capturability is guaranteed.

The capture zone is limited. This is due to the fact that the pursuers are not faster than the evader – when both pursuers or just one pursuer, are/is faster than the evader, global capturability is guaranteed. Interestingly though, while the area

17

of the Capture Zone is small, the pursuers can initially be far away from the evader and yet capturability is still guaranteed, provided the evader is in the narrow, gray, capturability zone.
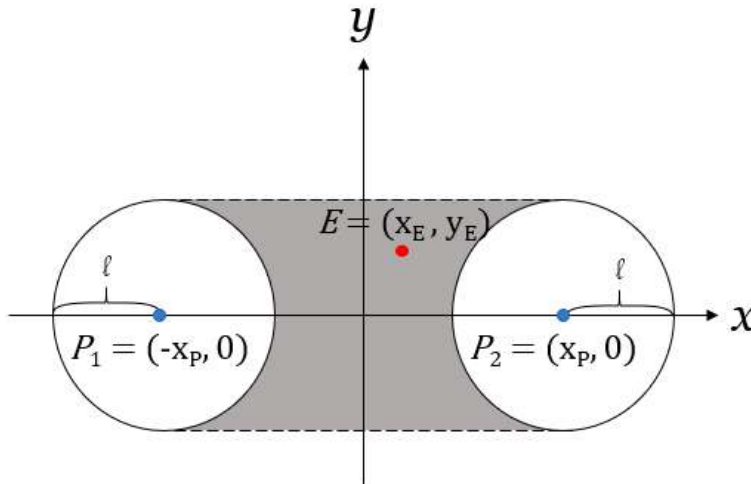
Figure 6: Region of Capture

3.5 Game of Degree

Suppose the initial state is in the capture zone as shown in Figure 6. We focus on the Capture Zone area which is in the first quadrant of the (x,y) plane, that is, $x_E > 0$, $y_E > 0$.

Because both pursuers with equal speed and equal capture radii must travel the same distance in the same time, the interception $\Delta I P_1 P_2$ is isosceles, so the vertex I of the BSR must be on the orthogonal bisector of the segment $\overline{P_1 P_2}$; therefore, the intercept point I is on the y-axis.

We now stipulate that the following must hold – see Fig. 7,

$$\sqrt{x_E^2 + (y - y_E)^2} = \sqrt{x_P^2 + y^2} - \ell,$$

as capture is only possible if $\overline{EI} = \overline{P_1 I} - \ell = \overline{P_2 I} - \ell$. Squaring both sides of the

18
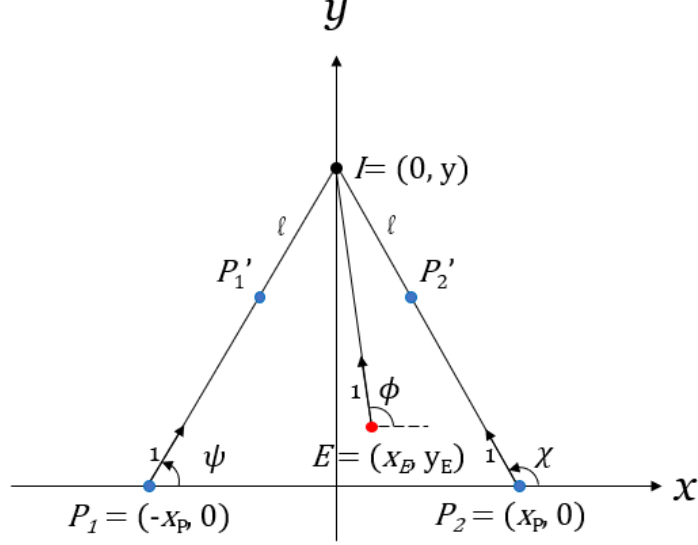
Figure 7: Optimal Trajectories

above equation, we obtain a quadratic equation in y

$$4(\ell^2 - y_E^2)y^2 - 4y_E(\ell^2 - y_E^2 + x_P^2 - x_E^2)y - (\ell^2 - y_E^2 + x_P^2 - x_E^2)^2 + 4\ell^2 x_P^2 = 0.$$

The discriminant must be non-negative. Thus, the following must be true:

$$4y_E^2(\ell^2 - y_E^2 + x_P^2 - x_E^2)^2 + 4(\ell^2 - y_E^2)(\ell^2 - y_E^2 + x_P^2 - x_E^2)^2 - 16\ell^2(\ell^2 - y_E^2)x_P^2 > 0$$

$$(\ell^2 - y_E^2 + x_P^2 - x_E^2)^2 - 4(\ell^2 - y_E^2)x_P^2 > 0$$

We know $\ell^2 - y_E^2 > 0$, $x_P^2 - x_E^2 > 0$, thus

$$\ell^2 - y_E^2 + x_P^2 - x_E^2 > 2\sqrt{\ell^2 - y_E^2}x_P.$$

We need

$$(x_P - \sqrt{\ell^2 - y_E^2} > x_E^2),$$

19

but in the Capture Zone

$$x_P - \sqrt{\ell^2 - y_E^2} > x_E.$$

Thus, as long as the state $(x_P,\ x_E,\ y_E) \in$ Capture Zone, the quadratic equation has two real roots. If $y_E \geq 0$,

$$y = \frac{y_E(\ell^2 - y_E^2 + x_P^2 - x_E^2)}{2(\ell^2 - y_E^2)} + \frac{\ell\sqrt{(\ell^2 - y_E^2 + x_P^2 - x_E^2)^2 - 4(\ell^2 - y_E^2)x_P^2}}{2(\ell^2 - y_E^2)} > 0 \quad (2)$$

The expression under the square root can be simplified so that eq. (2) can be written as

$$y(x_P, x_E, y_E) = \frac{\ell^2 - y_E^2 + x_P^2 - x_E^2}{2(\ell^2 - y_E^2)} y_E + \frac{\ell\sqrt{(x_P + \sqrt{\ell^2 - y_E^2})^2 - x_E^2} \cdot \sqrt{(x_P - \sqrt{\ell^2 - y_E^2})^2 - x_E^2}}{2(\ell^2 - y_E^2)} \quad (3)$$

Eq. (3) can be applied $\forall\ x_P > 0,\ x_E > 0,\ y_E > 0$ to the Capture Zone part which is in the first quadrant of the realistic (x,y) plane. The players' optimal state feedback strategies are

$$\sin \psi^* = \frac{y}{\sqrt{x_P^2 + y^2}}, \qquad\qquad \cos \psi^* = \frac{x_P}{\sqrt{x_P^2 + y^2}}$$

$$\sin \chi^* = \frac{y}{\sqrt{x_P^2 + y^2}}, \qquad\qquad \cos \chi^* = -\frac{x_P}{\sqrt{x_P^2 + y^2}}$$

$$\sin \phi^* = \frac{y - y_E}{\sqrt{x_E^2 + (y - y_E)^2}}, \qquad\qquad \cos \phi^* = -\frac{x_E}{\sqrt{x_E^2 + (y - y_E)^2}}$$

where the function $y(x_P, x_E, y_E)$ is given by eq. (3). The value function

$$V(x_P, x_E, y_E) = \sqrt{x_P^2 + y^2} - \ell.$$

When the state is symmetric $(x_E = 0)$

$$y(x_P, 0, y_E) = \frac{x_P^2 - (\ell - y_E)^2}{2(\ell - y_E)}$$

and the Value/time-to-capture

$$V(x_P, 0, 0) = \frac{x_P^2 - (\ell^2 - y_E^2)}{2(\ell - y_E)}$$

When $y_E = 0$,

$$y(x_P, x_E, 0) = \frac{\sqrt{(x_P + \ell)^2 - x_E^2} \cdot \sqrt{(x_P - \ell)^2 - x_E^2}}{2\ell}$$

3.6 Contact

Consider the case where the initial state is not in the interior of the gray capture zone and E is in contact with one of the pursuers, say P_2 – see Figure 8 – so

$$(x_P - x_E)^2 + y_E^2 = \ell^2$$

We insert this expression into eq. (3) and calculate the y-coordinate of the players' aim point,

$$y = \frac{x_P y_E}{x_P - x_E} \tag{4}$$

But note:

$$tan(\pi - \chi) = \frac{y_E}{x_P - x_E}$$

and we calculate

$$\overline{y} = x_P \, tan(\pi - \chi) = \frac{x_P y_E}{x_P - x_E}$$

21
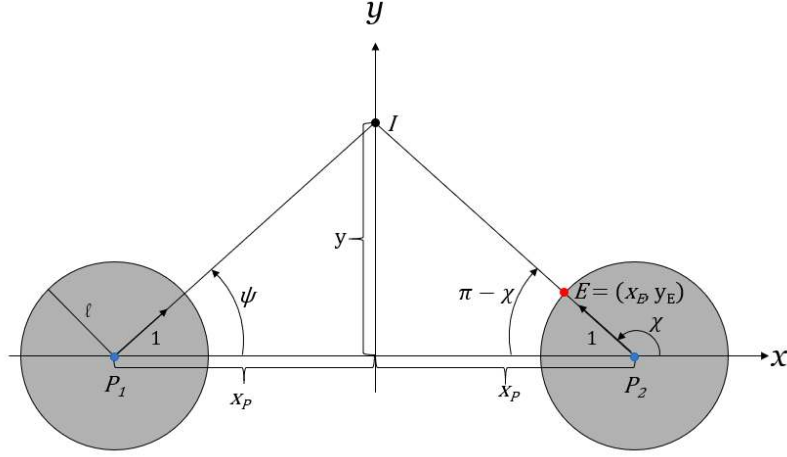
Figure 8: E in Contact with P_2

so,

$$\bar{y} = y$$

Thus, the optimal strategy of P_2 mandates that: Once in contact, P_2 pushes against E and does not let go of E. Once E reaches the y–axis which is the orthogonal bisector of the $\overline{P_1 P_2}$ segment, the captive, but not yet captured, E will be met by P_1 and capture will be effected.

In general, if E does not play optimally by heading toward the interception point $I = (0, y)$, where y is specified by eq. (3), he will prematurely come into contact with one of the Pursuers, whereupon, as discussed above, he'll be pushed toward the y–axis where he'll be met by the companion pursuer and he'll be captured. Indeed, see Fig. 9 – the Evader's SR is closed and, trying to escape, he'll therefore run into one of the hyperbolae, say the P_2, E hyperbola. He will be met by P_2 who, by playing optimally, will push toward the point I' on the y-axis where he'll encounter P_1 and capture will be effected. This play is illustrated in Figure 9:

E erred by not running toward the aim point I and prematurely established contact with P_2. Consequently, once contact is established, P_2 relentlessly pushed E to the

22
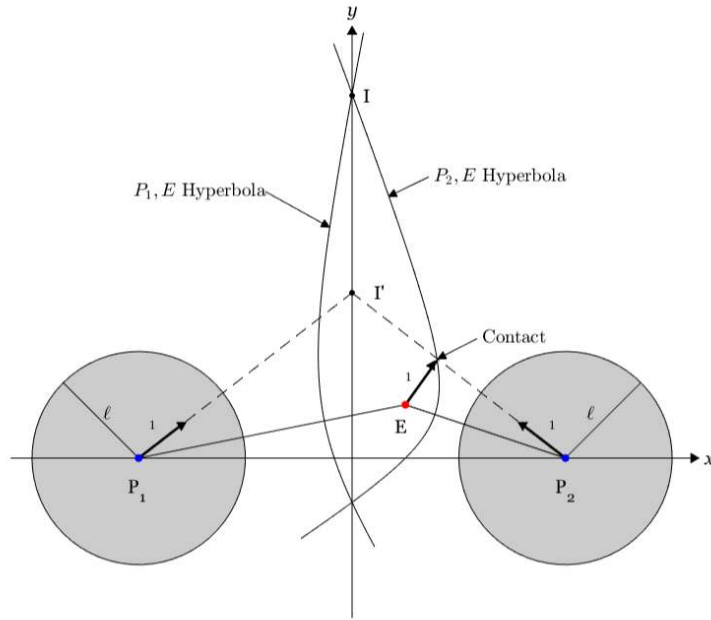
Figure 9: Suboptimal Play of Evader

new aim point I' on the y–axis, where E will be met by P_1 and will be isochronously captured by P_1 and P_2. This is not good for E because $\overline{P_1I'} = \overline{P_2I'} < \overline{P_1I} = \overline{P_2I}$; E was captured prematurely. A period of contact cannot arise in classical pursuit-evasion differential games where the pursuers are faster than the evader and this occurrence is unique to games where the pursuer's speed is the same, or even lower, than the evader's. When the speed ratio $\mu = \frac{v_E}{v_P}$, $0 < \mu < 1$, contact is immediately fatal for E.

3.7   Different Capture Ranges

We now consider the case where the Pursers are endowed with dissimilar capture ranges: $\ell_1 > \ell_2 \geq 0$. The intercept point I is no longer on the y-axis. Instead, the point of interception is defined by the intersections of three hyperbolae: the safe region-delimiting hyperbola whose foci are P_1 and E, the safe region-delimiting

hyperbola whose foci are P_2 and E, plus a third hyperbola whose foci are the positions of the pursuers, P_1 and P_2. The parameters for the latter are

$$a = \frac{\ell_2 - \ell_1}{2}, \quad b = \sqrt{x_P^2 - a^2}.$$

The geometry is illustrated in Figure 10. The three hyperbolae are concurrent at the point I, which is the three players' aim point.
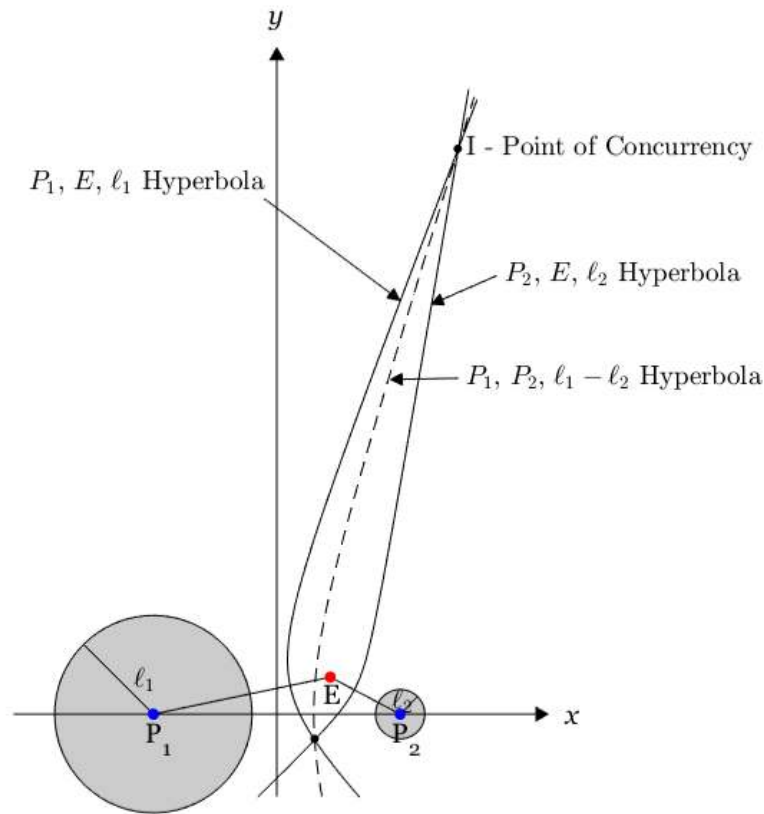
Figure 10: Non-Equal Capture Disks. $\ell_1 = 1.2$, $\ell_2 = 0.3$.

We can now also consider the case where one of the pursuers, say P_2, is not endowed with a capture disk, thus point capture by P_2 is then necessary. The geometry when $\ell_2 = 0$, is depicted in Figure 11. The aim point I, where, under optimal play by the three players the evader will be captured, is defined by the intersection of the

P_1, E hyperbola, the orthogonal bisector of the $\overline{EP_2}$ segment, and also the P_1, P_2 hyperbola; these three curves are concurrent at the aim point I.
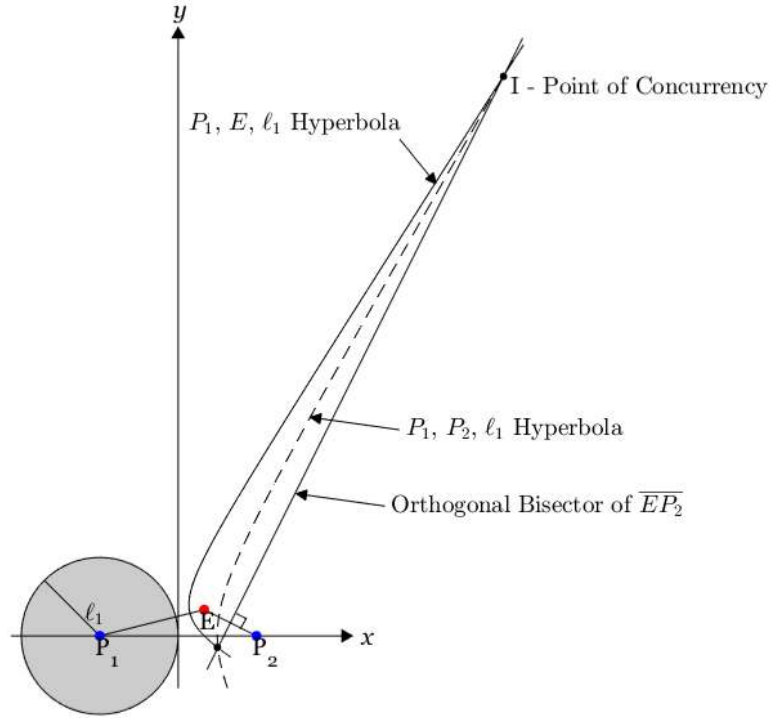
Figure 11: Point Capture in Conjunction with Capture by a Pursuer Endowed with a Capture Disk of Radius. $\ell_1 = 1.5$.

3.8 Conclusion

A pursuit-evasion differential game in which two pursuers engage an equal-speed evader was analyzed. For capture to be effected, at least one of the pursuers must be endowed with a circular capture disk. A geometric approach based on the solution of the max-min open loop optimal control problem, whose validity was assumed in [1] and proven in [8], is employed also when the pursuers have the same speed as the evader. In this paper, a streamlined derivation of the players' optimal state feedback strategies is provided. This, contingent on the evader being in the zone of capturability, as specified by the geometric solution of the Game of Kind. The zone

of capturability is rather restricted due to the fact that the pursuers have the same speed as the evader. In extension, the optimal feedback strategies for pursuers with unequal capture radii were determined. Included was also the case in which only one pursuer is endowed with a capture disk.

IV. Two-on-One Pursuit of an Equal Speed Evader

4.1 Abstract

The two-on-one pursuit-evasion differential game in the Euclidean plane is considered for the case where the holonomic players have equal speed, but at least one of the Pursuers is endowed with a circular capture disk. Necessary and sufficient conditions for capturability when the two Pursuers' respective capture disks radii are $\ell_1 \geq \ell_2 \geq 0$ are obtained, thus providing the solution of the Game of Kind. The solution to the Game of Degree is then derived, thus providing the optimal pursuit and evasion state feedback strategies for the two Pursuers and the Evader when all three have equal speed.

4.2 Introduction

The two-on-one pursuit-evasion differential game on the Euclidean plane with simple motion/honolomic players is analyzed under the stipulations that the Evader/Pursuers' speed ratio $\mu \triangleq \frac{v_E}{v_P} = 1$, but at least one of the Pursuers is endowed with a capture disk whose radius $\ell > 0$.

Isaacs, who formulated the two-on-one pursuit-evasion differential game under the header "The Two Cutters and Fugitive Ship" differential game, stipulated that the players have simple motion, the Pursuers are faster than the Evader, and point capture is required [1]. Wasz and Pachter [2] expanded on Isaacs' work through the introduction of Pursuer capture disks whose radii $\ell_1 = \ell_2 = \ell > 0$. In their work, they provided the solution to the Game of Kind by determining the regions in the state space where one of the Pursuers captures the Evader and the region where the two pursuers isochronously capture the Evader. They then turned to the Game of Degree and determined the optimal state feedback strategies for the Pursuers and the Evader.

In an extension to the previously mentioned work, Pachter and Wasz [3] and Vlassakis and Pachter [17] addressed the two-on-one pursuit-evasion differential game where the speed ratio $\mu = 1$ and the two Pursuers' capture disks radii are $\ell_1 = \ell_2 = \ell > 0$. The conditions for capturability were determined along with the optimal state feedback strategies for the Pursuers and the Evader. Also in their work, Vlassakis and Pachter [17] explored the case where the Pursuers are endowed with unequal capture disks $\ell_1 > \ell_2 \geq 0$. The solution to the Game of Degree was partially delineated. The case where there are many pursuers, the Evader is as fast as the Pursuers, and the game evolves in the Euclidean plane where the players have simple motion was addressed by Pshenichnyi in the seminal paper [18], however, point capture was required. The pursuit strategy in [18] was stroboscopic, that is, the Evader was discriminated. In our work, the two Pursuers are endowed with circular capture sets. Most importantly, in our work the players' optimal strategies are state feedback strategies.

The paper is organized as follows. In Section 4.3, the previous work concerning the Two-on-One pursuit of an equal speed Evader with unequal capture ranges is consolidated and extended. We obtain the complete solution to the Game of Kind for the case in which the Evader/Pursuers' speed ratio $\mu = 1$: The necessary and sufficient conditions for capturability are determined for both the cases in which the Pursuers' capture radii $\ell_1 > \ell_2 > 0$ and $\ell_1 > \ell_2 = 0$. The Capturability Zone is where the Game of Degree is played, and its solution, the Pursuers' and Evader's state feedback optimal strategies – are provided in Section 4.4. We analyze the two-on-one pursuit-evasion differential game, when the speed ratio $\mu = 1$, in a three-dimensional reduced state space and draw special attention to the conditions in the end game, at the moment of capture of the Evader by the two "slow" pursuers. A conjecture which characterizes the region of capturability, advanced in Section 4.3, is numerically validated by simulations, as discussed in Section 4.5. The Game of Kind and Game

of Degree in the case where one of the Pursuers employs point capture is analyzed in the respective Sections 4.6 and 4.7 and interesting special cases are fully analyzed in Section 4.8. Special attention is given in Section 4.9 to the geometry of the reduced state space of the Two-on-One pursuit-evasion differential game where the speed ratio $\mu = 1$ and the Pursuers' capture ranges are $\ell_1 \geq \ell_2 \geq 0$. In Section 4.10, we apply our solution of the Two-on-One pursuit-evasion differential game to the interesting game where a single Pursuer chases an equal speed Evader cornered against a wall. Conclusions follow in Section 4.11.

4.3   Unequal Capture Ranges: Game of Kind

When the capture ranges are $\ell_1 > \ell_2 > 0$, the results of references [3] and [17] bounds for the state space region R_c where capturability is guaranteed. This follows from the results reported in [17], where the Pursuers' capture ranges are equal, that is, $\ell_1 = \ell_2 = \ell \, (> 0)$, and the capture region is included between the tangents of the capture circles of radius ℓ – see Fig. 12:
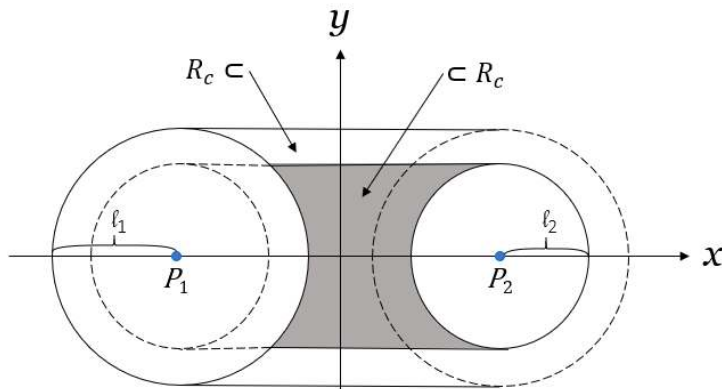
Figure 12: Capturability Region.

Obviously, when the capture ranges $\ell_1 > \ell_2 \geq 0$, the capture region R_c is smaller than the region included between the tangents of the circles of radius ℓ_1 and is larger than the region included between the tangents of the circles of radius ℓ_2.

In this respect, in reference to the Game of Kind, we have the following:

Conjecture 1 *In the Two-on-One differential game when the Pursuers' capture ranges $\ell_1 > \ell_2 \geq 0$, the capturability region R_C is the region included between the tangents to the capturability circles, as shown in Fig. 13.*

$$y = \frac{(\ell_1 + \ell_2)x_P - (\ell_1 - \ell_2)x}{\sqrt{4x_P^2 - (\ell_1 - \ell_2)^2}}$$
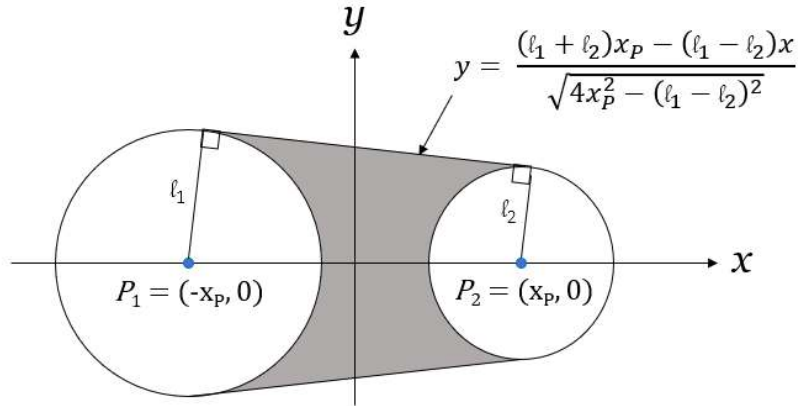
Figure 13: Capturability Region.

If the state (x_P, x_E, y_E) is in the blue shaded region shown in Fig. 13, the Evader cannot escape, provided the pursuers play optimally.

$$y_E < \frac{1}{\sqrt{4x_P^2 - (\ell_1 - \ell_2)^2}}[(\ell_2 - \ell_1)x_E + (\ell_1 + \ell_2)x_P], \tag{5}$$

$\square$

Referencing Fig. 14,

$$\tan \alpha = \frac{\ell_1 - \ell_2}{\sqrt{(2x_P)^2 - (\ell_1 - \ell_2)^2}}$$

30
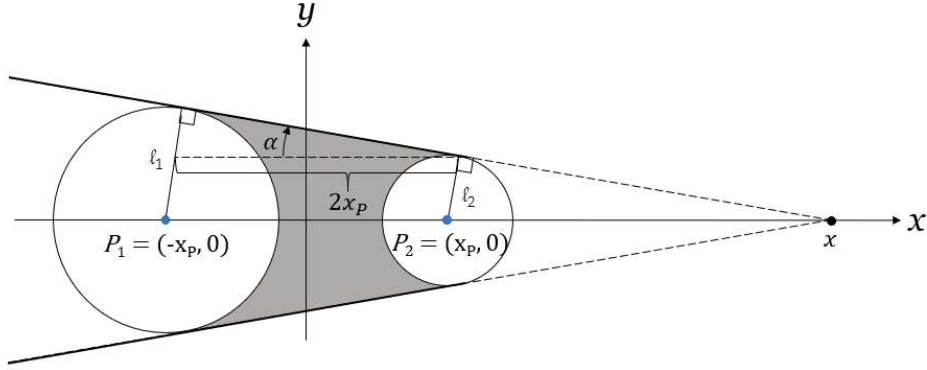
Figure 14: Capture Zone with Unequal Capture Radii

so the slope of the straight line which is tangent to the Pursuers' capture circles is $-\frac{\ell_1-\ell_2}{\sqrt{4x_P^2-(\ell_1-\ell_2)^2}}$ and, therefore, the tangent's equation is

$$y(x_E; x_P) = -\frac{\ell_1 - \ell_2}{\sqrt{4x_P^2 - (\ell_1 - \ell_2)^2}}x_E + c.$$

The tangent intersects the x-axis at the distance x from the origin, at $(x, 0)$. We calculate

$$\frac{x + x_P}{2x_P} = \frac{\ell_1}{\ell_1 - \ell_2}$$
$$x = \frac{\ell_1 + \ell_2}{\ell_1 - \ell_2}x_P$$

so

$$0 = -\frac{\ell_1 - \ell_2}{\sqrt{4x_P^2 - (\ell_1 - \ell_2)^2}} \cdot \frac{\ell_1 + \ell_2}{\ell_1 - \ell_2}x_P + c$$

31

$$\Rightarrow$$

$$c = \frac{\ell_1 + \ell_2}{\sqrt{4x_P^2 - (\ell_1 - \ell_2)^2}} x_P.$$

Hence, the conjectured capturability zone in the upper half plane where $y_E \geq 0$ is below the straight line (5). The capture zone is symmetric about the x-axis.

The validity of the conjecture is tested and "proved" by simulation in Section 4.5 after the Pursuers' and Evader's optimal state feedback strategies are developed in Section 4.4 below.

4.4   Unequal Capture Ranges: Game of Degree

Consider the frame (x, y) in the Euclidean plane where the x-axis passes through the positions P_1 and P_2 of the Pursuers and the y-axis is the orthogonal bisector of the segment $\overline{P_1 P_2}$ whose length is $2x_P$. The position of the Evader in the (x, y) frame is $E = (x_E, y_E)$.

The Interception point $I = (x, y)$ is on a hyperbola whose foci are P_1 and P_2 and the distance from P_1 to P_2 is $2x_P$. The hyperbola, depicted in Fig. 15, is

$$\frac{x^2}{a^2} - \frac{y^2}{b^2} = 1 \tag{6}$$

and its parameters are

$$a = \frac{1}{2}(\ell_1 - \ell_2), \qquad b = \sqrt{x_P^2 - \frac{1}{4}(\ell_1 - \ell_2)^2}.$$

Since the speed ratio $\mu = 1$, when the Evader's position is (x_E, y_E), the following must hold:

$$\sqrt{(x - x_E)^2 + (y - y_E)^2} = \sqrt{(x_P - x)^2 + y^2} - \ell_2. \tag{7}$$

32

where (x, y) are the coordinates of the Interception point I where E is captured by the Pursuers – see Fig. 15. We thus have two nonlinear equations, (6) and (7), in the two unknowns x and y, whose solution yields the Interception point $I = (x, y)$.
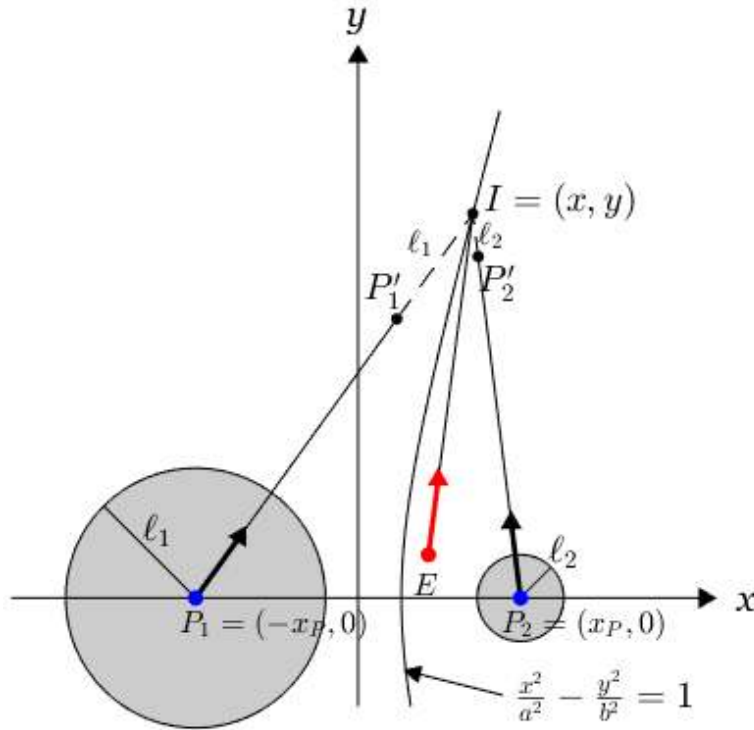
Figure 15: Interception is Effected on the Hyperbola whose foci are P_1 and P_2

We proceed as follows: squaring the two sides of eq. (7) yields

$$(x_E - x_P)x + y_E y + \frac{1}{2}(x_P^2 - x_E^2 - y_E^2 + \ell_2^2) = \ell_2\sqrt{(x_P - x)^2 + y^2}$$

Squaring again both sides of the above equation yields a quadratic equation in x and y

$$[(x_E - x_P)^2 - \ell_2^2]x^2 + (y_E^2 - \ell_2^2)y^2 + 2(x_E - x_P)y_E xy$$
$$+ [(x_E - x_P)w + 2\ell_2^2 x_P]x + wy_E y + \frac{1}{4}w^2 - \ell_2^2 x_P^2 = 0 \quad (8)$$

where

$$w \triangleq x_P^2 - x_E^2 - y_E^2 + \ell_2^2.$$

We have two second-order polynomial equations (6) and (8) in two variables, (x, y). We back out x from eq. (6):

$$x = \frac{a}{b}\sqrt{y^2 + b^2}.$$

Inserting the above expression into eq. (8) and squaring, we get a quartic equation in y. Quartic equations have an analytic solution. But, we should embark on the solution of the quartic equation only after the solution of the Game of Kind guarantees capturability – see Section 4.3, where it is mandated that E be under the tangents to the capture disks. The quartic equation will then have two real solutions, one of which – the point (x, y) farther from E – yields the players' aim point I.

If $\ell_1 = \ell_2 = \ell > 0$, eq. (6) is replaced by the equation $x = 0$ and setting $x = 0$ in eq. (8) yields a quadratic equation in y:

$$(y_E^2 - \ell^2)y^2 + (x_P^2 - x_E^2 - y_E^2 + \ell^2)y_E y + \frac{1}{4}(x_P^2 - x_E^2 - y_E^2 + \ell^2)^2 - \ell^2 x_P^2 = 0$$

We, however, now consider the case in which the two Pursuers, P_1 and P_2, are endowed with capture disks of unequal radii, ℓ_1 and ℓ_2. The reach of P_i is ℓ_i, $i = 1, 2$; without loss of generality $\ell_1 > \ell_2 \geq 0$, and, when $\ell_2 > 0$, we must solve a quartic equation; if however $\ell_2 = 0$, we must solve a quadratic equation as will be evident in the sequel.

We have capturability if and only if the Safe Region (SR) of E is closed. As in [3],
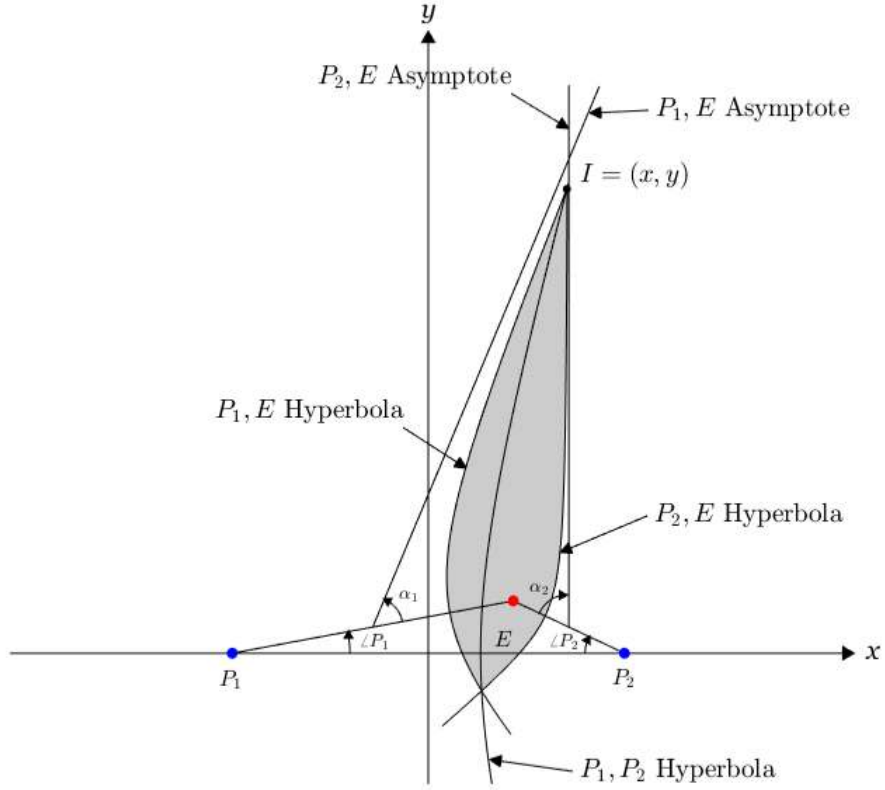
Figure 16: Safe Region of E. $\ell_1 = 1.2$. $\ell_2 = 0.4$.

the SR is formed by the P_1, E and the P_2, E hyperbolae, yet this is now a tale of three hyperbolae, the third hyperbola being the P_1, P_2 hyperbola. The three hyperbolae are concurrent at two points. The players' aim point I is the point of concurrency which is farther from E – see Fig. 16. Without (much) loss of generality, we have assumed $0 \leq x_E$, $y_E > 0$. Geometrically, referencing Fig. 16, we calculate:

$$\alpha_1 = Atan\left(\frac{\sqrt{(x_P + x_E)^2 + y_E^2 - \ell_1^2}}{\ell_1}\right),$$

$$\alpha_2 = Atan\left(\frac{\sqrt{(x_P - x_E)^2 + y_E^2 - \ell_2^2}}{\ell_2}\right),$$

$$\angle EP_1P_2 = Atan\left(\frac{y_E}{x_P + x_E}\right),$$

$$\angle EP_2P_1 = Atan\left(\frac{y_E}{x_P - x_E}\right).$$

We have capturability if and only if the state (x_P, x_E, y_E) is such that the upper asymptote of the East-opening of the P_1, E hyperbola and the upper asymptote of the West-opening of the P_2, E hyperbola meet/intersect. In this respect, we are interested in the $\angle EP_1P_2 + \alpha_1$ and $\angle EP_2P_1 + \alpha_2$ angles. Thus, let

$$a_1 \triangleq tan(\angle EP_1P_2 + \alpha_1) = \frac{\ell_1 y_E + (x_P + x_E)\sqrt{(x_P + x_E)^2 + y_E^2 - \ell_1^2}}{\ell_1(x_P + x_E) - y_E\sqrt{(x_P + x_E)^2 + y_E^2 - \ell_1^2}},$$

$$a_2 \triangleq tan(\angle EP_2P_1 + \alpha_2) = \frac{\ell_2 y_E + (x_P - x_E)\sqrt{(x_P - x_E)^2 + y_E^2 - \ell_2^2}}{\ell_2(x_P - x_E) - y_E\sqrt{(x_P - x_E)^2 + y_E^2 - \ell_2^2}}$$

The equation of the upper asymptote of the East-opening of the hyperbola whose foci are P_1 and E is

$$y = a_1 x + b_1.$$

Since the upper asymptote of the East opening of the hyperbola emanates from the point $\left(\frac{x_E - x_P}{2}, \frac{y_E}{2}\right)$,

$$\frac{y_E}{2} = a_1 \frac{x_E - x_P}{2} + b_1$$

where

$$b_1 \triangleq \frac{1}{2}[y_E - a_1(x_E - x_P)],$$

36

and we get

$$y = a_1 x + \frac{1}{2}[y_E - a_1(x_E - x_P)].$$

Similarly, the equation of the upper asymptote of the West-opening of the hyperbola whose foci are P_2 and E is

$$y = -a_2 x + \frac{1}{2}[y_E + a_2(x_P + x_E)]$$

We have two linear equations in the two unknowns x and y. We are interested in the solution

$$y = \frac{1}{2} \frac{a_1[y_E + a_2(x_P + x_E)] + a_2[y_E - a_1(x_E - x_P)]}{a_1 + a_2},$$

which is also written as

$$y = \frac{1}{2} y_E + \frac{1}{\frac{1}{a_1} + \frac{1}{a_2}} x_P.$$

The SR is closed – capturability is guaranteed – if and only if $a_1 + a_2 \neq 0$ and $y > 0$, where we calculate

$$\frac{y}{x_P} = \frac{\left\{ \begin{bmatrix} \ell_1 y_E + (x_P + x_E)\sqrt{(x_P + x_E)^2 + y_E^2 - \ell_1^2} \end{bmatrix} \\ \cdot \begin{bmatrix} \ell_2 y_E + (x_P - x_E)\sqrt{(x_P - x_E)^2 + y_E^2 - \ell_2^2} \end{bmatrix} \right\}}{\left\{ \begin{bmatrix} \ell_1(x_P + x_E) - y_E\sqrt{(x_P + x_E)^2 + y_E^2 - \ell_1^2} \end{bmatrix} \\ \cdot \begin{bmatrix} \ell_2 y_E + (x_P - x_E)\sqrt{(x_P - x_E)^2 + y_E^2 - \ell_2^2} \end{bmatrix} \\ + \begin{bmatrix} \ell_2(x_P - x_E) - y_E\sqrt{(x_P - x_E)^2 + y_E^2 - \ell_2^2} \end{bmatrix} \\ \cdot \begin{bmatrix} \ell_1 y_E + (x_P + x_E)\sqrt{(x_P + x_E)^2 + y_E^2 - \ell_1^2} \end{bmatrix} \right\}} + \frac{y_E}{2x_P} \tag{9}$$

The sufficient conditions for capturability can be described geometrically. In Fig. 16, we see that for capturability to be possible,

$$\angle EP_1P_2 + \alpha_1 < \frac{\pi}{2} \ \ and \ \ \angle EP_2P_1 + \alpha_2 < \frac{\pi}{2}.$$

37

These conditions can also be written as

$$\ell_1(x_P + x_E) > y_E\sqrt{(x_P + x_E)^2 + y_E^2 - \ell_1^2}$$

$$\ell_2(x_P - x_E) > y_E\sqrt{(x_P - x_E)^2 + y_E^2 - \ell_2^2},$$

and thus

$$\ell_1^2(x_P + x_E)^2 > [(x_P + x_E)^2 - \ell_1^2]y_E^2 + y_E^4$$

$$\ell_2^2(x_P - x_E)^2 > [(x_P - x_E)^2 - \ell_2^2]y_E^2 + y_E^4.$$

These conditions hold if and only if y_E is such that

$$|y_E| < \ell_1, \qquad |y_E| < \ell_2$$

Capturability is then guaranteed.

If $|y_E| > \ell_1$, the SR is open – E can escape, and if $|y_E| > \ell_2$, we need $\ell_1 > |y_E|$ for capturability.

The quartic equation has two real solutions when its "parameter" (x_P, x_E, y_E) is such that $a_1 + a_2 \neq 0$ and y given by eq. (9) is positive. For this to be the case, we need $|x_E| < x_P$. This is so because the SR of E must be closed.

If both $\ell_1 = \ell_2 = 0$, since the speed ratio $\mu = 1$, E can escape. However, isochronous capture is possible when $\ell_2 = 0$, provided $\ell_1 > 0$. We show this by replacing eq. (7) with

$$\sqrt{(x - x_E)^2 + (y - y_E)^2} = \sqrt{(x_P - x)^2 + y^2} \tag{10}$$

38

Squaring both sides of eq. (10) yields the linear relationship

$$(x_P - x_E)x - y_E y = \frac{1}{2}(x_P^2 - x_E^2 - y_E^2) \tag{11}$$

Eqs. (6) and (11) yield the quadratic equation in x

$$\left[\frac{1}{a^2} - \left(\frac{x_P - x_E}{by_E}\right)^2\right]x^2 + \frac{(x_P - x_E)(x_P^2 - x_E^2 - y_E^2)}{b^2 y_E^2}x - \frac{(x_P^2 - x_E^2 - y_E^2)^2}{4b^2 y_E^2} - 1 = 0$$

that is,

$$\left[\left(\frac{b}{a}\right)^2 y_E^2 - (x_P - x_E)^2\right]x^2 + (x_P - x_E)(x_P^2 - x_E^2 - y_E^2)x - \frac{1}{4}(x_P^2 - x_E^2 - y_E^2)^2 - b^2 y_E^2 = 0 \tag{12}$$

Here $a = \frac{1}{2}\ell_1$ and $b = \sqrt{x_P^2 - \frac{1}{4}\ell_1^2}$. We require $x_P > \frac{1}{2}\ell_1$, otherwise the triangle inequality will be violated; if $x_P < \frac{1}{2}\ell_1$, E cannot be (isochronously) captured by P_1 and P_2. And when $y_E = 0$, the aim point $I = (x, y)$ is

$$x = \frac{1}{2}(x_P + x_E), \quad y = \sqrt{x_P^2 - \frac{1}{4}\ell_1^2} \cdot \sqrt{\left(\frac{x_P + x_E}{\ell_1}\right)^2 - 1}.$$

Fig. 17 shows the case where $\ell_2 = 0$. If E is in the shaded state space region, capture is possible. We have capturability because although $\ell_2 = 0$, $\ell_1 > 0$. The aim point I is now at the intersection of the orthogonal bisector of the segment $\overline{EP_2}$ and the hyperbola whose foci are E and P_1, as shown in Fig. 17. We have capturability if and only if

$$\alpha_1 + \angle EP_1P_2 < \frac{\pi}{2} - \angle EP_2P_1$$
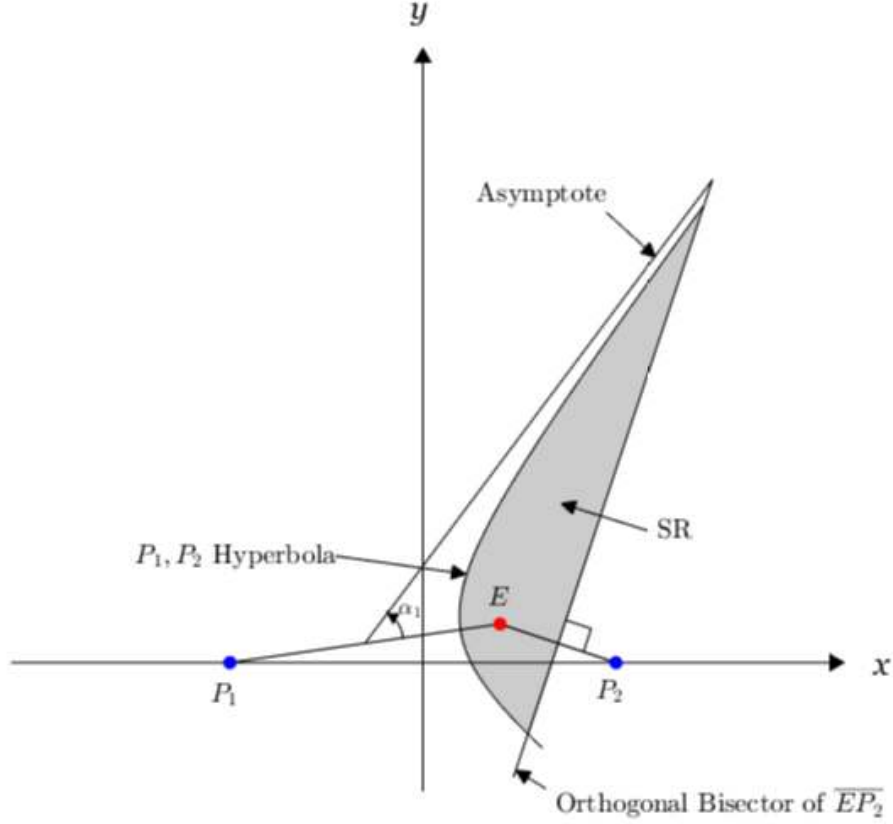
Figure 17: The Case where $\ell_2 = 0$.

that is, the state (x_P, x_E, y_E) is such that

$$\frac{\pi}{2} - \left[Atan \left(\frac{y_E}{x_P + x_E} \right) + Atan \left(\frac{y_E}{x_P - x_E} \right) \right] > Atan \left(\frac{\sqrt{(x_P + x_E)^2 + y_E^2 - \ell_1^2}}{\ell_1} \right)$$

which yields the condition

$$\frac{\sqrt{(x_P + x_E)^2 + y_E^2 - \ell_1^2}}{\ell_1} < \frac{x_P^2 - x_E^2 - y_E^2}{2 x_P y_E} \tag{13}$$

The quadratic equation (12) has two real solutions when the parameter (x_P, x_E, y_E) is such that eq. (13) holds. In this respect, consider the discriminant Δ of the quadratic

40

eq. (12). We calculate

$$\Delta = \alpha(x_P^2 - x_E^2 - y_E^2)^2 + (4x_P^2 - \ell_1^2)y_E^2 - \ell_1^2(x_P^2 - x_E^2)$$

We have capturability if

$$x_P^2 - x_E^2 < \frac{(x_P^2 - x_E^2 - y_E^2)^2 + (4x_P^2 - \ell_1^2)y_E^2}{\ell_1^2} \tag{14}$$

4.5   Simulation

Concerning Conjecture 1, and as a first step, consider the segment $[y_{E_{max}}, 0]$ on the y-axis, where $x_E = 0$. Thus, set $x_E = 0$ in eq. (9) and calculate

$$\frac{y(x_E = 0)}{x_P} = \frac{y_E}{2x_P} + \frac{\left[\ell_1 y_E + x_P\sqrt{x_P^2 + y_E^2 - \ell_1^2}\right]\left[\ell_2 y_E + x_P\sqrt{x_P^2 + y_E^2 - \ell_2^2}\right]}{\begin{array}{c}\left[\ell_1 x_P - y_E\sqrt{x_P^2 + y_E^2 - \ell_1^2}\right]\left[\ell_2 y_E + x_P\sqrt{x_P^2 + y_E^2 - \ell_2^2}\right] \\ + \left[\ell_2 x_P - y_E\sqrt{x_P^2 + y_E^2 - \ell_2^2}\right]\left[\ell_1 y_E + x_P\sqrt{x_P^2 + y_E^2 - \ell_1^2}\right]\end{array}}$$

We scan on $0 \le y_E < y_{E_{max}}$ the expression

$$\begin{aligned}\left[\ell_1 x_P - y_E\sqrt{x_P^2 + y_E^2 - \ell_1^2}\right] &\cdot \left[\ell_2 y_E + x_P\sqrt{x_P^2 + y_E^2 - \ell_2^2}\right] \\ + \left[\ell_2 x_P - y_E\sqrt{x_P^2 + y_E^2 - \ell_2^2}\right] &\cdot \left[\ell_1 y_E + x_P\sqrt{x_P^2 + y_E^2 - \ell_1^2}\right] > 0\end{aligned}$$

In conjunction with the work reported in [17], the case where $\ell_1 = \ell_2 = \ell$ collapses this expression to

$$\ell x_P - y_E\sqrt{x_P^2 + y_E^2 - \ell^2} > 0$$
$$\ell^2 x_P^2 > y_E^2 x_P^2 + y_E^4 - y_E^2 \ell^2$$
$$y_E^4 + (x_P^2 - \ell^2)y_E^2 - \ell^2 x_P^2 < 0$$

41

The roots of the above equation are

$$y_E^2 = 0, \ \ell^2,$$

thus, we need $-\ell < y_E < \ell$, which is indeed consistent with the result in [17].

The validity of Conjecture 1 when $x_E = 0$ is examined numerically. For each time step, the Interception point I was calculated using equations (9) and (6). The three-state nonlinear dynamics of the differential game are – see Fig. 18:

$$\dot{x}_P = \frac{1}{2}(cos\ \chi - cos\psi), \ x_P(0) = x_{P_0}$$
$$\dot{x}_E = cos\ \phi - \frac{1}{2}(cos\ \chi + cos\ \psi) + \frac{1}{2}\frac{y_E}{x_P}(sin\ \chi - sin\ \psi), \ x_E(0) = x_{E_0}$$
$$\dot{y}_E = sin\ \phi - \frac{1}{2}(sin\ \chi + sin\ \psi) - \frac{1}{2}\frac{x_E}{x_P}(sin\ \chi - sin\ \psi), \ y_E(0) = y_{E_0}$$

Fig. 18 shows the reduced state space in the realistic plane (X, Y). The optimal state feedback strategies are

$$sin\ \psi^* = \frac{y}{\sqrt{(x_P + x)^2 + y^2}},$$
$$cos\ \psi^* = \frac{x_P + x}{\sqrt{(x_P + x)^2 + y^2}}$$
$$sin\ \chi^* = \frac{y}{\sqrt{(x_P - x)^2 + y^2}},$$
$$cos\ \chi^* = -\frac{x_P - x}{\sqrt{(x_P - x)^2 + y^2}}$$
$$sin\ \phi^* = \frac{y - y_E}{\sqrt{(x_E - x)^2 + (y - y_E)^2}},$$
$$cos\ \phi^* = -\frac{x_E - x}{\sqrt{(x_E - x)^2 + (y - y_E)^2}}$$

where x, y are the coordinates of the players' aim point I.

The players' trajectories in the reduced state space are first obtained, including
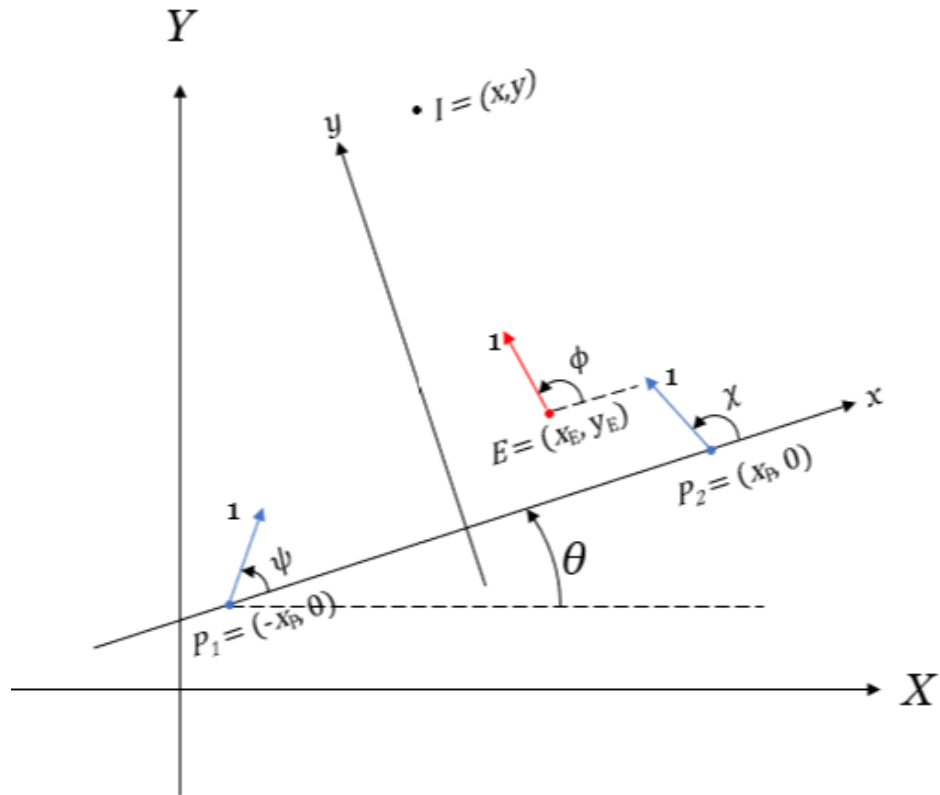
Figure 18: Reduced State Space in the Realistic Plane

their respective control time histories $\phi(t)$, $\psi(t)$, $\chi(t)$, $0 \leq t$. To transform the dynamics into the realistic plane, we first note that the initial conditions are the same for both the realistic plane and the reduced state space because the (x, y) and (X, Y) frames are initially aligned. The "free fall" closed-loop dynamics during optimal play

are

$$\dot{X}_{P_1} = cos(\psi + \theta), \qquad\qquad X_{P_1}(0) = -x_{P_0}$$

$$\dot{Y}_{P_1} = sin(\psi + \theta), \qquad\qquad Y_{P_1}(0) = 0$$

$$\dot{X}_{P_2} = cos(\chi + \theta), \qquad\qquad X_{P_2}(0) = x_{P_0}$$

$$\dot{Y}_{P_2} = sin(\chi + \theta), \qquad\qquad Y_{P_2}(0) = 0$$

$$\dot{X}_{E} = cos(\phi + \theta), \qquad\qquad X_{E}(0) = x_{E_0}$$

$$\dot{Y}_{E} = sin(\phi + \theta), \qquad\qquad Y_{E}(0) = y_{E_0}$$

where

$$sin\ \theta = \frac{Y_{P_2} - Y_{P_1}}{2x_p}, \quad cos\ \theta = \frac{X_{P_2} - X_{P_1}}{2x_p}$$

and the control time histories are known. Thus,

$$\dot{X}_{P_1} = \frac{X_{P_2} - X_{P_1}}{2x_p}cos\ \psi - \frac{Y_{P_2} - Y_{P_1}}{2x_p}sin\ \psi, \qquad X_{P_1}(0) = -x_{P_0}$$

$$\dot{Y}_{P_1} = \frac{X_{P_2} - X_{P_1}}{2x_p}sin\ \psi + \frac{Y_{P_2} - Y_{P_1}}{2x_p}cos\ \psi, \qquad Y_{P_1}(0) = 0$$

$$\dot{X}_{P_2} = \frac{X_{P_2} - X_{P_1}}{2x_p}cos\ \chi - \frac{Y_{P_2} - Y_{P_1}}{2x_p}sin\ \chi, \qquad X_{P_2}(0) = x_{P_0}$$

$$\dot{Y}_{P_2} = \frac{X_{P_2} - X_{P_1}}{2x_p}sin\ \chi + \frac{Y_{P_2} - Y_{P_1}}{2x_p}cos\ \chi, \qquad Y_{P_2}(0) = 0$$

$$\dot{X}_{E} = \frac{X_{P_2} - X_{P_1}}{2x_p}cos\ \phi - \frac{Y_{P_2} - Y_{P_1}}{2x_p}sin\ \phi, \qquad X_{E}(0) = x_{E_0}$$

$$\dot{Y}_{E} = \frac{X_{P_2} - X_{P_1}}{2x_p}sin\ \phi + \frac{Y_{P_2} - Y_{P_1}}{2x_p}cos\ \phi, \qquad Y_{E}(0) = y_{E_0}$$

We integrate the linear but time-dependent differential system

$$\dot{X} = A(t) \cdot X, \quad X(0) = X_0, 0 \le t \le t_f$$

where

$$X \triangleq \begin{bmatrix} X_{P_1} \\ Y_{P_1} \\ X_{P_2} \\ Y_{P_2} \\ X_E \\ Y_E \end{bmatrix}, \quad X_0 = (-x_{P_0}, \ 0, \ x_{P_0}, \ 0, \ x_{E_0}, \ y_{E_0}) \, ,$$

$$A(t) = \begin{bmatrix} -cos(\psi(t)) & sin(\psi(t)) & cos(\psi(t)) & -sin(\psi(t)) & 0 & 0 \\ -sin(\psi(t)) & -cos(\psi(t)) & sin(\psi(t)) & cos(\psi(t)) & 0 & 0 \\ -cos(\chi(t)) & sin(\chi(t)) & cos(\chi(t)) & -sin(\chi(t)) & 0 & 0 \\ -sin(\chi(t)) & -cos(\chi(t)) & sin(\chi(t)) & cos(\chi(t)) & 0 & 0 \\ -cos(\phi(t)) & sin(\phi(t)) & cos(\phi(t)) & -sin(\phi(t)) & 0 & 0 \\ -sin(\phi(t)) & -cos(\phi(t)) & sin(\phi(t)) & cos(\phi(t)) & 0 & 0 \end{bmatrix}$$

and obtain the players' trajectories in the realistic plane.

Numerical exploration of the shaded region in Fig. 13 confirms that indeed capturability is guaranteed.

4.6   Game of Kind: $\ell_2 = 0$

We revisit the case where $\ell_1 > \ell_2 = 0$. It behooves us to say that "point capture" means P_2 is endowed with a capture disk of radius $\epsilon > 0, \epsilon \to 0$. The following relationship is derived geometrically – see Fig. 20.

$$\alpha_1 = Atan \left(\frac{\sqrt{\overline{EP_1}^2 - \ell^2}}{\ell} \right)$$
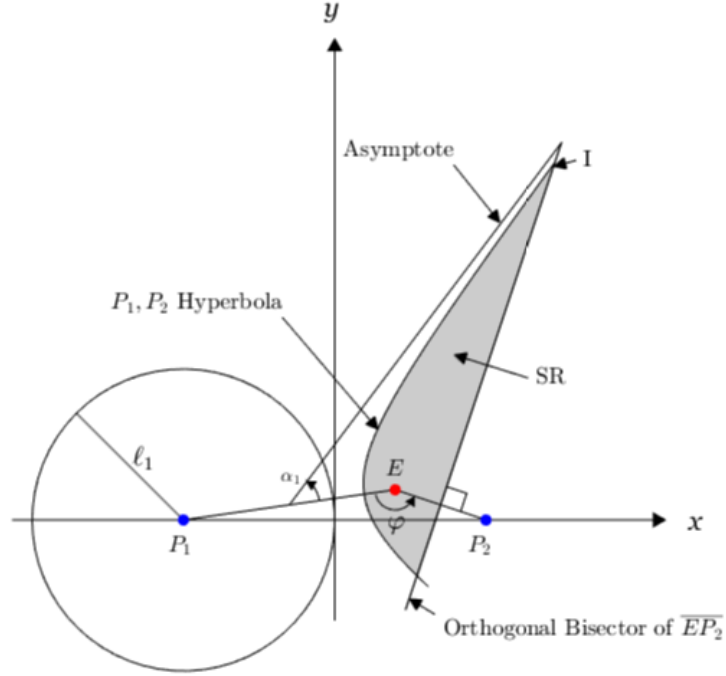
Figure 19: Isochronous Capture when P_1 is Endowed with a Capture Disk of Radius ℓ_1 and P_2 resorts to point capture.

We have capturability if and only if the state (x_P, x_E, y_E) is such that $\alpha_1 + \angle P_1 + \angle P_2 < \frac{\pi}{2}$. Since $\angle P_1 + \angle P_2 = \pi - \varphi$, the condition is

$$\varphi > \alpha_1 + \frac{\pi}{2} \left(> \frac{\pi}{2} \right)$$

The law of cosines yields:

$$\underbrace{4x_P^2}_{\overline{P_1 P_2}^2} = \underbrace{(x_P + x_E)^2 + y_E^2 + (x_P - x_E)^2 + y_E^2}_{\overline{EP_1}^2 + \overline{EP_2}^2} - 2\sqrt{\underbrace{[(x_P + x_E)^2 + y_E^2]}_{\overline{EP_1}} \cdot \underbrace{[(x_P - x_E)^2 + y_E^2]}_{\overline{EP_2}}} \cdot cos\varphi.$$

Simplifying the above expression yields

$$cos\ \varphi = -\frac{x_P^2 - x_E^2 - y_E^2}{\underbrace{\sqrt{(x_P^2 + x_E^2 + y_E^2)^2 - 4x_P^2 x_E^2}}_{\overline{EP_1} \cdot \overline{EP_2}}},$$

46

which can be rewritten as the following:

$$sin\ \alpha_1 < \underbrace{\frac{x_P^2 - x_E^2 - y_E^2}{\sqrt{(x_P^2 + x_E^2 + y_E^2)^2 - 4x_P^2 x_E^2}}}_{\overline{EP_1} \cdot \overline{EP_2}}$$

$$\frac{\sqrt{\overline{EP_1}^2 - \ell^2}}{\overline{EP_1}} < \underbrace{\frac{x_P^2 - x_E^2 - y_E^2}{\sqrt{(x_P^2 + x_E^2 + y_E^2)^2 - 4x_P^2 x_E^2}}}_{\overline{EP_1} \cdot \overline{EP_2}}.$$

The above expression further simplifies to

$$\sqrt{\overline{EP_1}^2 - \ell^2} \cdot \overline{EP_2} < x_P^2 - x_E^2 - y_E^2$$

$$\Rightarrow$$

$$(x_P^2 + x_E^2 + y_E^2)^2 - 4x_P^2 x_E^2$$

$$< \ell^2[(x_P - x_E)^2 + y_E^2] + (x_P^2 - x_E^2 - Y_E^2)$$

which finally yields the straight-line boundary of the capture zone

$$y_E < \frac{1}{2}\ell \cdot \frac{x_P - x_E}{\sqrt{x_P^2 - \left(\frac{\ell}{2}\right)^2}}.$$

The state component x_P must be such that $0 < \ell < 2x_P$.

If the Evader is on the y-axis $(x_E = 0)$, we have

$$x_E = 0 \Rightarrow y_E < \frac{1}{2}\ell \cdot \frac{1}{\sqrt{1 - \left(\frac{1}{2}\frac{\ell}{x_P}\right)^2}}.$$

The zone of capturability when $x_E = 0$ is then the thick line segment shown in Fig.

20.
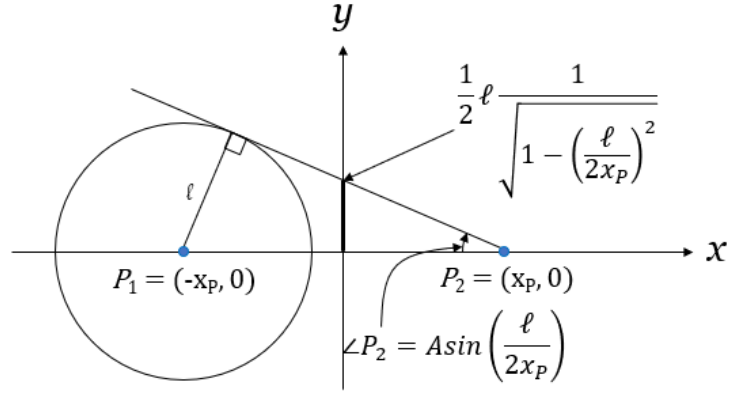
Figure 20: Capturability Condition.

We verify:

$$x_P \tan\left(A\sin\left(\frac{\ell}{2x_P}\right)\right) = \frac{1}{2}\ell \cdot \frac{1}{\sqrt{1 - \left(\frac{\ell}{2x_P}\right)^2}}$$

As expected, the complete zone of capturability is symmetric about the x-axis.

4.7   Game of Degree: $\ell_2 = 0$

The case in which $\ell = \ell_1 > \ell_2 = 0$ is now considered. The equation of the hyperbola whose foci are P_1 and P_2 when $\ell_2 = 0$ is given in (6), with parameters

$$a = \frac{1}{2}\ell, \quad b = \sqrt{x_P^2 - \frac{1}{4}\ell^2}.$$

Also,

$$\sqrt{(x - x_E)^2 + (y - y_E)^2} = \sqrt{(x - x_P)^2 + y^2},$$

which can be rewritten as

48

$$x = \frac{y_E}{x_P - x_E} \cdot y + \frac{1}{2}\frac{x_P^2 - x_E^2 - y_E^2}{x_P - x_E}. \tag{15a}$$

This is the equation of the orthogonal bisector of the $\overline{EP_2}$ segment. Let

$$e \triangleq \frac{y_E}{x_P - x_E}, \quad f \triangleq \frac{1}{2}\frac{x_P^2 - x_E^2 - y_E^2}{x_P - x_E},$$

so eq. (15a) is

$$x = ey + f \tag{15b}$$

We have two equations, (6) and (15b), in the two unknowns x and y. Inserting eq. (15b) into eq. (6) yields

$$(ey + f)^2 b^2 - a^2 y^2 = a^2 b^2.$$

We have the quadratic equation

$$(b^2 e^2 - a^2)y^2 = 2b^2 e f y + b^2(f^2 - a^2) = 0 \tag{16}$$

Its discriminant

$$\Delta = a^2 b^2 (f^2 + b^2 e^2 - a^2).$$

We calculate

$$f^2 \;+\; b^2 e^2 \;-\; a^2 \;=\; \frac{1}{4}\left[\frac{(x_P^2 - x_E^2 - y_E^2)^2}{(x_P - x_E)^2} + \frac{y_E^2}{(x_P - x_E)^2} \cdot (4x_P^2 - \ell^2) - \ell^2\right]$$

which is equivalent to

$$f^2 + b^2 e^2 - a^2 = \frac{1}{4}\frac{1}{(x_P - x_E)^2} \cdot \left[y_E^4 + 2\left(x_P^2 + x_E^2 - \frac{1}{2}\ell^2\right)y_E^2 + x_P^4 + x_E^4 - 2x_P^2 x_E^2 - \ell^2(x_p - x_E)^2\right]$$

For a solution to the Game of Degree to exist, we need the discriminant $\Delta > 0$; given x_P and x_E, the discriminant Δ depends on y_E.

$$\Delta \propto y_E^4 + 2\left(x_P^2 + x_E^2 - \frac{1}{2}\ell^2\right)y_E^2 + x_P^4 + x_E^4 - 2x_P^2 x_E^2 - \ell^2(x_P - x_E)^2 > 0$$

In this respect, consider the quartic equation which is now a biquadratic equation:

$$y_E^4 + 2\left(x_P^2 + x_E^2 - \frac{1}{2}\ell^2\right)y_E^2 + x_P^4 + x_E^4 - 2x_P^2 x_E^2 - \ell^2(x_P - x_E)^2 = 0$$

Its roots are
$$y_E^2 = \frac{1}{2}\ell^2 - x_P^2 - x_E^2 \pm \left|2x_P x_E - \frac{1}{2}\ell^2\right|$$

The roots of the biquadratic equation are

$$y_E^2 = -(x_P - x_E)^2 \;\; (< 0), \qquad y_E^2 = \ell^2 - (x_P + x_E)^2.$$

But we assume E has not yet been captured, so

$$(x_P + x_E)^2 + y_E^2 > \ell^2$$

which can be rewritten as
$$y_E^2 > \ell^2 - (x_P + x_E)^2,$$

and since the discriminant Δ is quadratic in y_E^2 – see Fig. 21 – the discriminant $\Delta > 0$ and we can proceed with the calculation of y, thus establishing the players' aim point $I = (x, y)$ – this, under the condition that the state (x_P, x_E, y_E) is indeed in the capture zone determined by the solution of the preliminary Game of Kind – see Fig. 20, where E must be under the tangent to the circle.

Using the two roots of the biquadratic equation, the discriminant Δ of the quadratic
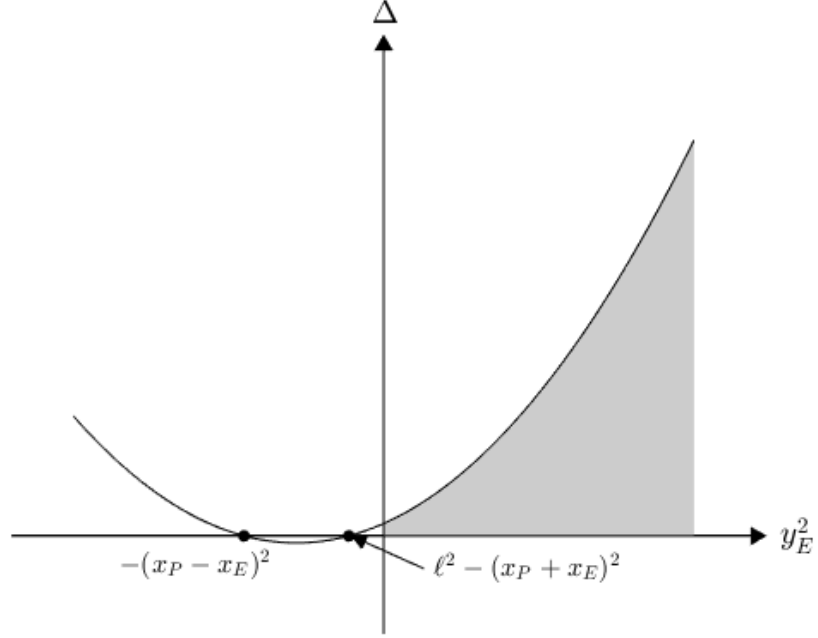
Figure 21: The Discriminant Dependence on y_E

equation in y, eq. (16), is

$$\Delta(x_P, x_E, y_E) = \frac{1}{64}\ell^2 \frac{1}{(x_P - x_E)^2}(4x_P^2 - \ell^2) \cdot [y_E^2 + (x_P - x_E)^2][y_E^2 + (x_P + x_E)^2 - \ell^2]$$

Hence, the explicit solution of the quadratic equation (16) is

$$y = \frac{1}{2}\sqrt{4x_P^2 - \ell^2} \cdot \left\{ \frac{y_E(x_P^2 - x_E^2 - y_E^2)\sqrt{4x_P^2 - \ell^2}}{\ell^2(x_P - x_E)\sqrt{[(x_P - x_E)^2 + y_E^2] \cdot [(x_P + x_E)^2 + y_E^2 - \ell^2]}}{\ell^2(x_P - x_E)^2 - y_E^2(4x_P^2 - \ell^2)} \right\} \tag{17}$$

This formula for the calculation of the players' aim point I applies to states $(x_P, x_E, y_E) \in$ Capture Zone (shown in Fig.20), and $(x_P + x_E)^2 + y_E^2 > \ell^2$, that is, E is not in contact with P_1. When the state $(x_P, x_E, y_E) \in$ Capture Zone and

51

$(x_P + x_E)^2 + y_E^2 = \ell^2$, that is, E is in contact with P_1, the aim point I is at the intersection of the radial from P_1 through E, with the orthogonal bisector of the segment $\overline{EP_2}$ – see Fig. 22. This is so because E is then a captive of P_1, being
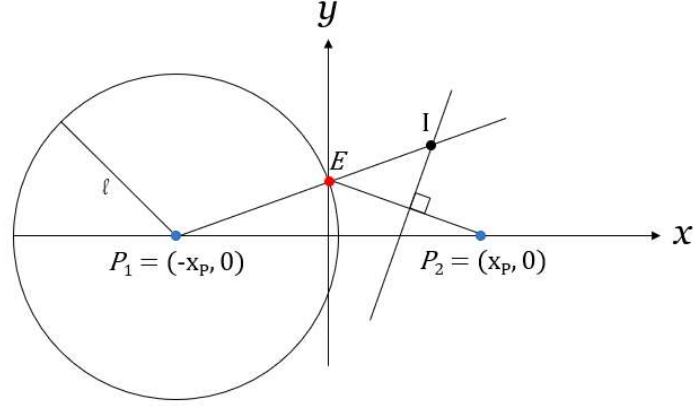
Figure 22: Contact with P_1

pushed around by P_1. If E does not move along with P_1, he will instantaneously be engulfed by the capture disk and capture will be effected.

The equation of the orthogonal bisector of the segment $\overline{EP_2}$ is given by eq. (15a) and the radial from P_1 through E is given by

$$y = \frac{y_E}{x_P + x_E}(x + x_P) \tag{18}$$

The solution of the linear equations (15a) and (18) is

$$x = \frac{1}{2}\frac{(x_P + x_E)^2 + y_E^2}{x_P^2 - x_E^2 - y_E^2} \cdot (x_P - x_E)$$
$$y = \frac{1}{2}y_E\left(1 + 2x_P\frac{x_P - x_E}{x_P^2 - x_E 62 - Y_E^2}\right)$$

During contact P_1 is in Pure Pursuit (PP) of E and P_2 is on a collision course toward the interception point $I = (x, y)$. E, in contact with P_1, flees from P_1, to be intercepted by P_2 at I and be captured. When the state $(x_P, x_E, y_E) \in$ Capture Zone

and E is in contact with P_2, that is, $x_E = x_P - \varepsilon, 0 < \varepsilon << 1$, P_2 will be in PP of E while E will be fleeing from P_2. P_1 will intercept E on the orthogonal bisector of the segment $\overline{P_1 P_2}$ where capture will be effected. When the state $(x_P, x_E, y_E) \in$ Capture Zone and E is not in contact with one of the Pursuers, the players head toward the aim point $I = (x, y)$, where y is given by eq. (17) and the x-coordinate of the players' aim point I is obtained by substituting the right-hand-side of (17) into (15a).

4.8 Special Cases

4.8.1 Evader at the Origin, $x_E = 0, \; y_E = 0$
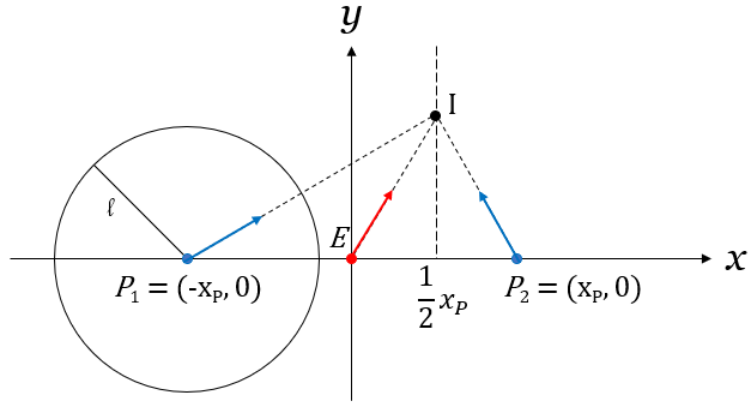
Figure 23: E at the Origin of the (x, y) Plane

We consider the case where the players are collinear: The Evader is situated at the origin of the (x, y) plane – see Fig. 23. Equations (15a) and (17) yield the aim point coordinates

$$x = \frac{1}{2} x_P, \quad y = \frac{1}{2} \frac{\sqrt{(4x_P^2 - \ell^2)(x_P^2 - \ell^2)}}{\ell}.$$

Obviously, here $x_P > \ell$ because E is at the origin.

53

4.8.2 Evader on the x-axis, $y_E = 0$
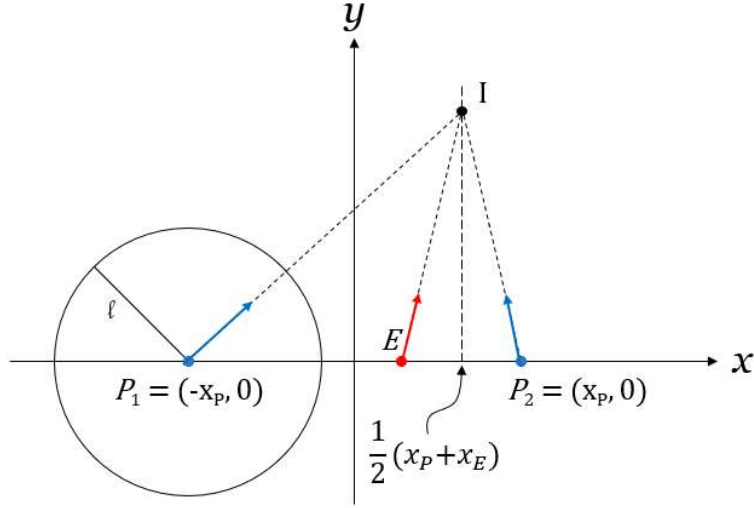
Figure 24: P_1, P_2 and E are collinear.

Equations (15a) and (17) yield the aim point coordinates

$$x = \frac{1}{2}(x_P + x_E), \quad y = \frac{1}{2}\frac{\sqrt{(4x_P^2 - \ell^2)[(x_P + x_E)^2 - \ell^2]}}{\ell}.$$

Obviously, $\ell < x_P + x_E$. In both case 4.8.1 and 4.8.2, E pulls away from the capture disk equipped Pursuer P_1 because it represents a greater threat than P_2 – as expected.

4.8.3 Evader on the y-axis, $x_E = 0$

When the Evader is initially located on the y-axis, the aim point I's coordinates are

$$y = \frac{1}{2}\sqrt{4x_P^2 - \ell} \cdot \frac{y_E(x_P^2 - y_E^2)\sqrt{4x_P^2 - \ell^2} + \ell x_P\sqrt{(x_P^2 + y_E^2)(x_P^2 + y_E^2 - \ell^2)}}{\ell^2(x_P^2 + y_E^2) - 4x_P^2 y_E^2},$$

$$x = \frac{y_E}{x_P}y + \frac{1}{2}\frac{x_P^2 - y_E^2}{x_P}$$

54
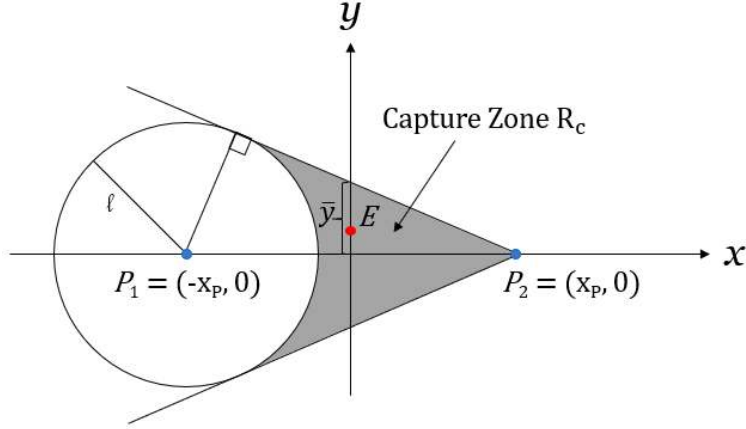
Figure 25: E is on the y-axis of the (x, y) Plane

We note that the denominator in the y-equation is positive if

$$y_E < \frac{\ell x_P}{\sqrt{4x_P^2 - \ell^2}}$$

But the maximal coordinate so that E is in the Capture Zone R_c,

$$\overline{y} = \frac{\ell x_P}{\sqrt{4x_P^2 - \ell^2}}$$

Thus, the denominator in the y-equation is positive as long as

$$y_E < \overline{y}$$

When the state is in the Capture Zone R_c the denominator in the y-equation is automatically positive. Indeed, the denominator in the y-equation is positive when the state $(x_P, x_E, y_E) \in$ Capture Zone R_c: for the denominator in the y-equation to be positive, the state (x_P, x_E, y_E) must be such that

$$y_E < \frac{\ell(x_P - x_E)}{\sqrt{4x_P^2 - \ell^2}}$$

55

Consider now the geometry of the Capture Zone.
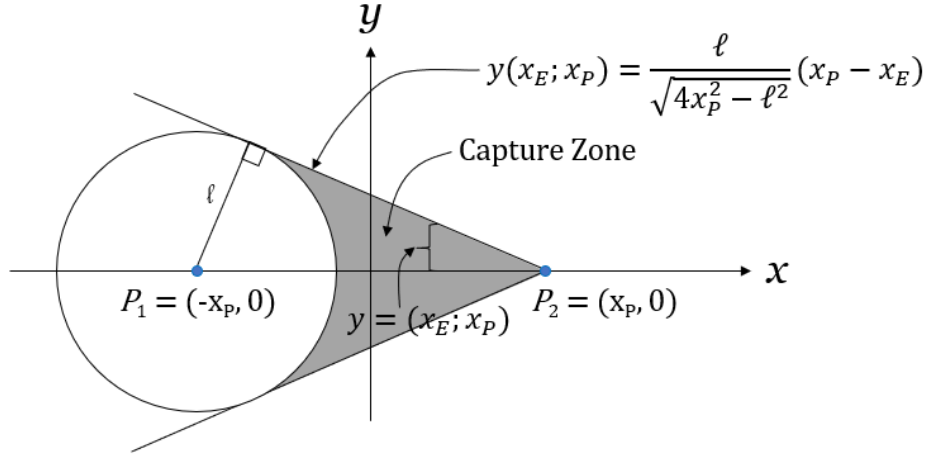
Figure 26: Capture Zone

$$y_E < y(x_E; x_P)$$

This means that the state is in the shaded region (Capture Zone). At the same time, the denominator in the y-equation is positive.

4.9   State Space

The axes of the rotating frame (x, y) are initially aligned with the (X, Y) axes of the realistic plane, and so Fig. 13 directly renders the capture zone in the realistic plane, given the positions of the Pursuers:

The two broken lines in Fig. 27, which form the boundary of the Capture Zone R_c, are not part of the Capture Zone. If the state (x_P, x_E, y_E) is on a broken line in the realistic plane (X, Y), E can escape by heading in the direction normal to the broken line; he might as well announce his course ahead of time and the Pursuers won't be able to catch up with him. When E is just below the upper-broken line/above the
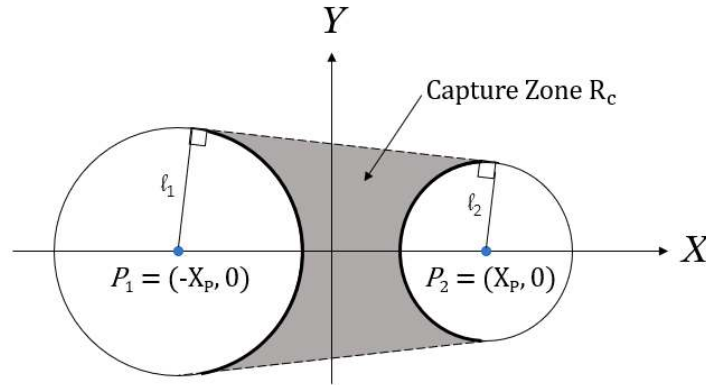
Figure 27: The Capture Zone in the Realistic Plane (X, Y)

lower-broken line, the time-to-capture is very long and it approaches infinity as E is (initially) closer to the broken line.

In the interior of the Capture Zone the optimal state feedback strategies of the players and the Value Function are determined by the solution of the quartic equation, which comes from squaring equation (8), or, if $\ell_2 = 0$, by the solution of the quadratic equation (16). Not so if in the realistic plane (X, Y), while in the Capture Zone, E is located on a thick line, which designates the circumference of a capture disk of P_1 or P_2. E is then in contact with one of the Pursuers. In this case, and as far as E is concerned, he is faced with the solution of a non-normal optimal control problem: During contact with a Pursuer's capture disk, E has no choice but to run away from the Pursuer. Concerning the Pursuer who is in contact with E, his optimal strategy is Pure Pursuit (PP) – he pushed against E. The second Pursuer goes on a collision course with E to meet E on the East-West opening of a hyperbola whose foci are P_1 and P_2, and the distance difference is $\ell_1 - \ell_2$. The Pursuers' optimal strategies are, as before, contingent on the solution of the quartic equation, derived from eqs. (8) and (6), or, if $\ell_2 = 0$, the solution of the quadratic equation (16).

Thus, the thick lines on the circumference of the capture disks which are on the boundary of the Capture Zone are included in the Capture Zone. When E is on a

thick line, the solution of the quartic equation yields Pursuer strategies which are Pure Pursuit (PP) for the Pursuer in contact with E and Collision Course (CC) guidance for the second Purser.

4.9.1 Reduced State Space (x_P, x_E, y_E)
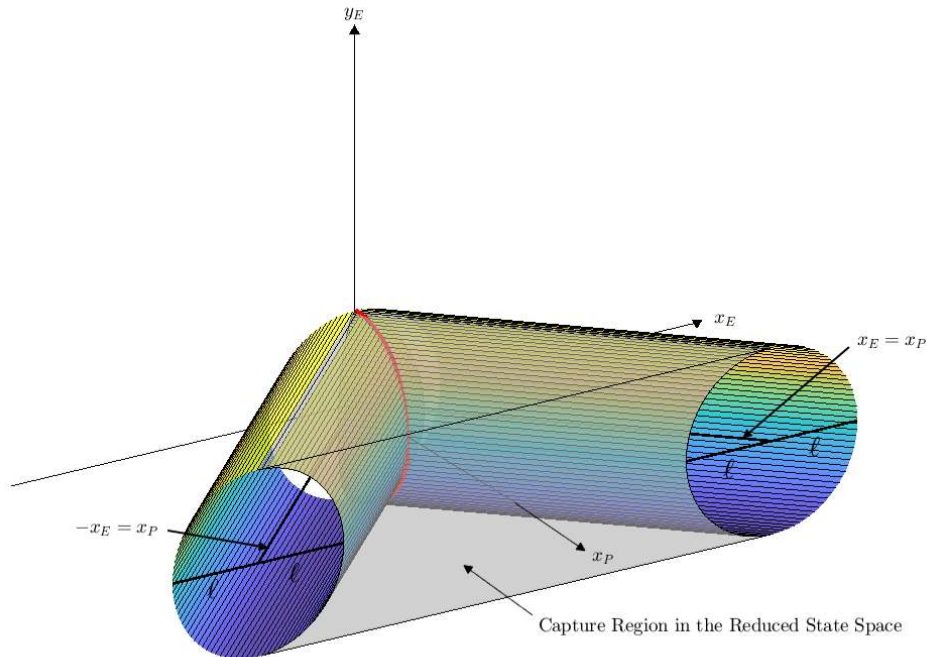
Figure 28: Reduced State Space. $\ell_1 = \ell_2 > 0$.

The 3-dimensional reduced state space, S, depicted in Fig. 28 when $\ell_1 = \ell_2 = \ell > 0$, is

$$S = \{(x_P, x_E, y_E)|x_P > 0\} \subset \mathbb{R}^3.$$

The Capture Zone R_c is defined in Fig. 28 by the 3-Dimensional shape whose reach in the direction of the y_E axis is delimited by the height ℓ of the cylinders and on the x_E axis by the surface of the cylinders. Due to symmetry, it is sufficient to consider

the first quadrant of $\mathbb{R}^3$

$$S_1 = \{(x_P, x_E, y_E)|x_P > 0, y_E \geq 0\},$$

and since $\ell_1 = \ell_2$, it is sufficient to consider the positive orthant of $\mathbb{R}^3$,

$$S_+ = \{(x_P, x_E, y_E)|x_P > 0, x_E \geq 0, y_E \geq 0\}.$$

The dimension of the reduced state space is 3, but when the speed ratio $\mu = 1$, and therefore isochronous capture is mandated, the terminal manifold is rank deficient: it is not of co-dimension 1, that is, it is not two-dimensional. The terminal manifold is now one-dimensional. It is a curve in the 3-D reduced state space – the red curve at the intersection of the two cylinders – see Fig. 28. And when the Pursuer P_2 relies on point capture, the terminal manifold shrinks to a point.

The optimal trajectories terminate at a point I where the two capture disks intersect – see Fig. 29. In the realistic plane, before capture of the Evader E, the
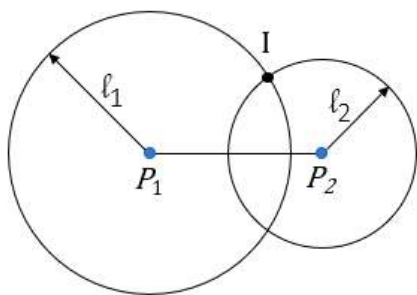
Figure 29: Point of Interception

geometry is shown in Fig. 30. Since the speed ratio $\mu = 1$, capture of E is only effected isochronously when both Pursuers, P_1 and P_2, come into contact with E. It is necessary that the Pursuers' capture disks come together. The capture disks intersect the first time when they just touch (from the outside) – see Fig. 31a. Because E can
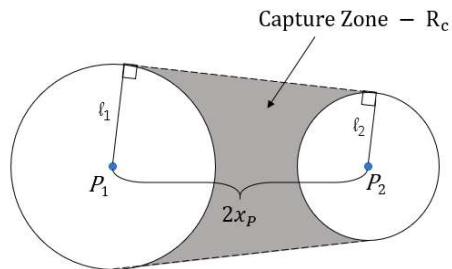
Figure 30: Point of Interception

only be isochronously captured by P_1 and P_2, the $P_1 - P_2$ separation $2x_P$ cannot be too big: From Fig. 31a we see that for capture to occur, we need

(a) First Contact   (b) Last Contact
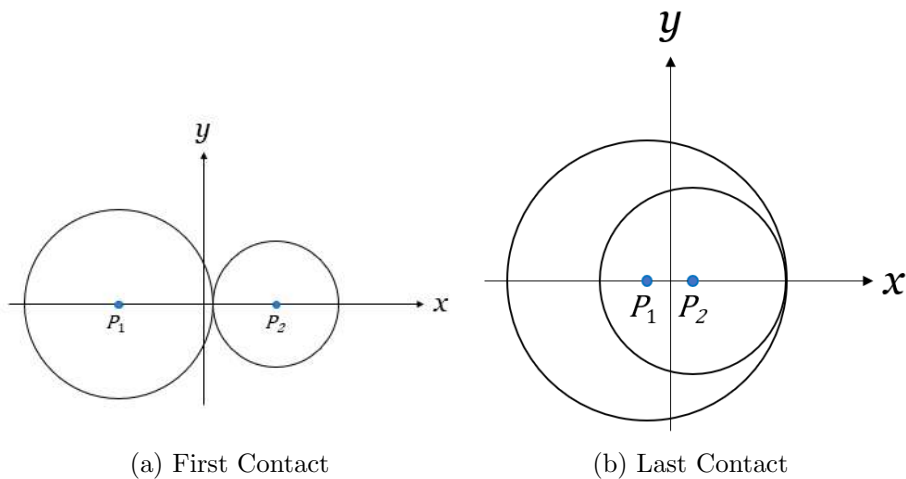
Figure 31: Contact of Capture Disks.

$$x_P \leq \frac{1}{2}(\ell_1 + \ell_2)$$

By the same token, P_1 and P_2 cannot be too close for isochronous capture to be possible. The critical configuration is shown in 31b. Thus it is necessary for

$$x_P \geq \frac{1}{2}(\ell_2 - \ell_1)$$

Now, in the reduced state space, isochronous capture occurs when the state

60

(x_p, x_E, y_E) is such that

$$(x_E + x_P)^2 + y_E^2 = \ell_1^2$$

$$(x_E - x_P)^2 + y_E^2 = \ell_2^2$$

Isochronous capture occurs on the terminal manifold which is now a curve in 3-D. This curve lies at the intersection of the above two-dimensional (red) orthogonal cylinders, as shown in Fig. 32. Thus, in parametric form this curve, in red, is

$$x_E(x_P) = \frac{1}{4x_P}(\ell_1^2 - \ell_2^2),$$

$$y_E(x_P) = \pm \sqrt{\ell_1^2 - \left[\frac{1}{4}(\ell_1^2 - \ell_2^2) \cdot \frac{1}{x_P} + x_P\right]^2}, \qquad \frac{1}{2}(\ell_1 - \ell_2) \le x_P \le \frac{1}{2}(\ell_1 + \ell_2)$$

(19)

The red curve at the intersection of the cylinders in Fig. 32 is the terminal manifold.
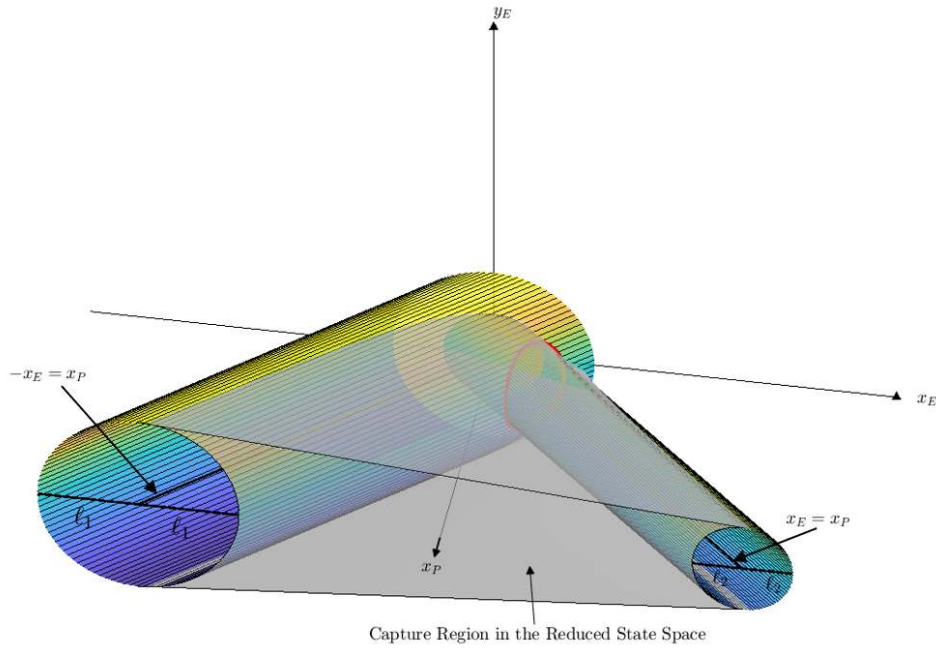
Figure 32: Capture Region in the Reduced State Space when $\ell_1 > \ell_2 > 0$.

When $\ell_1 = \ell_2 = \ell$, the terminal manifold is the curve:

$$x_E(x_P) = 0, \quad y_E(x_P) = \sqrt{\ell^2 - x_P^2}, \quad 0 \leq x_P \leq \ell.$$

It is the red curve shown in Fig. 33.
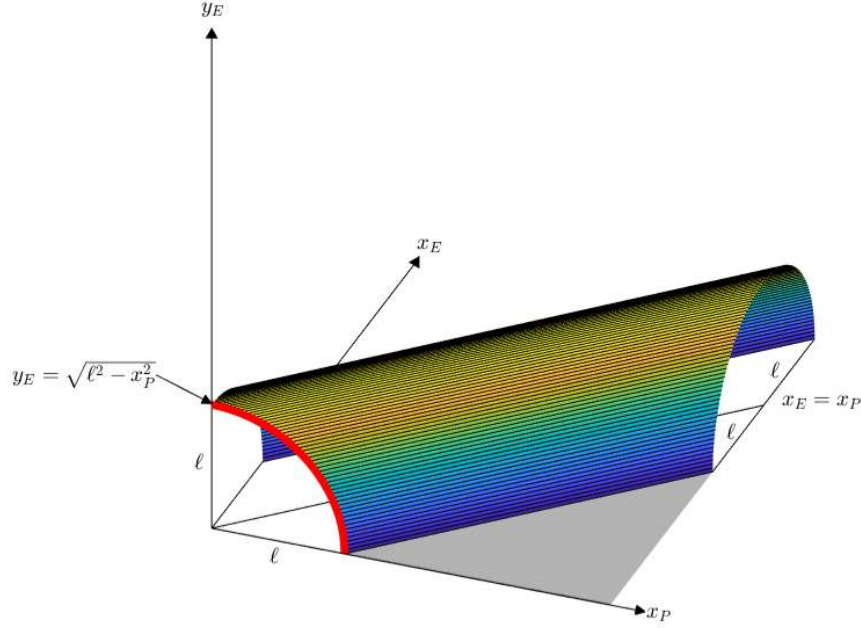
Figure 33: The Upper Part (in red) of the Terminal Manifold

When $\ell_2 = 0$, the terminal manifold shrinks to the point in 3-D space

$$x_P = \frac{1}{2}\ell_1, \quad x_E = \frac{1}{2}\ell_1, \quad y_E = 0,$$

and the reduced state space is shown in Fig. 34. The red dot is the terminal manifold.

The capture zone in the reduced state space (x_P, x_E, y_E) is delimited by two ruled surfaces formed by the tangents to the two capture circles at each fixed x_P, $x_P \geq \frac{1}{2}(\ell_2 - \ell_1)$. In our two-on-one pursuit-evasion differential game when the speed
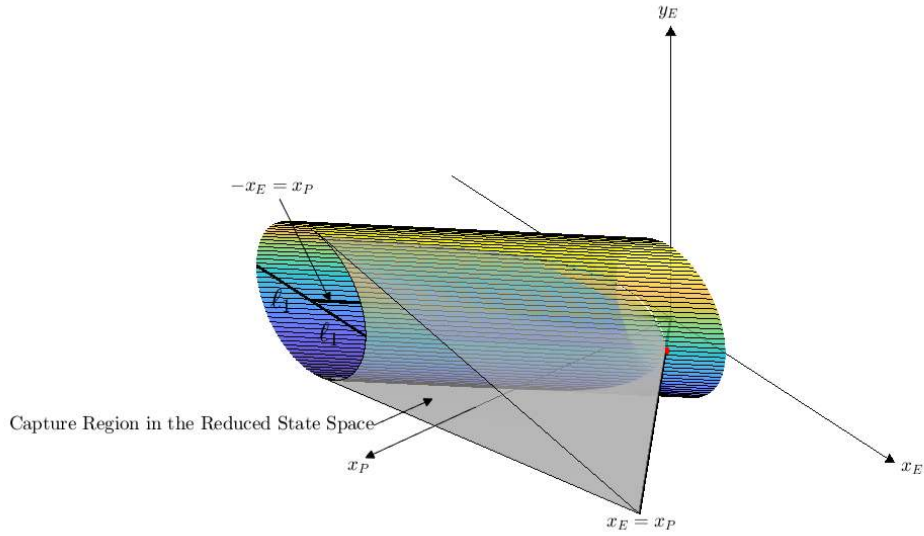
Figure 34: Reduced State Space with Terminal Manifold. $\ell_1 > \ell_2 = 0$.

ratio $\mu = 1$, the terminal manifold is a curve, and as such, dimension deficient. Hence, the terminal costate for optimal trajectories is

$$
\begin{pmatrix} \lambda_{x_P} \\ \lambda_{x_E} \\ \lambda_{y_E} \end{pmatrix} \Bigg|_{t_f} = -a \begin{pmatrix} \cos \xi \\ b \\ \sin \xi \end{pmatrix}, 0 \leq \xi \leq \frac{\pi}{2}, \quad a > 0,
$$

and for optimal trajectory in the positive orthant where $x_E \geq 0$, $b < 0$. This is similar to the situation in the Two Cutters and Fugitive Ship Differential Game [8] where the speed ratio $\mu \triangleq \frac{v_E}{v_P} < 1$, in the state space region where the Evader is isochronously captured by P_1 and P_2.

In the case where $\ell_1 > \ell_2 = 0$, the terminal manifold is reduced to a point. The

terminal costate is now

$$\left.\begin{pmatrix} \lambda_{x_P} \\ \lambda_{x_E} \\ \lambda_{y_E} \end{pmatrix}\right|_{t_f} = -a \begin{pmatrix} cos\ \xi \\ b \\ sin\ \xi \end{pmatrix}, 0 \le \xi \le \frac{\pi}{2}, \quad a > 0, \quad b \in \mathbb{R}.$$

Thus, the family of optimal trajectories is now parameterized by two parameters, ξ and $b \in \mathbb{R}$, and as such can cover the 3-D space.

It is important to note that the costates are the partial derivatives of the game's Value function $V(x_P, x_E, y_E)$, albeit with a negative sign, so

$$\lambda_{x_P}(t_f) = -V_{x_P}(t_f),$$

$$\lambda_{x_E}(t_f) = -V_{x_E}(t_f),$$

$$\lambda_{y_E}(t_f) = -V_{y_E}(t_f)$$

Lastly, we compare the (x_P, x_E, y_E) reduced state spaces when $\mu < 1$ and when $\mu = 1$. As derived in [2] and [8], the region in the reduced state space, where E is isochronously captured by P_1 and P_2 when $\mu < 1$ is delimited by the surface

$$y_E = \frac{x_P - x_E}{\mu x_P - x_E} \sqrt{\mu^2 \ell^2 - (\mu x_P - x_E)^2},$$

Combining the two equations above yields the cyan surfaces shown in Fig. 35, which are asymptotic to the planes $\pm x_E = \mu x_P$.

A cross-section of Fig. 35 is shown in Fig. 36. The shaded blue, hourglass-shaped region is the portion of the reduced state space in which, when the speed ratio $\mu < 1$, isochronous capture is guaranteed. The shaded gray region is the section of the reduced state space in which isochronous capture occurs when $\mu = 1$. Obviously, when $\mu < 1$, the region of capturability in the reduced state space is infinite, and

64
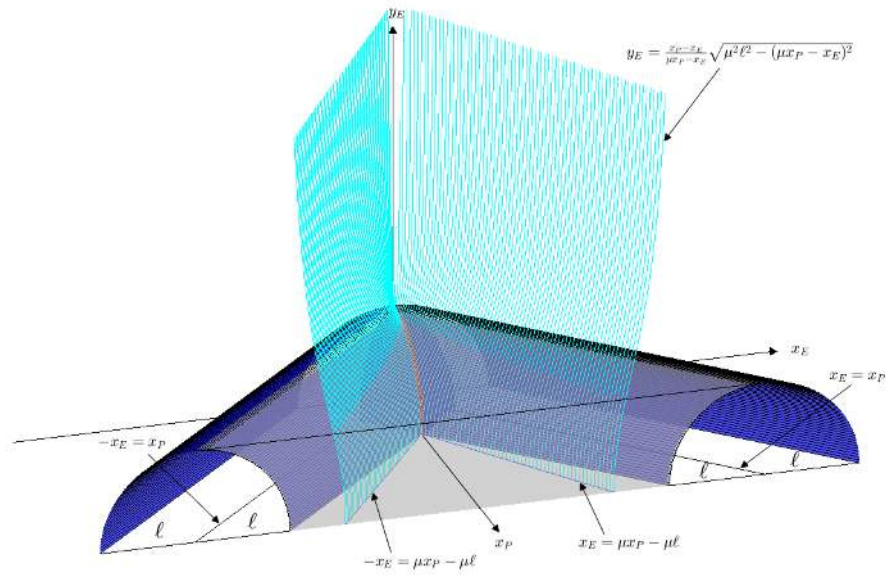
Figure 35: State Spaces Comparison: $\mu = 1$ and $\mu = \frac{\sqrt{2}}{2} < 1$, $\ell_1 = \ell_2 = \ell > 0$

thus, the winning region for the Pursuers is much larger than when the speed ratio $\mu = 1$, as expected.
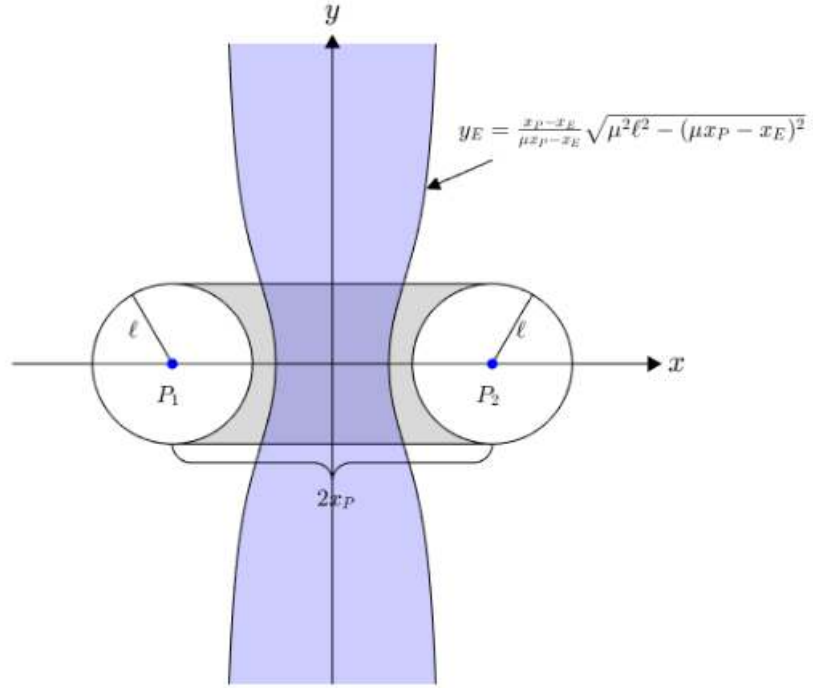
Figure 36: Cross-Section Comparison in the Reduced State Space: $\mu = 1$ and $\mu = \frac{\sqrt{2}}{2}$, $\ell_1 = \ell_2 = \ell > 0$, $x_P = 2$.

4.10 Cornered Rat

The pursuit-evasion differential game where an Evader is hemmed in between a Pursuer and a wall, a variation of the "Cornered Rat" scenario from [1], is considered – see Fig. 37. The Pursuer and Evader have simple motion/are holonomic, as usual, and the Pursuer and Evader now have the same speed; the speed ratio $\mu = \frac{v_E}{v_P} = 1$. The Purser's capture range $\ell > 0$. The following holds:

Theorem 2 *In the "Cornered Rat" game illustrated in Fig. 37, where the Pursuer's and Evader's speeds are equal, under optimal play, the Pursuer captures the Evader provided the latter is in the shaded region shown in Fig. 39. Capture is effected at the wall. The Pursuer's and Evader's optimal state feedback strategies for min-max*

66
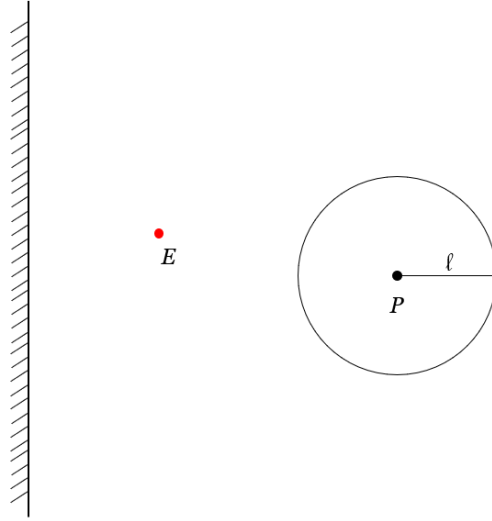
Figure 37: Cornered Rat, $\mu = 1$, $\ell > 0$

time-to-capture are given in Section 4.4.

Proof. Consider two-on-one pursuit with the speed ratio $\mu = 1$ and the Pursuers' capture ranges $\ell_1 = \ell_2 = \ell > 0$. We have the solution to the Game of Kind, given in Section 4.3 – see Fig. 27, reproduced herein as Fig. 38 for the special case where the two Pursuers' capture ranges are equal, as was the case in reference [17]. Since now $\ell_1 = \ell_2 = \ell$, the capture region (shaded) is as shown in Fig. 38.
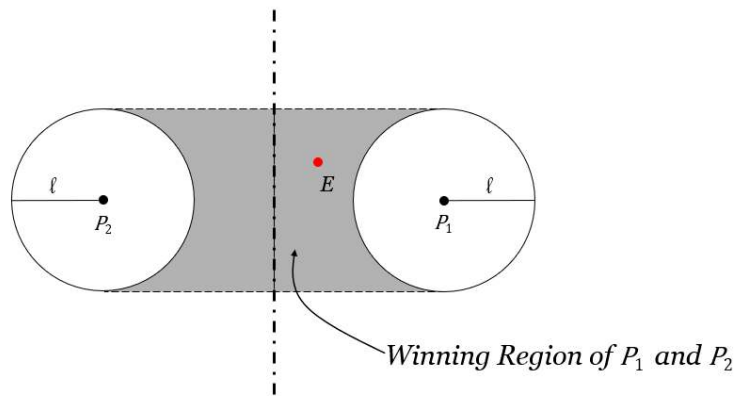
Figure 38: Solution to the Game of Kind, $\mu = 1$, $\ell > 0$

P_2, in conjunction with P_1, work to capture E in minimum time while E tries to

67

maximize the time-to-capture. We now assert that the presence of P_2 is equivalent to the presence of a wall at the orthogonal bisector of the segment $\overline{P_1 P_2}$, as shown in Fig. 39.
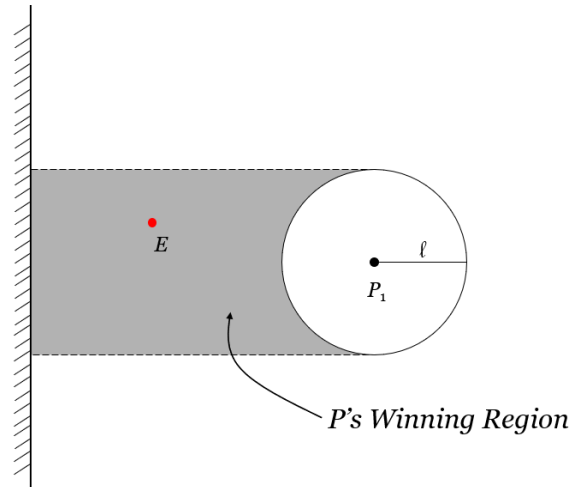
Figure 39: Cornered Rat Game of Kind, $\mu = 1$, $\ell > 0$

E has no hope of escaping P_1 (P in Fig. 37) by running away from P_1 in a Westerly direction because he then runs into the embrace of P_2. During optimal play by the Pursuers – P_1 and the virtual Pursuer P_2, which mirrors P_1's controls, the effect of a virtual wall halfway between P_1 and P_2 materializes. Hence, the optimal pursuit and evasion strategies derived in Section 4.4 are directly applicable to the Cornered Rat game when the speed ratio $\mu = 1$. Just as the Evader is captured in the Two-on-One pursuit-evasion differential game along the y axis when $\ell_1 = \ell_2 = \ell$, in our Cornered Rat game, the Evader/Rat is now captured with his back to the wall.

$\square$

An interesting special case ensues when the Evader is on the wall. The solution of Isaacs' Wall Pursuit differential game when the speed ratio $\mu = \frac{v_E}{v_P} = 1$ is as follows:

Corollary 3 *Consider the Wall Pursuit game where the Pursuer's and Evader's speeds are equal, $\mu = 1$, and the Pursuer is endowed with a capture disk of radius ℓ. If the Evader is in the shadow cast on the wall by the Pursuer's capture disk, he will be captured. Outside this narrow band, the Evader escapes by running along the wall. The Pursuer's optimal state feedback strategy is specified in Section 4.4.*

$\square$

4.11   Conclusion

The complete solution of the Two-on-One pursuit-evasion differential game where the players have simple motion, the speed of the Evader is equal to the speed of the Pursuers, and the two pursuers are endowed with capture disks of radii $\ell_1 > \ell_2 \geq 0$ is presented. Concerning the Game of Kind, in the case where one of the Pursuers resorts to point capture, that is, $\ell_2 = 0$, it was determined that, in the realistic plane, the Capturability Zone is the interior of the region between the tangents from P_2 to the capture disk of radius ℓ_1 of P_1. In this vein, for the case where $\ell_1 > \ell_2 > 0$, we conjecture that the Capturability Region in the realistic plane is the interior of the region between the two tangents to the Pursuers' capture disks. If the Evader is in this zone, his capture under optimal play by the two pursuers is guaranteed. If the Evader is on one of the tangent lines, capture is not possible, and the Evader's escape, by running in a direction normal to this line, is guaranteed. This was validated in interesting special cases, and numerically validated by simulation. The optimal pursuit and evasion state feedback strategies for the two Pursuers and the Evader are derived, thus providing the solution of the Game of Degree: Each player should travel toward an aim point I whose location is geometrically determined by the intersection of three hyperbolae as discussed in Section 4.4: the P_1, E hyperbola, P_2, E hyperbola, and the P_1, P_2 hyperbola. Computationally, this comes down to the solution of a

quartic equation and when $\ell_2 = 0$, it entails the solution of a quadratic equation. Lastly, we examined the geometry of the three-dimensional reduced state space of the Two-on-One pursuit-evasion differential game. In the Two-on-One differential game, the terminal "manifold" is rank deficient, it is a curve. It was explicitly determined, along with the terminal costates required for generating, in retrograde fashion, the optimal flow field in the reduced state space. The optimal trajectories/characteristics are a family of straight lines which fill the capture zone determined by the Game of Kind. There are no singular surfaces except the benign Evader's dispersal surface $\{(x_P, x_E, y_E) | \ x_P > 0, y_E = 0\}$. The complete solution of the Two-on-One pursuit-evasion differential game when the Evader is as fast as the pursuers has been obtained.

V. Pure Pursuit of an Equal Speed Evader

5.1 Abstract

The classical problem of pure pursuit is revisited. The off-the-beaten path case is considered where the Pursuer's speed is equal to the speed of the Evader, whereupon the terminal separation between the Pursuer and Evader must be less than the capture range l to ensure capture. The instance where two pursuers are at work is then considered, and conditions are given that determine if capture of the Evader is possible, and if so, the solution of the Evader's optimal control problem of maximizing the time-to-capture is provided.

5.2 Introduction

This research is motivated by the work of Rufus Isaacs, who in 1951 started developing the theory of differential games, with an emphasis on pursuit-evasion [1]. In his work, he discussed strategies for minimum time capture in the face of Evader maneuvers. It is often times stipulated that the protagonists have simple motion/are holonomic, that is, they can instantaneously choose their heading. Also of interest are Pure Pursuit (PP) scenarios in which the Pursuer instantaneously directs his/her heading toward the Evader for all time. Pure pursuit when the Pursuer is faster than the Evader has been considered since the 18th century [4], [5] but closed form solutions have been obtained only for the case where the Pursuer is initially abeam of the Evader. Only fairly recently have Barton and Eliezer [6] developed an analytical solution for the Pursuer's path in a PP scenario where the Evader's course is not restricted to being perpendicular to the initial line of sight. Also, point capture is exclusively considered. This paper first revisits the pursuit problem discussed in [6], with the provision that the Pursuer is endowed with a capture circle of radius l. In

71

this paper, an extension of the work from [6] is undertaken to derive a closed form solutions for the case where the speed ratio $\mu \triangleq \frac{V_E}{V_P} = 1$, which so far has not been considered in the context of PP.

5.3   Course-Holding Evader

It is assumed that the Evader (E) holds the course θ, thus moving along a straight-line in the realistic plane (x,y), as depicted in Figure 40, while the Pursuer (P) starts at the origin. The initial P-E separation is d. The speed ratio μ is defined as the ratio of the Evader's speed V_E to the Pursuer's speed V_P, $\mu \triangleq \frac{V_E}{V_P}$. It is customarily stipulated that the speed ratio $\mu < 1$, a standard assumption in the pursuit-evasion literature.
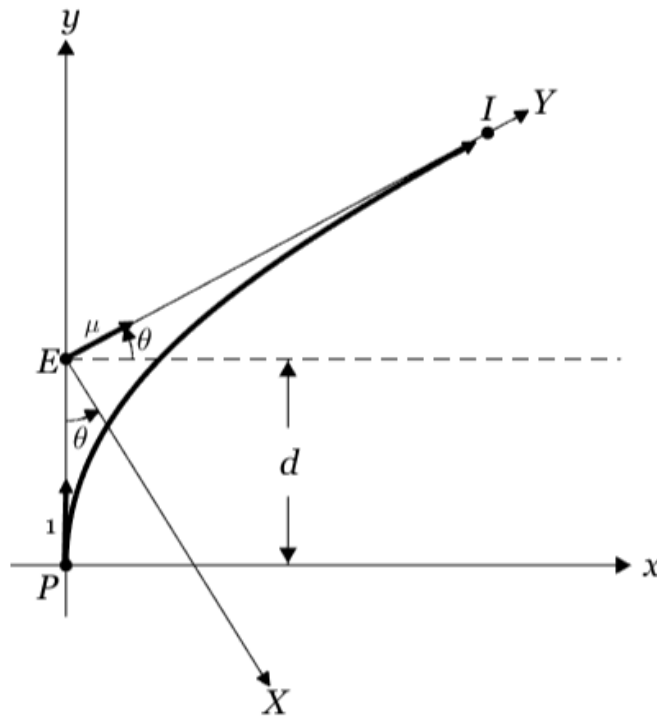

Figure 40: Pure Pursuit Curve. $d = 1$, $\theta = \frac{\pi}{6}$, $\mu = 0.9$.

Without loss of generality set the Pursuer's speed at 1, so the Evader's speed is μ.

The coordinates of the Evader in the (x,y) frame, when his course angle is θ, are $(\mu\ t\ cos\ \theta, d + \mu\ t\ sin\ \theta)$.

Barton and Eliezer [6] analytically derived a formula for the position of the Pursuer along the pursuit curve using a rotated frame (X,Y), where the Y-axis is aligned with the Evader's path, as shown in Figure 40. The pursuit curve in the (X,Y) frame is:

$$\frac{Y_P}{h} = \frac{\mu}{1 - \mu^2}(sec\ \theta + \mu\ tan\ \theta) + \frac{1}{2}\left\{\frac{1}{1 + \mu}w\left(\frac{X_P}{h}\right)^{1+\mu} - \frac{1}{1 - \mu}w^{-1}\left(\frac{X_P}{h}\right)^{1-\mu}\right\} \quad (20)$$

where

$$w \triangleq sec\ \theta - tan\ \theta.$$

$$h = d\ cos\ \theta$$

Using (20), the time of point capture t_c is determined by setting in eq. (20) $X_P = 0$. Since $t_c = \frac{Y_P(X_P=0)}{\mu}$, the capture time

$$t_c = \frac{1}{1 - \mu^2}(1 + \mu\ sin\ \theta)d\ , \quad (21)$$

The aspect angle at the time capture is 0 – the Pursuer captures the Evader from behind.

Eq. (20) allows us to explore the relationship between the capture time, the heading angle θ, and the speed ratio μ. As Figure 41 shows, the capture time is monotonically increasing in θ; to outrun the Pursuer, the Evader must turn away from the Pursuer.

Unfortunately, when the speed ratio $\mu = 1$, eq. (20) is not applicable.
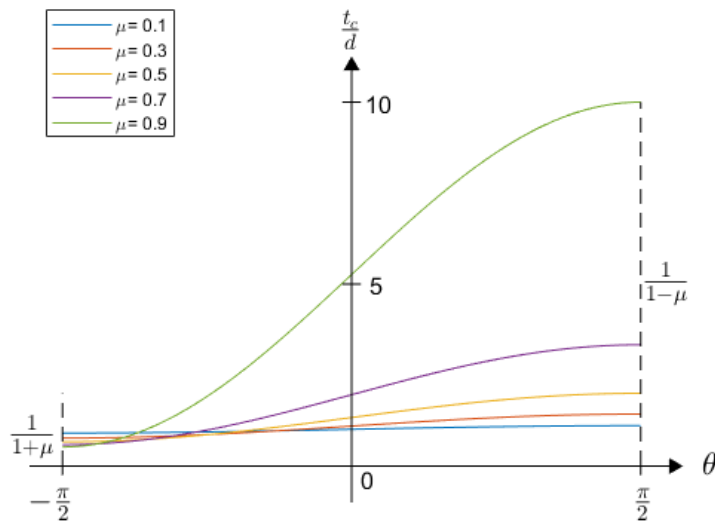
Figure 41: Capture Time vs θ for $\mu < 1$.

5.4 Pure Pursuit when the Speed Ratio $\mu = 1$

5.4.1 Single Pursuer

A PP strategy will always result in failure to capture the Evader. However, if the Pursuer is endowed with a capture circle of radius l, the Evader may be captured if he must hold course and does not flee directly away from the Pursuer, or if more than one Pursuer gives chase. During PP, the *P-E* distance is monotonically decreasing, and it asymptotically settles on a constant distance behind the Evader, except if E runs away from P whereupon the initial *P-E* separation does not change.

Point capture is now out of the question. To capture a course-holding Evader, the Pursuer must be endowed with a capture disk of radius $l > 0$. In order to determine if capture is possible, we must first determine the limiting separation r between the Pursuer and Evader as time approaches infinity. Since the two players are traveling at the same speed, they will asymptotically achieve a final *P-E* separation r_∞, P trailing behind E. The following holds.

Proposition 4 *If P engages in PP and the speed ratio is μ=1, point capture is not possible. If E holds the course θ, the pursuit always ends with a tail chase where asymptotically P maintains a constant distance r_∞ behind E,*

$$r_\infty(\theta) = \frac{1 + \sin\theta}{2} r_0. \tag{22}$$

Proof. When the speed ratio $\mu = 1$, (20) does not hold. To determine the terminal miss distance r_∞, we must derive ab initio the pursuit curve when the speed ratio $\mu = 1$. To do so, we use polar coordinates (r, ϕ), which specify E's position relative to P, and start with the equations of motion – see Figure 42 –

$$\dot{r} = -1 + \cos(\phi - \theta) \tag{23}$$

$$\dot{\phi} = -\frac{1}{r}\sin(\phi - \theta) \tag{24}$$

with initial conditions $r(0) = r_0$, $\phi(0) = \pi/2$. Figure 42 provides a visual representation at two instantaneous points in time that show the change in distance and bearing of E as time increases. The axes (X,Y) represent a stationary, inertial frame, while the moving frame's axes (X_0, Y_0), (X_1, Y_1) are centered on the Pursuer's instantaneous position but remain aligned with the inertial (X,Y) frame. We must solve the system of differential equations (23) and (24) to get an analytical solution for the path of the Pursuer.

E's bearing ϕ is monotonically decreasing, so we divide eqs. (23) and (24):

$$\frac{1}{r}\frac{dr}{d\phi} = \frac{1 - \cos(\phi - \theta)}{\sin(\phi - \theta)} \tag{25}$$

The solution by separation of variables of the differential equation (25) is reduced to an integration. E's bearing ϕ is such that $\theta \leq \phi \leq \pi/2$. Integrating both sides of the
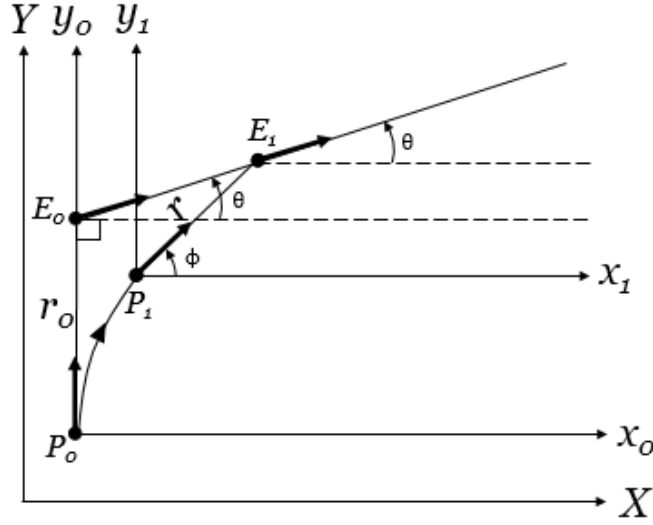
Figure 42: Pursuit Curve Determination Using Polar Coordinates.

differential equation (25) yields

$$ln\left(\frac{r(\phi)}{r_0}\right) = \int_{\pi/2}^{\phi} \frac{1 - cos(\phi - \theta)}{sin(\phi - \theta)} d\phi. \tag{26}$$

To obtain $r(\phi)$, we introduce the function

$$I(\phi) \triangleq -\int_{\pi/2-\theta}^{\phi-\theta} \frac{1 - cos\ x}{sin\ x} dx.$$

The integral

$$\int \frac{1 - cos\ x}{sin\ x} dx = -ln(1 + cos\ x),$$

so

$$I(\phi) = ln\left(\frac{1 + cos(\phi - \theta)}{1 + sin\ \theta}\right). \tag{27}$$

We relate (26) and (27) to get

$$ln\left(\frac{r(\phi)}{r_0}\right) = -ln\left(\frac{1 + cos(\phi - \theta)}{1 + sin\ \theta}\right) \tag{28}$$

76

which yields the pursuit curve in polar form when the speed ratio is $\mu = 1$ and E's course θ, $-\frac{\pi}{2} < \theta \leq \frac{\pi}{2}$, is arbitrary, and not necessarily $\theta = 0$:

$$r(\phi) = \frac{1 + sin\ \theta}{1 + cos(\phi - \theta)} r_0, \quad \theta \leq \phi \leq \pi/2. \tag{29}$$

With (29), we can determine the asymptotic P-E separation r_∞ by evaluating (29) at $\phi = \theta$. The terminal miss distance is

$$r_\infty(\theta) = \frac{1 + sin\ \theta}{2} r_0.$$

$\square$

If the Pursuer is endowed with a capture radius $l > r_\infty$, the course-holding Evader will be captured. Thus, the following holds

Corollary 5 *If the initial P-E separation is r_0 and the Evader holds the course θ, $-\frac{\pi}{2} \leq \theta < \frac{\pi}{2}$, he/she will be captured by an equal speed Pursuer P which employs PP, provided the Pursuer is endowed with a capture circle of radius*

$$\frac{1}{2}(1 + sin\ \theta)\ r_0 < l < r_0. \tag{30}$$

$\square$

To determine r with respect to time we must first determine the function $\phi(t)$, namely, the temporal behavior of the bearing angle ϕ. To this end, we insert eq. (29) into eq. (24):

$$\frac{d\phi}{dt} = -\frac{1}{1 + sin\ \theta} \frac{1}{r_0}[1 + cos(\phi - \theta)]sin(\phi - \theta), \tag{31}$$

77

and so

$$\frac{1}{r_0}\frac{1}{1+sin\ \theta}t = -\int_{\pi/2}^{\phi}\frac{d\phi}{[1+cos(\phi-\theta)]sin(\phi-\theta)}$$

that is

$$\frac{1}{r_0}\frac{1}{1+sin\ \theta}t = -\int_{\pi/2-\theta}^{\phi-\theta}\frac{dx}{[1+cos(x)]sin(x)}. \tag{32}$$

Upon integrating, we get

$$\frac{1}{r_0}\frac{1}{1+sin\ \theta}t = \frac{1}{4}\left[\frac{1}{cos^2(\frac{\pi}{4}-\frac{\theta}{2})}-\frac{1}{cos^2(\frac{\phi}{2}-\frac{\theta}{2})}\right] - \frac{1}{2}\ ln\left(\frac{tan(\frac{\phi}{2}-\frac{\theta}{2})}{tan(\frac{\pi}{4}-\frac{\theta}{2})}\right),$$

which gives

$$t = r_0(1+sin\ \theta)*\left\{\frac{1}{4}\left[\frac{1}{cos^2(\frac{\pi}{4}-\frac{\theta}{2})}-\frac{1}{cos^2(\frac{\phi}{2}-\frac{\theta}{2})}\right] - \frac{1}{2}\ ln\left(\frac{tan(\frac{\phi}{2}-\frac{\theta}{2})}{tan(\frac{\pi}{4}-\frac{\theta}{2})}\right)\right\}. \tag{33}$$

Equation (33) provides t as a function of ϕ, given θ and r_0. Plotting (33) for a fixed θ and r_0 gives the plot shown in Figure 43.
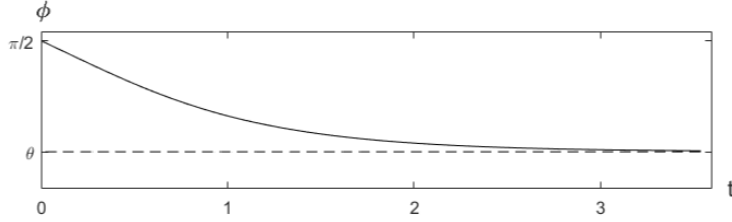

Figure 43: $r_0 = 1$, $\theta = \frac{\pi}{8}$. The Function $\phi(t)$ is Monotonically Decreasing.

We can now calculate r($\phi(t)$), which will allow us to get the equation of the pursuit curve in parametric form. First, we define:

$$a(t) \triangleq r(\phi(t))cos(\phi(t))$$

$$b(t) \triangleq r(\phi(t))sin(\phi(t))$$

78

Next, we map the pursuit curve into the Cartesian frame (X,Y):

$$X_P(t) = t \ cos \ \theta - a(t)$$

$$Y_P(t) = r_0 + t \ sin \ \theta - b(t)$$

where $t \geq 0$. The pursuit curve in the Cartesian plane (X,Y) can also be parameterized in terms of ϕ:

$$X_P(\phi) = t(\phi) \ cos \ \theta - r(\phi) \ cos \ \phi \tag{34}$$

$$Y_P(\phi) = r_0 + t(\phi) \ sin \ \theta - r(\phi) \ sin \ \phi, \tag{35}$$

where $t(\phi)$ is given by eq. (33) and $\theta \leq \phi \leq \pi/2$. Combining (29), (33), (34), and (35) produces equations parameterized by ϕ that describe the pursuit curve in the realistic plane (X,Y). In the classical case where $\theta = 0$, the pursuit curve in parametric form is

$$X_P(\phi) = -\frac{1}{2} \left[\frac{cos \ \phi}{1 + cos \ \phi} + ln \left(tan \left(\frac{\phi}{2} \right) \right) \right] r_0$$

$$Y_P(\phi) = \left(1 - \frac{sin \ \phi}{1 + cos \ \phi} \right) r_0, \ 0 < \phi \leq \frac{\pi}{2}.$$

We calculate

$$\frac{sin \ \phi}{1 + cos \ \phi} = tan \left(\frac{\phi}{2} \right)$$

$$\frac{cos \ \phi}{1 + cos \ \phi} = \frac{1}{2} \left[1 - tan^2 \left(\frac{\phi}{2} \right) \right].$$

Now

$$\frac{Y_P}{r_0} = 1 - tan \left(\frac{\phi}{2} \right)$$

79

and thus

$$tan\left(\frac{\phi}{2}\right) = 1 - \frac{Y_P}{r_0}.$$

Hence when $\mu = 1$ and $\theta = 0$ the classical pursuit curve in Cartesian coordinates is

$$\frac{X_P}{r_0} = -\frac{1}{2}\left\{\frac{1}{2}\left[1 - \left(1 - \frac{Y_P}{r_0}\right)^2\right] + ln\left(1 - \frac{Y_P}{r_0}\right)\right\},$$

which simplifies to

$$\frac{X_P}{r_0} = -\frac{1}{2}\left[\frac{Y_P}{r_0} - \frac{1}{2}\left(\frac{Y_P}{r_0}\right)^2 + ln\left(1 - \frac{Y_P}{r_0}\right)\right] \tag{36}$$

Equation (36) allows us to plot the pursuit curve in the Cartesian frame (X,Y) when E's course $\theta = 0$ and $\mu = 1$ – see Figure 44.
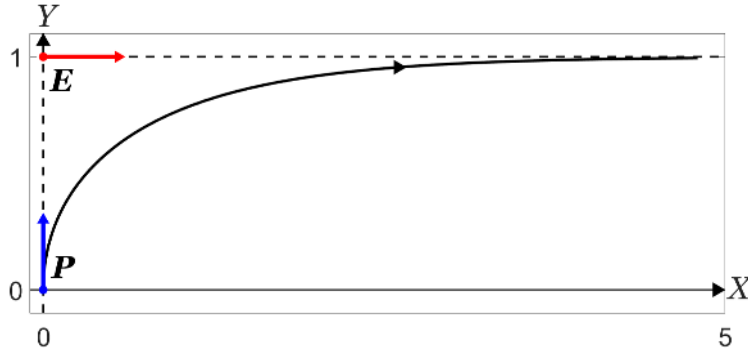

Figure 44: $\theta = 0$. Pursuit Curve in the Cartesian Frame (X,Y) when $\mu = 1$.

Using Corollary 5, we can establish the condition which guarantees that a course-holding Evader can escape when $\mu = 1$: If his/her course angle

$$\theta > Asin\left(2\frac{l}{r_0} - 1\right), \tag{37}$$

the Evader will escape the single Pursuer. Figure 45a depicts the conical safe region,

delimited by a critical angle A,

$$A \triangleq Asin(2\frac{l}{r_0} - 1),$$

in the case where the pursuer's capture range l is greater than half of r_0. In this case, the Escape Cone is convex. Heading into the Escape Cone allows E to escape. If the capture range l is less than half of r_0, the Escape Cone is no longer convex (Figure 45b) where the critical angle $A = Asin\left(1 - 2\frac{l}{r_0}\right)$.

(a) $r_0 > l > \frac{r_0}{2}$ (b) $l < \frac{r_0}{2}$
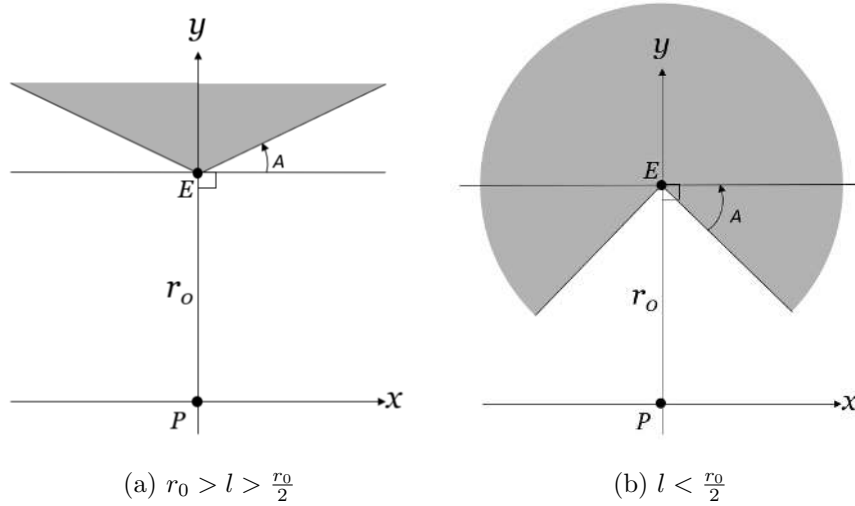
Figure 45: Escape Cones

5.4.2 Two Pursuers

Consider now the pursuit scenario with two pursuers in PP, but the speed ratio $\mu = 1$, as shown in Figure 46. The state is (r_1, r_2, φ). First, we will assume that the capture ranges of the pursuers are such that $l_i > \frac{r_i}{2}$, $i = 1, 2$; thus, the critical angles are $A_i = Asin\left(2\frac{l_i}{r_i} - 1\right)$, $i = 1, 2$ and both Escape Cones will be convex.

We analyze the game from the perspective of each player. Using the theory developed in Section 5.4.1, we determine the Escape Cones with respect to each Pursuer,

Figure 46: The State of the Game When There Are Two Pursuers.

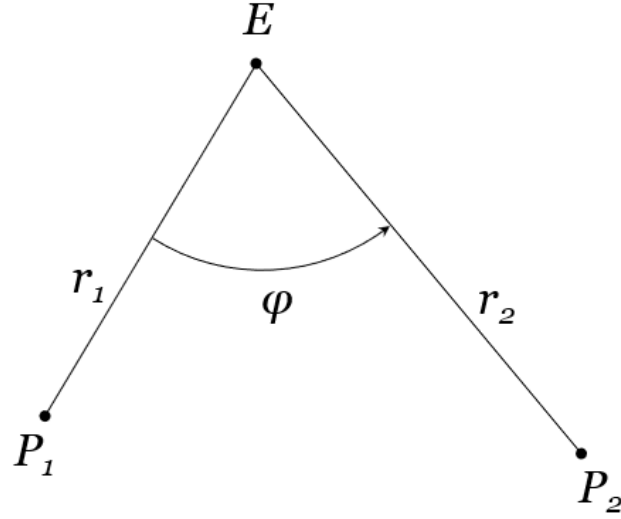as illustrated in Figure 47. The shaded black region C_1 and the shaded blue region C_2 are the Escape Cones from P_1 and P_2, respectively. If E chooses a straight-line trajectory within C_2, it will escape from P_2. However, the same trajectory will result in capture by P_1. Thus, for escape to be possible, there must be a region where the two Escape Cones intersect:

$$C_1 \cap C_2 \neq \emptyset. \tag{38}$$

If the condition (38) holds, the Evader can escape both pursuers by heading into the cone $C_1 \cap C_2$ and holding course. If however $C_1 \cap C_2 = \emptyset$, capturability is guaranteed, irrespective of what E does.

Concerning capturability, for $C_1 \cap C_2 = \emptyset$, the following geometric condition must hold – see Figure 47:

$$\varphi > \frac{\pi}{2} - A_1 + \frac{\pi}{2} - A_2, \tag{39}$$
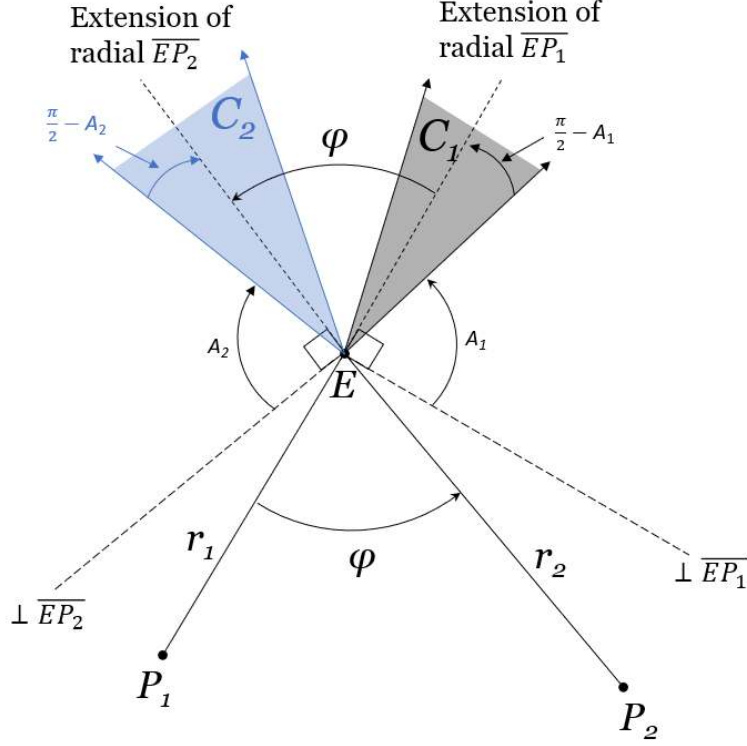
Figure 47: Escape Cones when $l_i > \frac{r_i}{2}$, $i = 1, 2$.

where, recall, we have $A_i = Asin\left(2\frac{l_i}{r_i} - 1\right)$, $i = 1, 2$. The following holds,

Theorem 6 *When two pursuers using PP and endowed with circular capture disks with radii l_i, $i = 1, 2$, are after an Evader, the speed ratio $\mu = 1$, and the initial configuration/state (r_1, r_2, φ) is as shown in Figure 46, capture will be effected, if and only if the Pursuers' lethal ranges $\frac{r_1}{2} < l_1 < r_1$, $\frac{r_2}{2} < l_2 < r_2$ are such that*

$$Asin(2\frac{l_1}{r_1} - 1) + Asin(2\frac{l_2}{r_2} - 1) > \pi - \varphi. \tag{40}$$

$\square$

Consider now the case where the capture range of the first Pursuer is such that $l_1 < \frac{r_1}{2}$, while the second Pursuer's capture range satisfies $l_2 > \frac{r_2}{2}$; this scenario is depicted in

Figure 48. In this case, the Escape Cones C_1 and C_2 will intersect and consequently escape will be possible if

$$Asin\left(2\frac{l_2}{r_2} - 1\right) - Asin\left(1 - 2\frac{l_1}{r_1}\right) < \pi - \varphi. \tag{41}$$

The Evader will head into the cone $C_1 \cap C_2$; he/she might as well hold course.
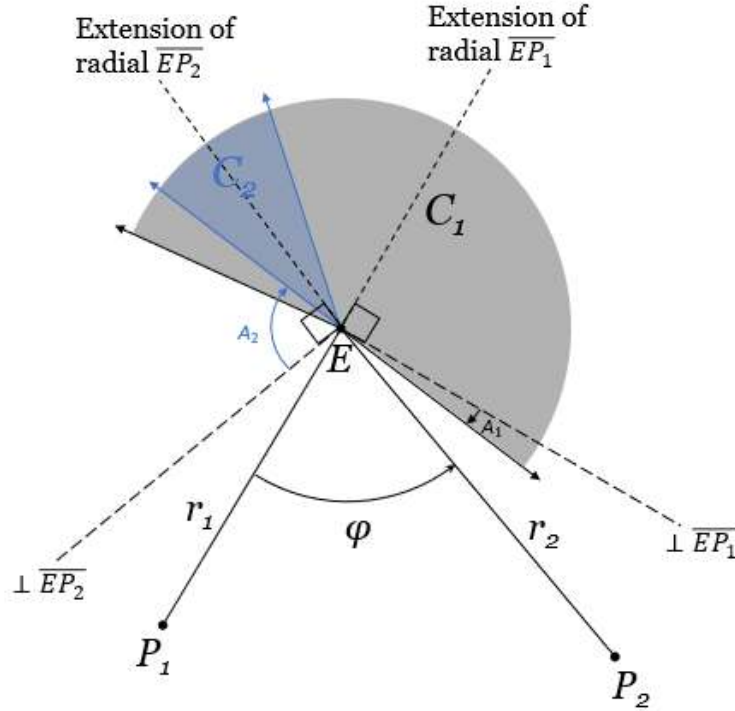
Figure 48: Escape Cones when $l_1 < \frac{r_1}{2}$, $r_2 > l_2 > \frac{r_2}{2}$.

If both capture circles have a smaller diameter than the initial range r_0, then E can escape $\forall\ 0 \le \varphi \le \pi$, $r_1 > l_1$, $r_2 > l_2$. Figure 49 shows an example in which $l_1 < \frac{r_1}{2}$, $l_2 < \frac{r_2}{2}$:

At the same time, in the special case where the initial configuration is such that $\varphi = \pi$ (Figure 50) where E is hemmed in by P_1 and P_2, assuming $l_i > \frac{r_i}{2}$, capture is inevitable. Referencing (39), we know that if $\varphi = \pi$, the right side of the equation is 0, while the left side will be greater than zero.

84

Figure 49: Escape Cones when $l_i < \frac{r_i}{2}$, $i = 1, 2$.

Figure 50: The State of the Game when $\varphi = \pi$.

If $\varphi = \pi$ but $l_1 > \frac{r_i}{2}, l_2 < \frac{r_i}{2}$ (Figure 51), then for capture to be possible the following condition must hold $A_1 > A_2$, that is
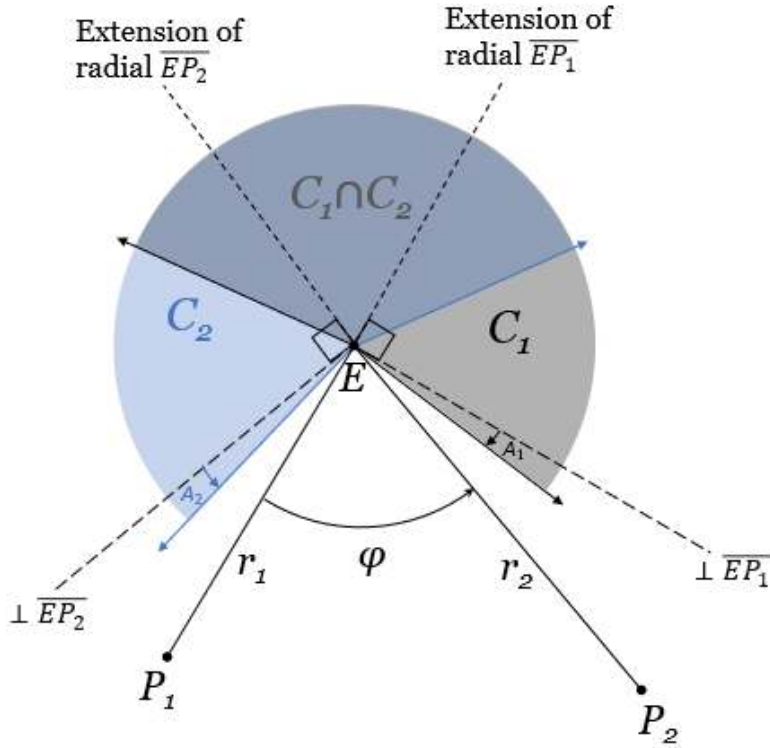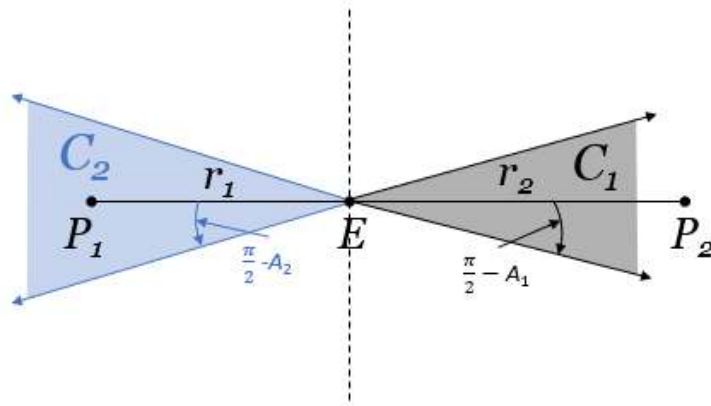
$$Asin\left(2\frac{l_1}{r_1} - 1\right) > Asin\left(1 - 2\frac{l_2}{r_2}\right). \tag{42}$$
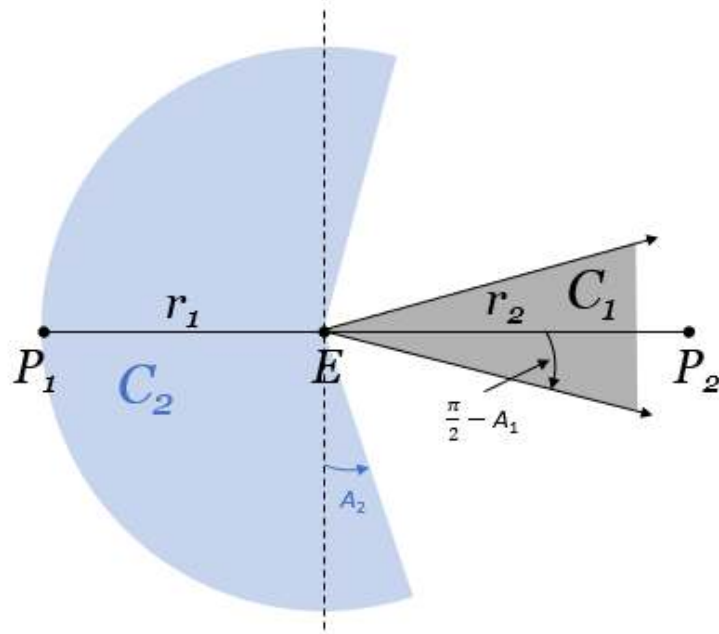
Figure 51: Escape Cones when $\varphi = \pi$, $r_1 > l_1 > \frac{r_1}{2}$, $l_2 < \frac{r_0}{2}$.

Lastly, if both capture radii are less than $\frac{r_i}{2}$, then $C_1 \cap C_2 \neq \emptyset$, and E can escape by heading into the sector formed by the intersection of the two Escape Cones.

5.5 Conclusion

The interception in pure pursuit of a course-holding Evader whose speed equals the speed of the Pursuer is considered. The pure pursuit curve in which the Pursuer and Evader have equal speed is analytically derived. For capture to occur, the Pursuer must be endowed with a capture disk of radius l, as point capture is not possible when the speed ratio is $\mu = 1$. If the capture range l is greater than the asymptotic separation between the Pursuer and Evader, as specified in Corollary 5, capture is possible. This result was applied to a two-on-one pursuit evasion scenario where the speed ratio $\mu = 1$. Necessary and sufficient conditions for capture were obtained for two-on-one engagement.

VI. Pure Pursuit in Defense of a Target

6.1 Abstract

A target-defense scenario is considered where an attacker heading toward the target is to be intercepted by a defender in Pure Pursuit (PP). The case where the target defender's speed is greater than the attacker's is analyzed and the result is compared to the outcome when an optimal interception strategy is used in defense of a target. The case is also considered where the attacker's speed is equal to the speed of the defender, but the defender is endowed with a capture disk of radius l. Necessary and sufficient conditions are given that determine if capture in PP of the attacker before he reaches the target is possible.

6.2 Introduction

A target-defense scenario where a Defender (D) is tasked with guarding a Target (T) coming under attack from an Attacker (A) is considered. The protagonists A and D have simple motion à la Isaacs/are holonomic and the Target is a point target. A wants to come as close as possible to T and perhaps reach T, whereas D strives to intercept A as far away from T as possible. The solution of this differential game was provided by Isaacs [1]: if A and D have the same speed, they both head toward the aim point I, which is the point on the orthogonal bisector of the $\overline{AD}$ segment which is closest to T. In this paper, the scenario where A heads straight toward the Target and D employs Pure Pursuit (PP) is considered. The objective is to determine the region in the plane wherefrom A can reach T before being intercepted by D. The kinematics of Pure Pursuit (PP) have been studied since the 18th century [4],[5], but closed form solutions were developed under the assumption that the Pursuer (P) was faster than the Evader (E), who initially traveled abeam of the Pursuer. Only fairly

87

recently [6] has the pursuit curve been derived for the case where the Evader is not necessarily initially abeam of the fast Pursuer. We build on the results obtained in [6] and also consider the case where the speed of the Evader is equal to the speed of the Pursuer.

This paper first revisits Pure Pursuit (PP) of a course-holding Evader where the speed ratio $\mu \triangleq \frac{V_A}{V_D} < 1$, as in [4]–[6], and applies the closed form formula for a pursuit curve developed in[6] to the target-defense scenario. The target-defense scenario in which the speed ratio $\mu = 1$, as in Isaacs' target-defense differential game, and, in addition, the Defender is endowed with a capture disk of radius l, and employs PP, is investigated.

6.3 Pure Pursuit of Course-Holding Evader

Consider the case when an Evader (E) holds the course θ, thus moving along a straight-line in the realistic plane (x,y), as depicted in Fig. 52, while the Pursuer (P) starts at the origin. In the literature, it is customarily assumed that E's course $\theta = 0$, but in [6] it is allowed for $-\frac{\pi}{2} \leq \theta \leq \frac{\pi}{2}$. The initial P-E separation is d. The speed ratio parameter μ is defined as the ratio of the Evader's speed V_E to the Pursuer's speed V_P, $\mu \triangleq \frac{V_E}{V_P}$. It is customarily stipulated that the speed ratio $\mu < 1$, a standard assumption in the pursuit-evasion literature.

Without loss of generality set the Pursuer's speed at 1, so the Evader's speed is μ. The trajectory of the Evader in the (x,y) frame, where his course angle is θ, is $(\mu\ t\ cos\ \theta, d + \mu\ t\ sin\ \theta)$.

Barton and Eliezer [6] analytically derived a formula for the pursuit curve using a rotated frame (X,Y), where the Y-axis is aligned with the Evader's path, as shown in Fig. 52. The Pursuer's position in the (X,Y) frame is (X_P, Y_P) and the pursuit
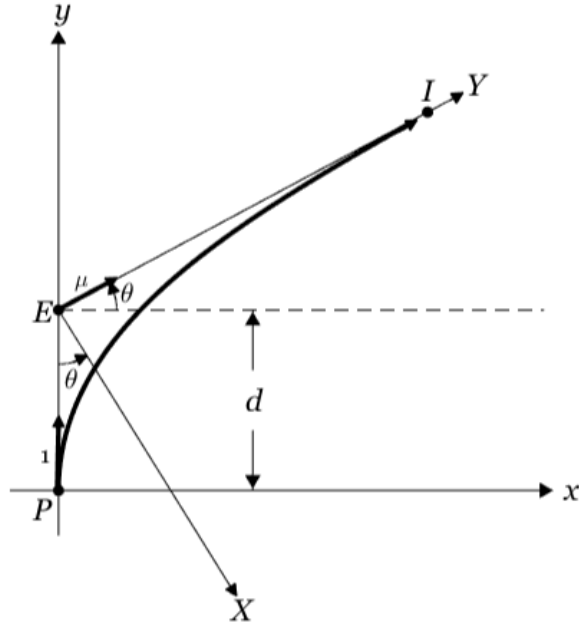
Figure 52: Capture Occurs at Point I – Point Capture

curve $Y_P(X_P)$ is:

$$\frac{Y_P}{h} = \frac{\mu}{1-\mu^2}(sec\ \theta + \mu\ tan\ \theta) + \frac{1}{2}\left\{\frac{1}{1+\mu}w\left(\frac{X_P}{h}\right)^{1+\mu} - \frac{1}{1-\mu}w^{-1}\left(\frac{X_P}{h}\right)^{1-\mu}\right\} \quad (43)$$

where

$$w \triangleq sec\ \theta - tan\ \theta, \quad h = d\ cos\ \theta$$

Using (43), we calculate the time of point capture of E, t_c: It is determined by setting in Eq. (43) $X_P = 0$. Since $t_c = \frac{Y_P(X_P=0)}{\mu}$, the capture time

$$t_c = \frac{1}{1-\mu^2}(1+\mu\ sin\ \theta)d \quad (44)$$

The aspect angle at the time of capture is always 0 – in PP the Pursuer captures the Evader from behind.

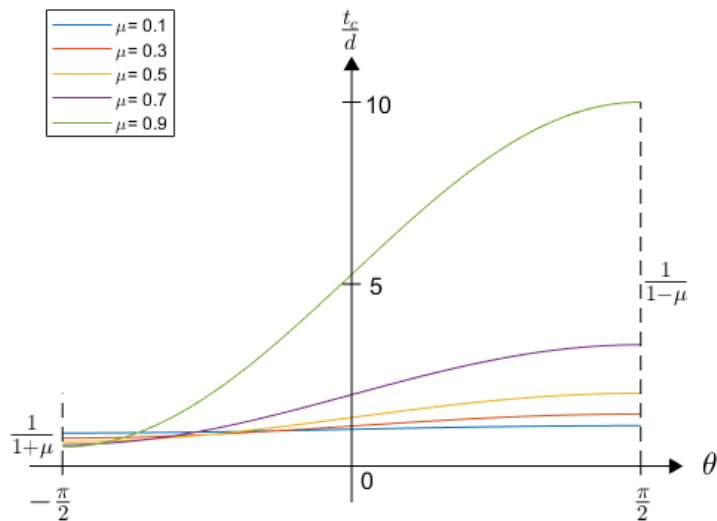Equation (44) allows us to explore the relationship between the capture time, the

Figure 53: Capture Time vs the Course Angle θ for the Speed Ratio $\mu < 1$.

Evader's course angle θ, and the speed ratio parameter μ. As Fig. 53 shows, the capture time is monotonically increasing in θ; to try to outrun the Pursuer, the Evader must turn away from the Pursuer, and preferably, run away from the Pursuer.

Unfortunately, when the speed ratio $\mu = 1$, Eq. (43) is not applicable.

6.4 Target Defense

The target defense differential game is now considered, where the Pursuer assumes the role of the Defender (D) and the Evader is the Attacker (A). The Attacker holds course while heading straight toward the Target (T) while the Defender employs PP, hoping to intercept A before the latter reaches T – see Fig. 54, where the initial distance from D to A is d, A holds the course θ by heading toward the Target and his/her initial distance from the point target T is r. In the target defense scenario, the state is (d, r, θ).

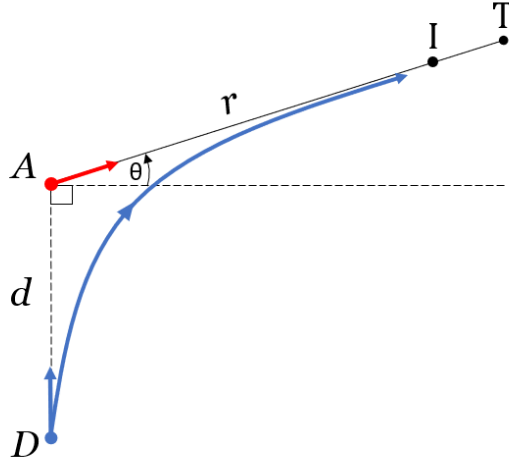Using Eq. (44), we compare the capture time t_c to the time $\frac{r}{\mu}$ it would take A to

Figure 54: The Target Defense Scenario.

reach the target. If $\frac{r}{\mu} < t_c$, that is,

$$\frac{r}{\mu} < \frac{1}{1 - \mu^2}(1 + \mu \ sin \ \theta)d,$$

the Attacker will reach T before being captured by D in PP. Hence, if the state (d, r, θ) of the "game" is such that

$$\frac{r}{d} < \frac{\mu}{1 - \mu^2}(1 + \mu \ sin \ \theta), \tag{45}$$

the Defender D, who's strategy is PP, is not able to defend the Target by capturing the Attacker A before the latter reaches T.

Now suppose (45) does not hold. Can A nevertheless reach T before being intercepted by D by maneuvering rather than holding course? The answer is no. This is so because the A/D speed ratio $0 < \mu < 1$ and therefore, away from T, player A is continuously exposed to capture by the fast Defender. By following a straight-line trajectory to T, A minimizes his exposure time to D. When (45) does not hold, A can significantly increase the time-to-capture by instantaneously choosing the new

course $\theta = \frac{\pi}{2}$, to be captured at time $t_c = \frac{1}{1-\mu}d > \frac{1}{1-\mu^2}(1 + \mu \, sin \, \theta)d$, but A will then be captured and will not reach T. When (45) does not hold, maneuvering away from a straight-line dash to T will not help A reach T before being intercepted by the fast Defender D who employs PP. Thus, the following holds,

Proposition 7 *When the state is (d, r, θ) and D employs PP, A is successful if and only if condition (45) holds.*

$\square$

Proposition 7 allows us to characterize the region in the state space (d, r, θ) in which A can reach T prior to being captured by D in PP. Let $\psi \triangleq \frac{\pi}{2} - \theta$.

The boundary of the safe region of T in polar coordinates (r, ψ) is

$$r(\psi) = \frac{\mu}{1 - \mu^2}(1 + \mu \, cos \, \psi) \, d, \; 0 \leq \psi \leq \pi. \tag{46}$$

Equation (46) delimits a cardioid-shaped region, whose boundary is B, shown in Fig. 55. If T is inside this region, A will reach T before being captured in PP by D. The range of r is $\frac{\mu}{1+\mu} \, d \leq r \leq \frac{\mu}{1-\mu} \, d$.
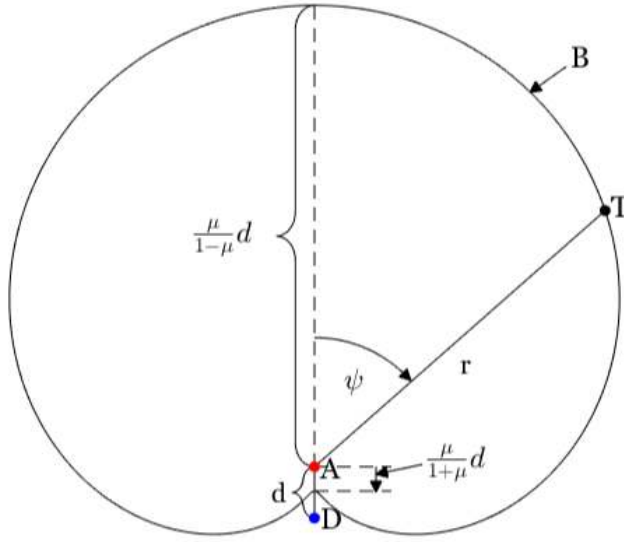
Figure 55: A's Winning Region. $\mu = 0.9, \ d = 1$.

6.5   Pure Pursuit vs. Optimal Interception

Consider now the differential game of guarding a Target [16] where A and D play optimally, that is, the Attacker wants to come as close as possible to the Target before being intercepted by the Defender and the Defender wants to capture A as far away from the Target as possible. The answer to the question: where should T be in order for A to be able to reach it before being intercepted by D, is as follows [16]:

A reaches T before being captured by D if and only if T is inside the Apollonius disk whose foci are A and D, where $dist(A, D) = d$, and the ratio used to construct the Apollonius circle is the A/D speed ratio $\mu < 1$. The radius of the Apollonius circle $\rho = \frac{\mu}{1-\mu^2}d$ and the distance $\overline{AO} = \frac{\mu^2}{1-\mu^2}d$ – see Fig. 56. Hence, the effectiveness of the Defender's PP strategy vis a vis the optimal strategy provided by the solution of the Target-Defense Differential Game [16], is illustrated in Fig. 57.

The Apollonius circle fits snugly in the boundary B, which delimits A's winning region when D employs PP, as discussed in Section 6.4. When D plays optimally, as
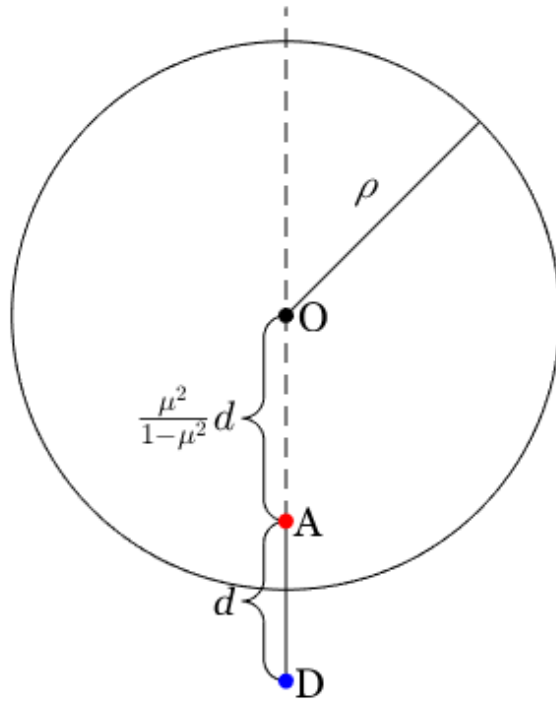
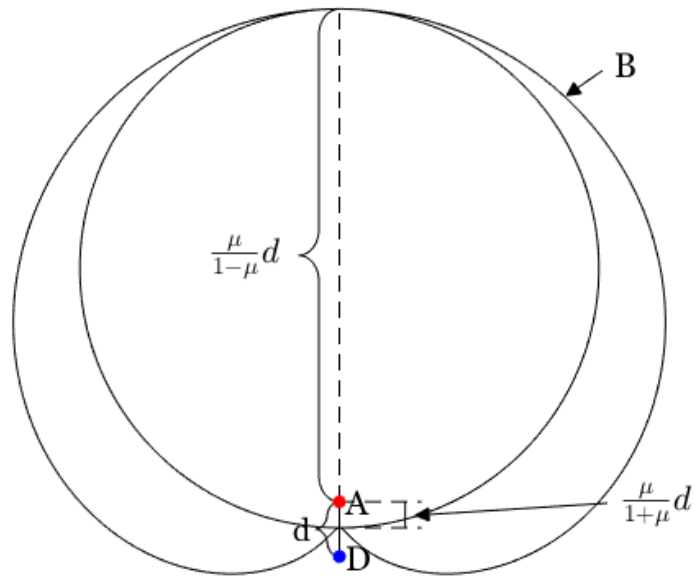Figure 56: A Wins if T is Inside the Apollonius Circle.

Figure 57: Optimal Pursuit v. Pure Pursuit.

94

opposed to employing the PP strategy, A's winning region is reduced – as expected.

In order to consider the classical target defense scenario of [1] where the Attacker and Defender have the same speed, one must first gain a better understanding of PP when the speed ratio $\mu = 1$.

6.6   Pure Pursuit When the Speed Ratio $\mu = 1$

When the speed ratio $\mu = 1$, a PP strategy will always result in failure to capture the Evader, except in the case where a suicidal Evader runs toward the Pursuer. However, if the Pursuer is endowed with a capture circle of radius l, the Evader may be captured if he holds course and does not flee directly away from the Pursuer, or if more than one Pursuer gives chase – see, e.g. [17]. During PP, also when the speed ratio $\mu = 1$, the P-E distance is monotonically decreasing, and it asymptotically settles on a constant distance behind the Evader, except if E runs away from P whereupon the initial P-E separation does not change throughout the pursuit.

Since the speed ratio $\mu = 1$, we now consider a Pursuer endowed with a capture circle of radius l. In the case where the speed ratio $\mu = 1$, Eq. (43) is not applicable. Thus, to find the time-to-capture t_c, we pick up where reference [6] left, at Eq. (25). For $\mu = 1$, the Pursuer's position satisfies the differential equation

$$\frac{dY_P}{dX_P} = \frac{1}{2}\left(\frac{X_P}{X_0} - \frac{X_0}{X_P}\right), \quad Y_P(d\ cos\ \theta) = -d\ sin\ \theta. \tag{47}$$

where

$$X_0 \triangleq (1 + sin\ \theta)\ d.$$

Upon integrating the differential equation (47) and applying the initial condition,

95

we obtain the pursuit curve when the speed ratio $\mu = 1$ and $-\frac{\pi}{2} \leq \theta \leq \frac{\pi}{2}$:

$$Y_P\ (X_P) = \frac{1}{4} \left[(1 - \sin\ \theta) \left(\frac{X_P}{d\ \cos\ \theta} \right)^2 - 3\ \sin\ \theta - 1 - 2(1 + \sin\ \theta) ln \left(\frac{X_P}{d\ \cos\ \theta} \right) \right] d,$$
$$0 < X_P \leq d\ \cos\ \theta \tag{48}$$

and in the classical case where $\theta = 0$, the pursuit curve is

$$Y_P\ (X_P) = \frac{1}{4} \left[\left(\frac{X_P}{d} \right)^2 - 2\ ln \left(\frac{X_P}{d} \right) - 1 \right] d, \quad 0 < X_P \leq d. \tag{49}$$

To determine the time-to-capture t_c when the speed ratio $\mu = 1$, we must deter-mine where capture occurs along the Pursuer's trajectory, say at X_c; recall that now the capture range $l > 0$. Fig. 58 depicts the moment the Evader enters the Pursuer's capture disk of radius l. This is determined by the following Optimality Principle whereby:

At capture time, the $\overline{PE}$ segment, which is of length l, is tangent to the pursuit curve at the instant of capture when the Pursuer is at $P' = (X_c, Y_c(X_c))$ – see Fig. 58.

We know

$$\frac{X_c}{l} = \sin\ \alpha$$

and

$$\tan\ \alpha = - \left. \frac{dX_P}{dY_P} \right|_{X_c},$$

which, when combined with Eq. (47), yields

$$\frac{\sqrt{l^2 - X_c^2}}{X_c} = \frac{1}{2} \left(\frac{X_0}{X_c} - \frac{X_0}{X_c} \right).$$

96
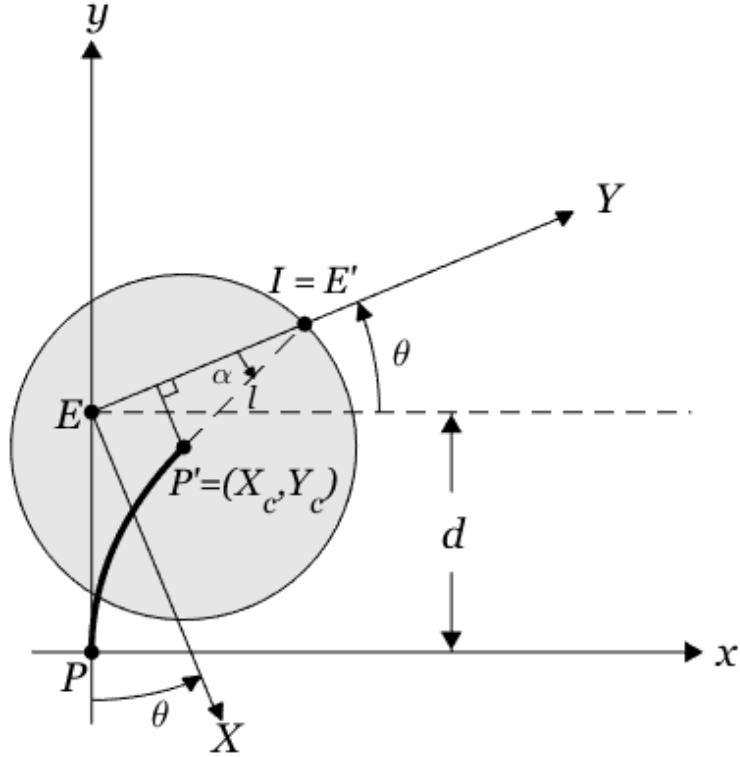
Figure 58: Geometry at Capture. $d = 1$, $\theta = \frac{\pi}{8}$, $l = 0.72$

This equation simplifies to the biquadratic equation in X_c

$$X_c^4 + 2X_0^2 X_c^2 + X_0^2(X_0^2 - 4l^2) = 0. \tag{50}$$

The solution of the biquadratic equation is

$$X_c = \sqrt{(1 + sin\ \theta)\left(2\frac{l}{d} - 1 - sin\ \theta\right)}\ d. \tag{51}$$

Evidently, for capture to be possible in the first place, need

$$sin\ \theta < 2\frac{l}{d} - 1$$

97

That is,

$$-\frac{\pi}{2} \le \theta \le \begin{cases} Asin\left(2\frac{l}{d} - 1\right) & \text{if } l \ge \frac{1}{2}d \\ -Asin\left(1 - 2\frac{l}{d}\right) & \text{if } l \le \frac{1}{2}d \end{cases} \tag{52}$$

The solution X_c must satisfy $X_c < l$. Indeed

$$l^2 - X_c^2 = l^2 - (1 + sin\ \theta)\left(2\frac{l}{d} - 1 - sin\ \theta\right)d^2,$$

and thus

$$l^2 - X_c^2 = \left(1 + sin\ \theta - \frac{l}{d}\right)^2 d^2 > 0.$$

Given X_c and $Y_c = Y_P(X_c)$, we can determine the capture time.

$$t_c = Y_P(X_c) + \sqrt{l^2 - X_c^2} \tag{53}$$

Substituting (48) for Y_P in (53) yields the following result.

When the speed ratio $\mu = 1$ and the Pursuer's capture range is l,

$$t_c(\theta, d; l) = \frac{1}{4}\left[2\left(1 - \frac{l}{d}\right) - (1 + sin\ \theta)\ ln\left(\frac{2\frac{l}{d} - 1 - sin\ \theta}{1 - sin\ \theta}\right)\right]d. \tag{54}$$

With the equation for capture time in (54), we can explore the relationship between capture time, the Evader's course angle θ, and the ratio of the initial separation and the capture disk radius l – see Fig. 59. But first and foremost, given the "state" (d, θ), for capture to be possible in the first place, we need – see Eq. (54)
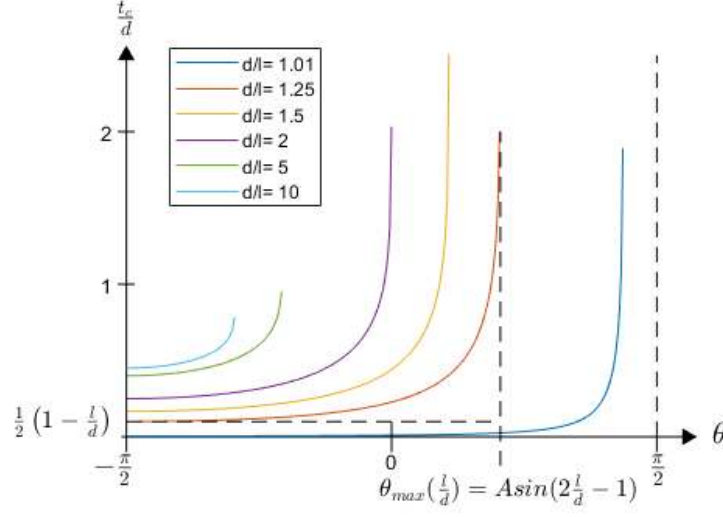
$$l > \frac{1 + sin\ \theta}{2}d$$

98

Figure 59: Capture Time vs the Course Angle θ for the Speed Ratio $\mu = 1$.

6.7 Target Defense When $\mu = 1$

When the A/D speed ratio $\mu = 1$, A reaches T unmolested by D in PP if and only if

$$t_c < r$$

Using the result (54) and, as before, setting $\psi \triangleq \frac{\pi}{2} - \theta$, we obtain the boundary B of A's winning region in polar coordinates (r, ψ):

$$r(\psi; d, l) = \frac{1}{4} \left[2 \left(1 - \frac{l}{d} \right) - (1 + \cos \theta) \ln \left(\frac{2\frac{l}{d} - 1 - \cos \theta}{1 - \cos \theta} \right) \right] d.$$

The range of ψ is

$$\pi \geq \psi \geq \begin{cases} \frac{\pi}{2} - Asin \left(2\frac{l}{d} - 1 \right) & \text{if } l > \frac{1}{2}d \\ \frac{\pi}{2} + Asin \left(1 - 2\frac{l}{d} \right) & \text{if } l < \frac{1}{2}d \end{cases}$$

For A to win the, Target T needs to be located above the boundary B. A's winning region is now open and is depicted in Fig. 60.

99

(a) $l > \frac{1}{2}d$ (b) $l < \frac{1}{2}d$

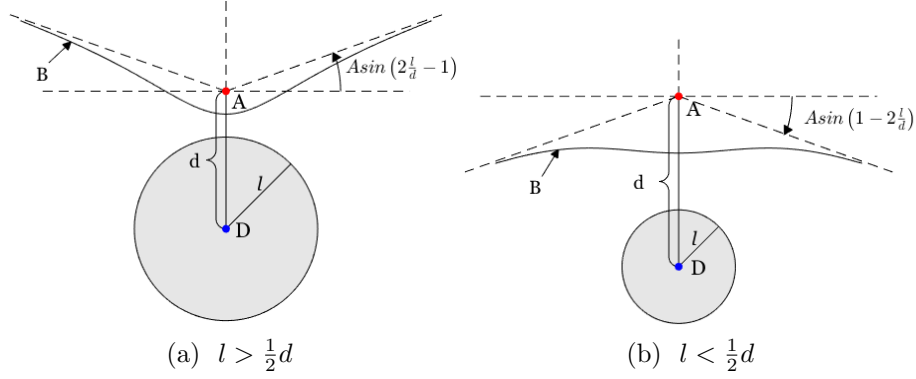Figure 60: A's Winning Region

6.8   Conclusion

The scenario involving a target-guarding Defender who employs PP against a target-seeking Attacker is considered. In the case where the Defender is faster than the Attacker – the speed ratio $\mu < 1$ – the conditions for capture of the Attacker prior to him reaching the Target are derived. The operationally relevant case in which the Attacker and Defender have similar capability, so the speed ratio parameter $\mu = 1$, was analyzed. An Attacker "Winning Region" wherefrom the Attacker is able to reach the Target before being captured by the Defender is characterized.

6.9   Appendix: Flight-or-Fight Response

As Figures 53 and 59 show, the capture time t_c increases as θ increases. To flee, the Evader turns away from the Pursuer. But what about the flight-or-fight response. Consider now the case where the Purser's maneuverability is limited by a minimal turn radius ρ while the pursuer employs PP, the radius of curvature of the pursuit curve cannot exceed ρ. Will it benefit the Evader to choose a smaller heading θ, that is, turn into the pursuer, to saturate the Pursuer's turning capability and thus break off the engagement?

Having derived the pursuit curve, $Y_P(X_P)$, the radius of curvature ρ is calculated

100

as

$$\rho(X_P) = \left| \frac{\left[1 + \left(\frac{dY_P}{dX_P} \right)^2 \right]^{\frac{3}{2}}}{\frac{d^2Y_P}{dX_P^2}} \right| \tag{55}$$

To obtain the radius of curvature $\rho(X_P)$, $X_c \le X_P \le d \cos \theta$, we start with Eq. (25) from [4] reproduced here as Eq. (56):

$$\frac{dY_P}{dX_P} = \frac{1}{2} \left[w \left(\frac{X_P}{h} \right)^{\mu} - \frac{1}{w} \left(\frac{X_P}{h} \right)^{-\mu} \right] \tag{56}$$

where

$$h \triangleq d \cos \theta, \quad w \triangleq \frac{1 - \sin \theta}{\cos \theta}.$$

Taking the derivative of Eq. (56), we get

$$\frac{d^2Y_P}{dX_P^2} = \frac{\mu}{2h} \left[w \left(\frac{X_P}{h} \right)^{\mu-1} + \frac{1}{w} \left(\frac{h}{X_P} \right)^{\mu+1} \right], \tag{57}$$

and substituting (56) and (57) into (55) yields

$$\frac{\rho}{h} = \frac{1}{4\mu} \left[w^2 \left(\frac{X_P}{h} \right)^{1+2\mu} + \frac{1}{w^2} \left(\frac{X_P}{h} \right)^{1-2\mu} + 2\frac{X_P}{h} \right]. \tag{58}$$

In the classical case of an abeam engagement when $\theta = 0$, $w = 1$ and $h = d$, so

$$\frac{\rho}{h} = \frac{1}{4\mu} \left[\left(\frac{X_P}{d} \right)^{1+2\mu} + \left(\frac{X_P}{d} \right)^{1-2\mu} + 2\frac{X_P}{d} \right].$$

To determine the minimum turn radius, we need to find the minimum of the function $\rho(X_P)$.

$$\frac{d\rho}{dX_P} \propto (1 + 2\mu)z + (1 - 2\mu)\frac{1}{z} + 2 \tag{59}$$

101

where

$$z \triangleq \left(\frac{X_P}{h}\right)^{2\mu} w^2, \quad 0 \le z \le \frac{1 - sin \ \theta}{1 + sin \ \theta}.$$

Setting the R.H.S. of Eq.(59) equal to 0, we get the quadratic equation in z

$$(1 + 2\mu)z^2 + 2z + 1 - 2\mu = 0.$$

We have a real solution if

$$1 - (1 + 2\mu)(1 - 2\mu) > 0,$$

which is always the case. The solution of the quadratic equation is

$$z = \frac{2\mu - 1}{2\mu + 1}$$

When the speed ratio $0 < \mu < \frac{1}{2}$, the radius of curvature is monotonically increasing in X_P. In other words, ρ_{max} is attained at $t = 0$, so the curvature of the pure pursuit path increases until the end point of the time of capture – see Fig. (61).

If, however, the speed ratio $\frac{1}{2} < \mu < 1$, as shown in Fig. 62, the radius of curvature attains its minimum at

$$\frac{X_P^*}{h} = \left(\frac{1}{w^2}\frac{2\mu - 1}{2\mu + 1}\right)^{\frac{1}{2\mu}}$$

which can also be written as

$$\frac{X_P^*}{h} = \left(\frac{1 + sin \ \theta}{1 - sin \ \theta}\frac{2\mu - 1}{2\mu + 1}\right)^{\frac{1}{2\mu}},$$

provided

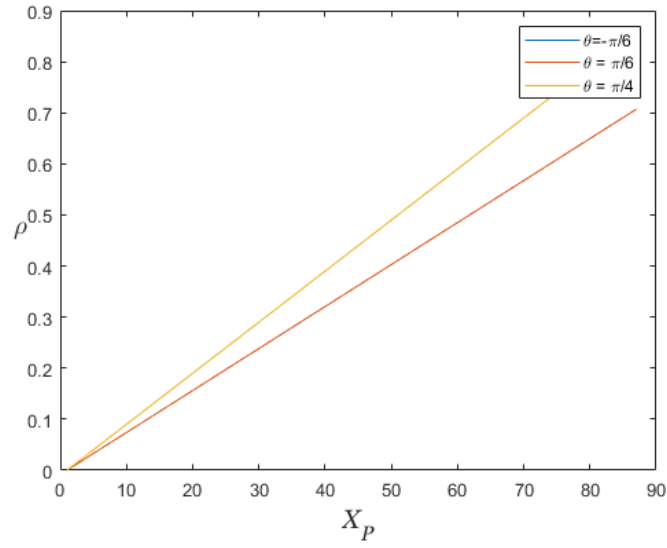$$\left(\frac{1 + sin \ \theta}{1 - sin \ \theta}\frac{2\mu - 1}{2\mu + 1}\right)^{\frac{1}{2\mu}} \le 1$$
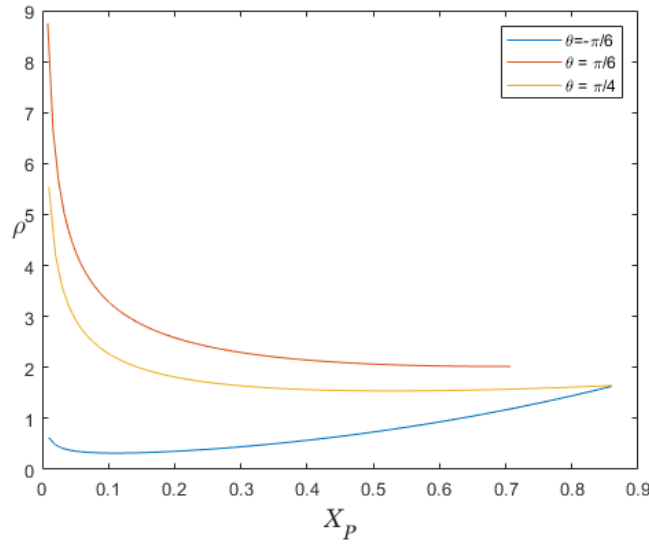
Figure 61: Radius of Curvature. $\mu = 0.3$.

Figure 62: Radius of Curvature. $\mu = 0.7$.

Hence, if the speed ratio $\frac{1}{2} < \mu < 1$, the radius of curvature attains its minimum at

$$\frac{X_P^*}{h} = \left(\frac{1 + sin\ \theta}{1 - sin\ \theta} \frac{2\mu - 1}{2\mu + 1} \right)^{\frac{1}{2\mu}}, \tag{60}$$

provided

$$\theta < Asin\left(\frac{1}{2\mu}\right).$$

If $\frac{1}{2} < \mu < 1$ and $\theta < Asin(\frac{1}{2\mu})$, the minimal radius of curvature

$$\frac{\rho^*}{h} = \frac{1}{4\mu}\left(\frac{X_P^*}{h}\right)\left(\frac{2\mu-1}{2\mu+1} + \frac{2\mu+1}{2\mu-1} + 2\right)$$

which is simplified to

$$\frac{\rho^*}{h} = \frac{4\mu}{4\mu^2 - 1}\left(\frac{X_P^*}{h}\right). \tag{61}$$

Substituting (60) into (61) yields

$$\frac{\rho^*}{h} = \frac{4\mu}{4\mu^2 - 1}\left(\frac{1 + sin\ \theta}{1 - sin\ \theta}\frac{2\mu-1}{2\mu+1}\right)^{\frac{1}{2\mu}}. \tag{62}$$

The Evader can judiciously choose his course angle θ according to equation (62) and instead of running away from the Pursuer to maximize the time-to-capture, by saturating the Pursuer's maneuverability, the Evader/Attacker can escape altogether.

VII. Many on One Pursuit and Evasion

7.1   Abstract

In an extension to Isaacs' "Two Cutters and Fugitive Ship" differential game, this paper analyzes the effects of a third pursuer joining the chase. We analyze evasion strategies to prolong the life of the evader when facing both "optimal" Collision Course (CC) and Pure Pursuit (PP) guidance by the three pursuers. Cases where traditionally "optimal" evasion result in a premature capture when compared to alternative strategies are illustrated. We provide evidence that conventional wisdom for "optimal" play by the evader is incorrect.

7.2   Introduction

In this paper, pursuit-evasion differential games with more than one purser are investigated. The players are assumed to have simple motion *à la* Isaacs, that is, they are holonomic, and the pursuit takes place in the Euclidean plane. We begin by revisiting the "Two Cutters and Fugitive Ship" differential game as outlined by Rufus Isaacs in [1], where the fugitive ship is slower than the two cutters and point capture is required.The solution to the differential game employs the geometric construct of an Apollonius circle. An Apollonius circle is the set of points whose distances from two fixed points, in this case the positions of the Pursuer and the Evader, are a constant ratio $\mu = \frac{v_E}{v_P}$, where v_E and v_P are the speeds of the Evader and the Pursuer, respectively – see Fig. 63. Under optimal play, capture occurs at the intersection of two Apollonius circles whose foci are the two pursuers' and the evader's instantaneous positions – see Fig. 64.
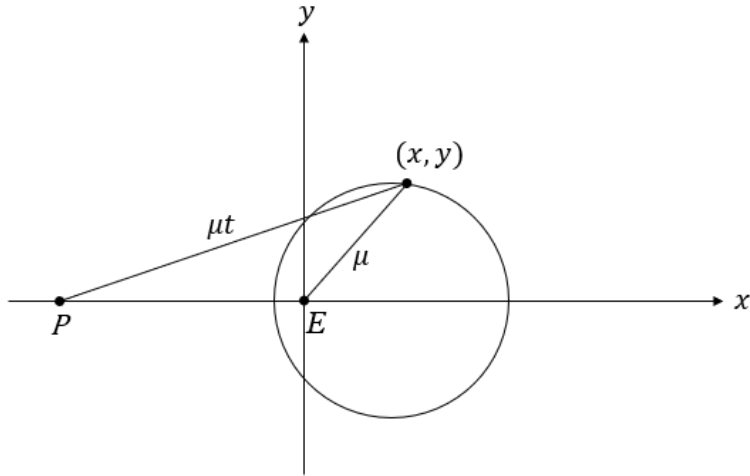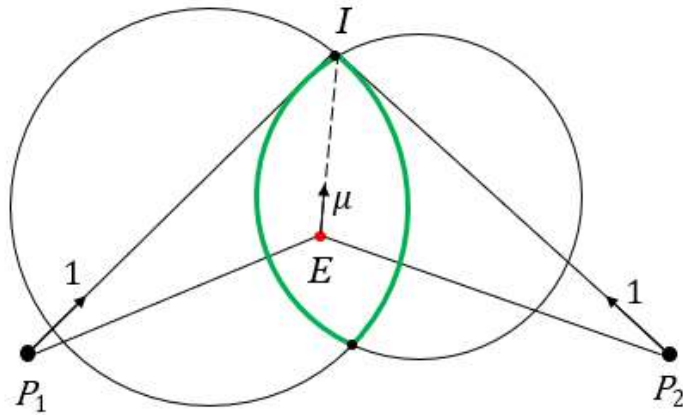
Figure 63: Apollonius Circle. $\mu < 1$, $\ell = 0$.

Figure 64: Construction of Aim Point I. $\mu < 1$, $\ell = 0$.

7.3   Extensions

Wasz and Pachter [2] extended the "Two Cutters and Fugitive Ship" game formulation by endowing the cutters with capture ranges of radius $\ell > 0$. In this case, the optimal feedback strategies change, as the safe region is no longer defined by the intersection of two Apollonius circles. Rather, it is defined by the intersection of two Cartesian ovals, a family of which is displayed in Fig. 65. Wasz, Pachter, and
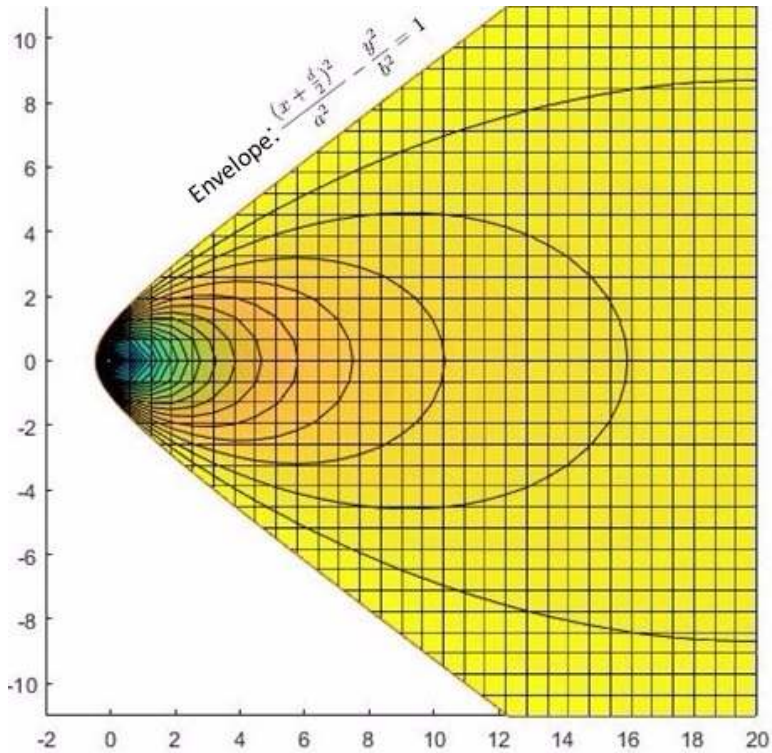
Figure 65: Family of Cartesian Ovals. $\mu < 1$, $\ell > 0$.

Vlassakis in [3] and [17] further explored the case where the pursuers have a capture range $\ell > 0$ but the speed ratio between the pursuers and the evader $\mu = \frac{v_E}{v_P} = 1$. Wasz and Pachter [3] delineated the state space region where capture is guaranteed – see Fig. 66 – and they synthesized the players' optimal state feedback strategies.

If E is in the shaded region in Fig. 66 and the pursuers player optimally, E will be captured. In [17], Vlassakis and Pachter streamlined the derivation for the optimal feedback strategies. Given the instantaneous positions of the two pursuers and the evader, the boundary of the Safe Region when the speed ratio $\mu = 1$ is depicted in Fig. 67 by the blue lines whcih are arcs of hyperbolae. The players' optimal strategies entail heading toward the aimpoint I, shown in Fig. 67. A simulation to illustrate the solutions to the Game of Kind and Game of Degree when E does not play optimally was developed.
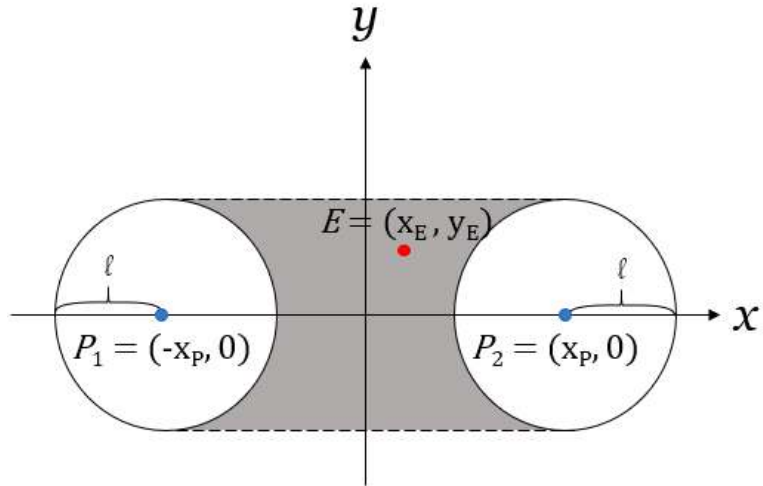
Figure 66: Solution to the Game of Kind. $\mu = 1$, $\ell > 0$.
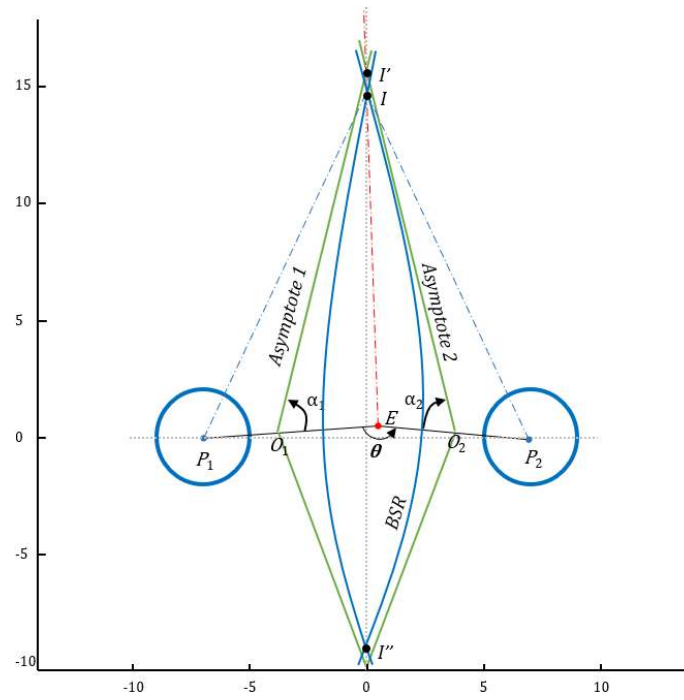

Figure 67: Two-on-One with Capture Ranges. $\mu = 1$, $\ell > 0$.

7.4   Three Pursuers

Von Moll, Pachter, Garcia, Casbeer, and Milutinovic [7] expanded the study of pursuit-evasion games with the inclusion of a third pursuer. This increases the complexity of the pursuit-evasion problem. Thus, it is instructive to consider an initial configuration which is fully symmetric, with the evader initially at the circumcenter of the equilateral triangle $\triangle P_1 P_2 P_3$ formed by the three pursuers, as shown in Fig. 68. Fig. 68 shows the three Apollonius circles formed by each of the pursuers
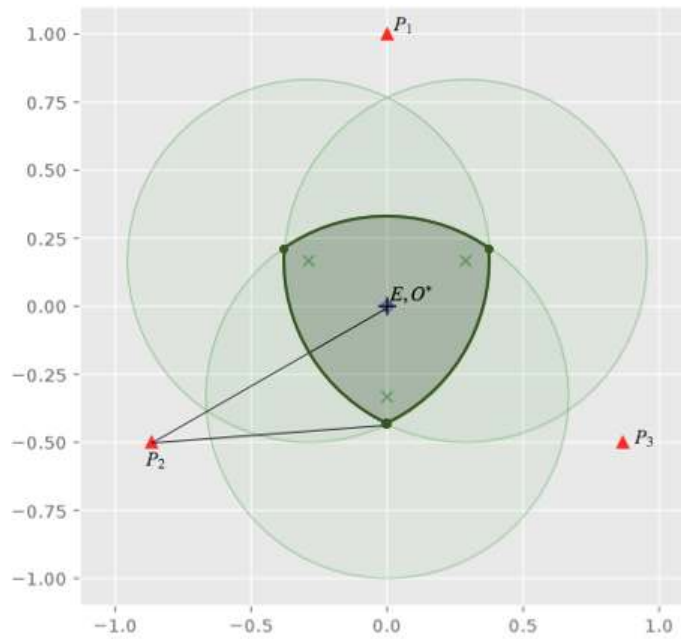

Figure 68: Three Pursuers.

and the evader, whose intersection creates the "Safe Region" whose vertices, in the two-on-one pursuit scenario, provided a candidate optimal aimpoint for the Evader to maximize his time-to-capture – ditto for the pursuers, who strive to minimize the time-to-capture. In the symmetric three-on-one case, however, the circumcenter of the equilateral triangle $\triangle P_1 P_2 P_3$, where the evader is initially located, provides the longest distance for each of the pursuers to travel, as has correctly been pointed out

by Alexander Von Moll in [7] and further analyzed in [10]. Thus, it would seem that the Evader should not head toward a vertex of the "safe region", but should stay stationary at the circumcenter O^*: thus, doing nothing, the Evader prolongs his time to capture. In [10], the three-on-one pursuit-evasion scenario was anaylzed when the Evader moves away from P_1 as illustratetd in Fig. 69 under the stipulation that the pursers employed the "optimal" strategy of Collision Course (CC) guidance as in Isaacs' Two Cutters and Fugitive Ship game [1].

Thus, we consider the three-on-one pursuit evasion game with CC guidance and analyze traditionally "optimal" evasion strategy. We look into the three-on-one case where the pursuers employ both CC guidance and Pure Pursuit (PP), and we try to improve on what one could naively think is the "optimal" evasion strategies.

7.5 Collision Course Guidance

If the Pursuers play "optimally", that is, they employ Collision Course (CC) guidance as in the two-on-one scenario, the geometry is illustrated in Figure 69.
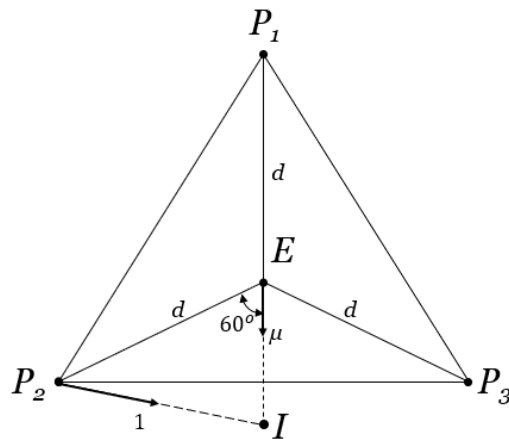

Figure 69: Pursuers use Collision Course Guidance.

110

Consider the triangle $\triangle EP_2I$: The time-to-capture

$$t_{c_{CC}} = \frac{-\mu + \sqrt{4 - 3\mu^2}}{2(1 - \mu^2)} \cdot d$$

Now

$$t_{c_{CC}} < d \Leftrightarrow \frac{-\mu + \sqrt{4 - 3\mu^2}}{2(1 - \mu^2)} < 1$$

$$\Leftrightarrow$$

$$\mu^3 - \mu^2 - \mu + 1 > 0, \ 0 \leq \mu < 1$$

$$\Leftrightarrow$$

$$(1 - \mu)(1 - \mu^2) > 0,$$

which is always the case. Thus, it appears that E should stay put, $\forall \ 0 \leq \mu < 1$. But in [7] it is shown that, when the Pursuers employ CC guidance, the state enters a dispersal surface. Depending on the speed ratio μ, E can do better – prolong his time-to-capture – by going South.

7.6   Pure Pursuit

We now consider the case where three fast Pursuers chase a slow Evader in Pure Pursuit (PP) and the speed ratio $\mu = \frac{v_E}{v_P} < 1$. As before, the configuration/initial state considered is fully symmetric, as shown in Figure 70, where the Evader is initially at the circumcenter of the equilateral $\triangle P_1 P_2 P_3$.

Given the speed ratio $\mu < 1$, it is clear that the Evader will be captured. The question is, how can E maximize the time to capture, given the three Pursuers are in PP?

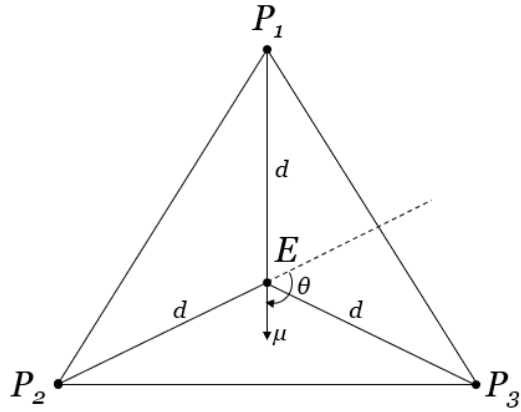We know [6] the capture time when the Pursuer employs PP and the Evader is

Figure 70: Three Pursuers Fully Symmetric State.

slower than the Pursuer ($\mu < 1$). The configuration is as shown in Figure 71:
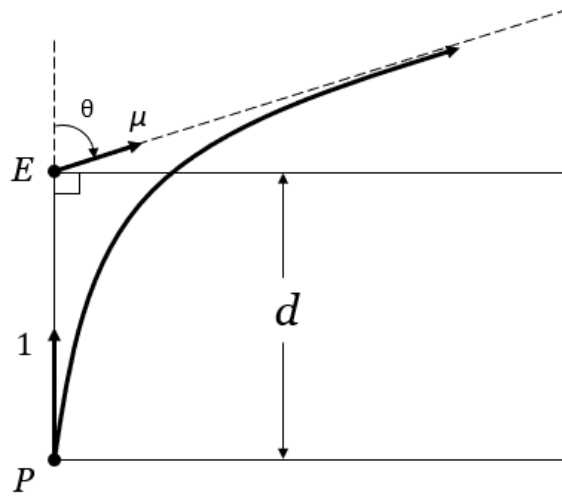

Figure 71: Pure Pursuit Scenario.

The time-to-capture in PP

$$t_{c_{PP}} = \frac{1}{1 - \mu^2}(1 + \mu \; cos\theta) \cdot d \tag{63}$$

In the fully symmetric configuration, depicted in Fig. 70, if E chooses a heading

112

directly away from P_1, as far as the Pursuers P_2 and P_3 are concerned, $\theta = \frac{2}{3}\pi$, so eq. (63) yields the time to capture in PP

$$t_{c_{PP}} = \frac{1}{1-\mu^2}\left(1 - \frac{1}{2}\mu\right) \cdot d \qquad (64)$$

E will isochronously be captured by P_2 and P_3 while P_1 is redundant. Next, consider the case where E stays put at its initial position. The time to capture is then

$$t_{c_P} = d \qquad (65)$$

Comparing equations (64) and (65):

$$t_{c_P} > t_{c_{PP}}$$

if and only if

$$d > \frac{1}{1-\mu^2}\left(1 - \frac{1}{2}\mu\right) \cdot d$$

which allows us to conclude: When the speed ratio $\mu < \frac{1}{2}$, the capture time is greater when the Evader is stationary – similar to the phenomenon encountered in [10] and [7], and discussed in Section 7.5, where the Pursuer employed "optimal" CC guidance.

7.7 Proactive Evader

In the case where the speed ratio $\mu < \frac{1}{2}$, if the Evader vacillates at high frequency by moving a distance $\delta\mu$ – North-South or East-West, as shown in Figure 72 – will this increase the capture time above and beyond $t_c = 1$ by making the Pursuers follow an oscillatory and therefore longer trajectory while the Evader is practically stationary? The design parameter δ sets the frequency of the Evader's oscillatory motion. It is the time the Evader runs away from its initial position before turning around, and since
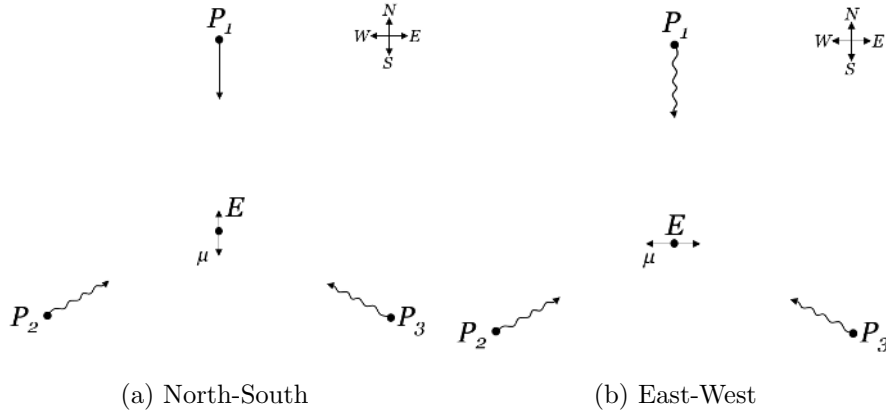
113

(a) North-South   (b) East-West

Figure 72: Dithering Evader.

the velocity of the Evader μ is constant, it determines the frequency of oscillation. As δ increases, that is, the Evader's oscillation frequency decreases, the Evader will draw the Pursuers further off course. However, too great of δ might result in a decreased capture time when compared to a stationary Evader. Thus, finding the optimal δ is of interest.

7.7.1   North-South Oscillation

In the case where the Evader oscillates North-South, as shown in Figure 72a, we know that if E is captured at any point above the circumcenter of the equilateral triangle $\triangle P_1 P_2 P_3$, it will result in a decrease in capture time when compared to a stationary Evader. This is because P_1 is not drawn off course by the Evader's North-South oscillatory motion, and thus will reach the circumcenter of the equilateral triangle $\triangle P_1 P_2 P_3$ in the same amount of time (nominally $t_C = 1$ sec.) regardless of the Evader's motion. Therefore, for capture time to increase when compared to a stationary evader, capture by P_1 or by P_2 and P_3 must occur some distance below the circumcenter of the equilateral triangle, in the region R below the broken line shown in Fig. 73.

The Evader's North-South oscillation strategy was simulated to determine which δ
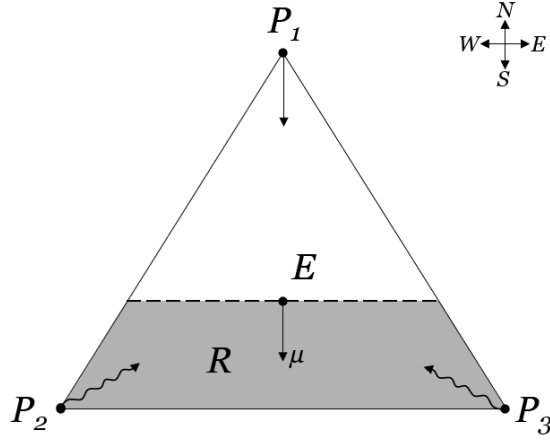
114

Figure 73: North-South Safe Region.

prolonged the life of the Evader when compared to staying put at the circumcenter. The pursuit curves were numerically calculated using Euler's integration method with a time step of 1e-5 seconds – this, compared to the time required to reach a stationary E in 1 second. The Evader initially travels South for time δ at speed μ, then changes direction to have traveled a distance $2\delta\mu$ so that it returns to the circumcenter of the equilateral triangle $\triangle P_1 P_2 P_3$ and continues to travel North for a distance $\delta\mu$, etc. – see Fig. 74.

The Evader was subject to the control policy shown in Fig 74 with varying δ's. Figure 75 shows the resulting capture times t_c for a range of δ's when the speed ratio $\mu = 0.2$. As shown in Fig. 75, there were δ's which extended the Evader's life. In the best case, $\delta = 0.518$, the oscillatory motion drew the pursuers off-course enough to extend the Evader's life by 0.006 seconds – this, compared to a nominal 1 sec capture time. The Evader changed direction once, and was captured 0.0062 units, or 0.62% of d, below its initial position at the circumcenter of the equilateral triangle $\triangle P_1 P_2 P_3$.

Next, we wanted to see the effects of varying δ for the case when the Evader first travels South for δ, then returns to a position $y(t_f)$ below the circumcenter of the equilateral triangle $\triangle P_1 P_2 P_3$ and stops – see Fig. 76. We use the parameter y'_f to
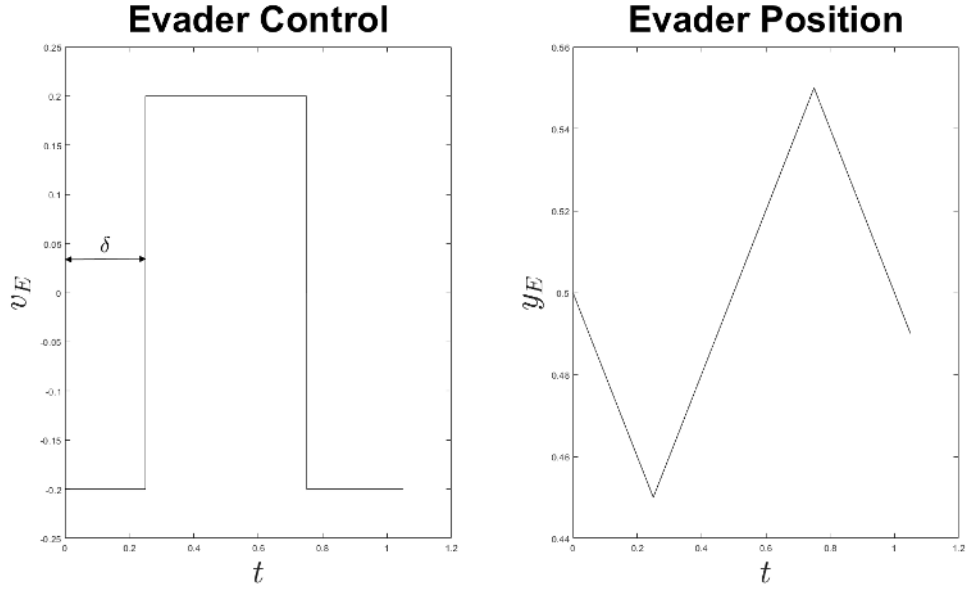
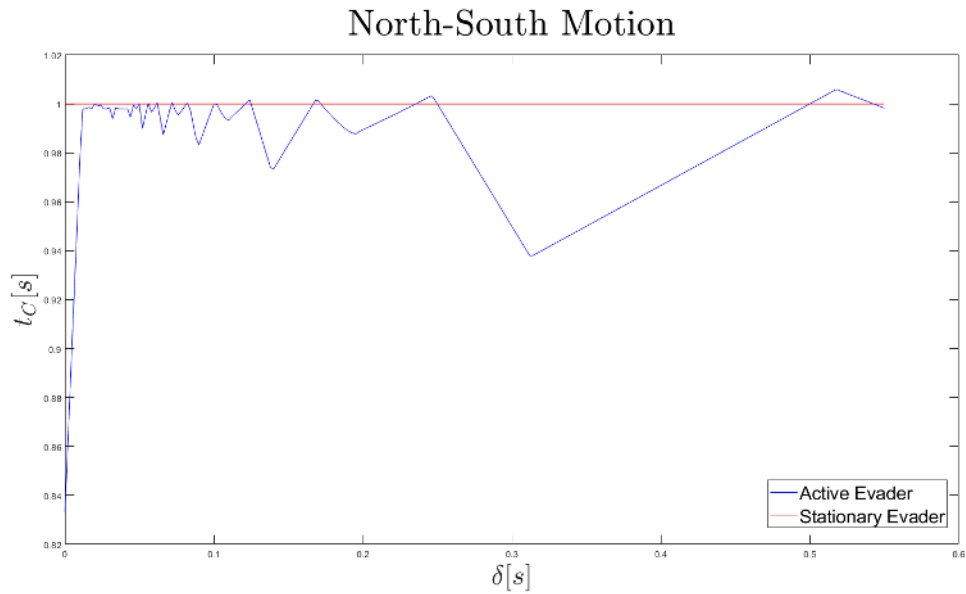Figure 74: Evader Control and Position. $\mu = .2,\ \delta = .25$.

Figure 75: Capture Time t_c vs. δ. $\mu = 0.2$.

signify the distance the Evader stops below its initial position at the center of the equilateral triangle.
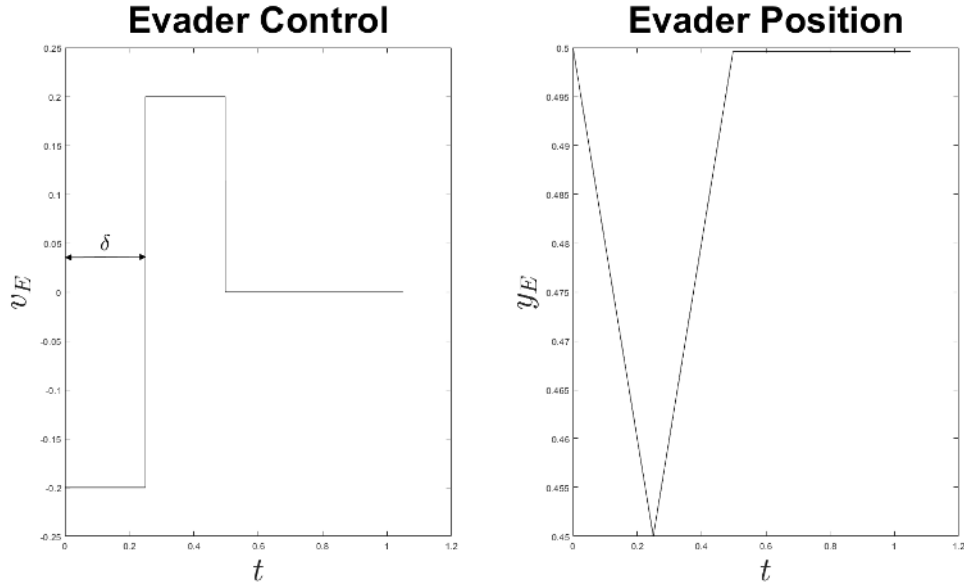
$$y'_f = y(t_f) - y_E(0)$$

116

Figure 76: Evader Control and Position with Stoppage. $\mu = .2,\ \delta = .25$.

Fig. 77 shows the case where the Evader stops at $y'_f = -0.002$. We see that when $\delta > 0.224$, the Evader's motion increases the time to capture t_c. In the best case, $\delta = 0.518$ yields $t_c = 1.006$ seconds.
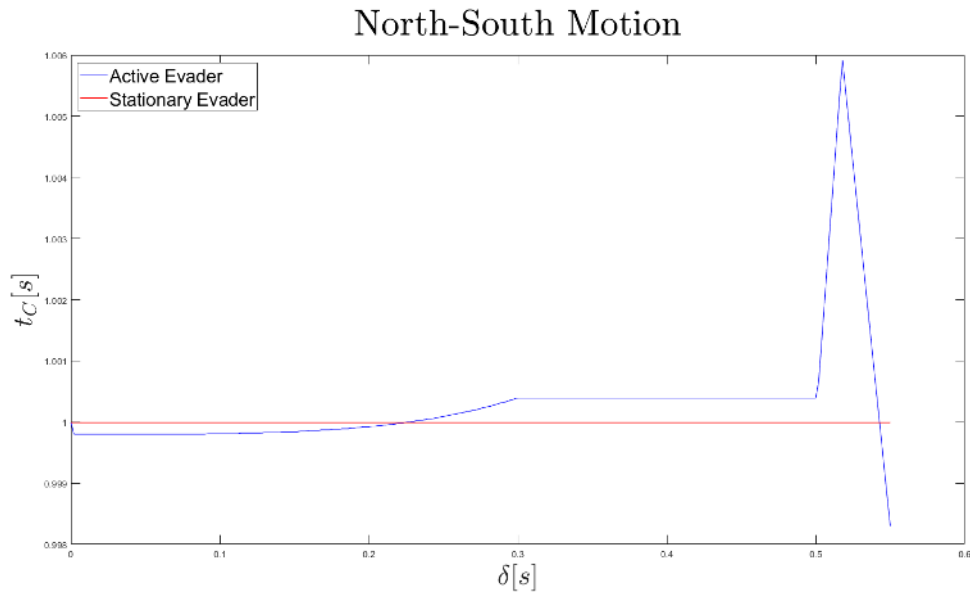

Figure 77: Capture Time t_c vs. δ with Evader Stoppage. $\mu = 0.2,\ y'_f = -0.002$.

7.7.2 East-West Oscillation

If the Evader oscillates East-West, as shown in Figure 72b, the Evader's motion
will draw all three Pursuers off course. We explore the possibility that the Evader's
motion increases the time to capture t_c when compared to a stationary Evader at
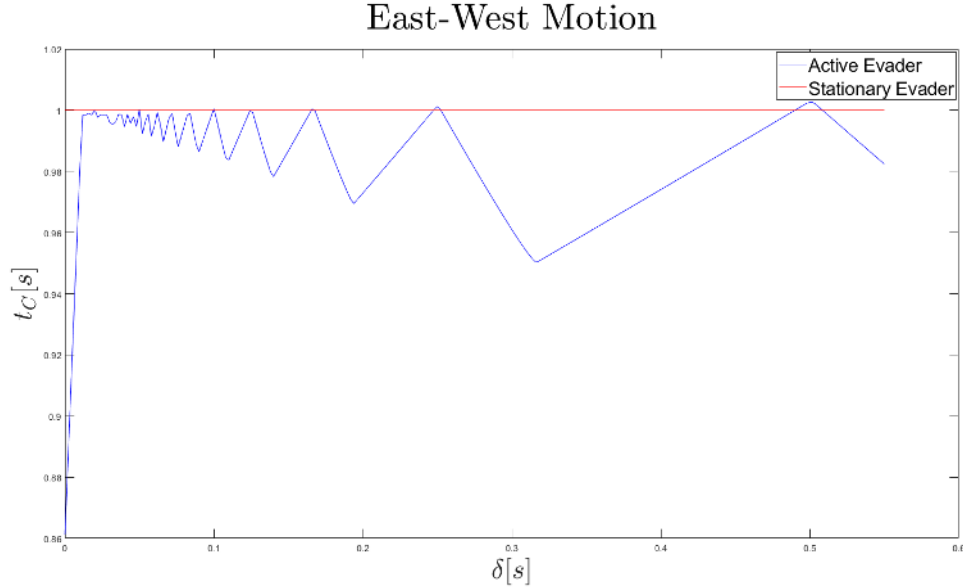O^*. As Fig. 78 shows, a mobile Evader is able to outlast a stationary Evader under

Figure 78: East-West Capture Time t_c vs. δ. $\mu = 0.2$.

certain frequencies of oscillation. An increase in capture time t_c occurs when the
Evader returns to its initial position at the circumcenter of the equilateral triangle
$\triangle P_1 P_2 P_3$. The δ which yeilds the largest increase in capture time is at $\delta = 0.5$, where
the mobile Evader is captured 0.003 seconds later than had he stayed stationary at
the circumcenter O^*. Once again, we also explore the case where the Evader changes
direction once, then returns to its initial position. In this case, we want zero separation
between the final position and the initial position, thus $y'_f = 0$.
As Fig. 79 shows, the higher frequency/smaller δ cases do not draw the Pursuers off
course enough to increase the time to capture. Once $\delta > 0.49$, we see an increase in
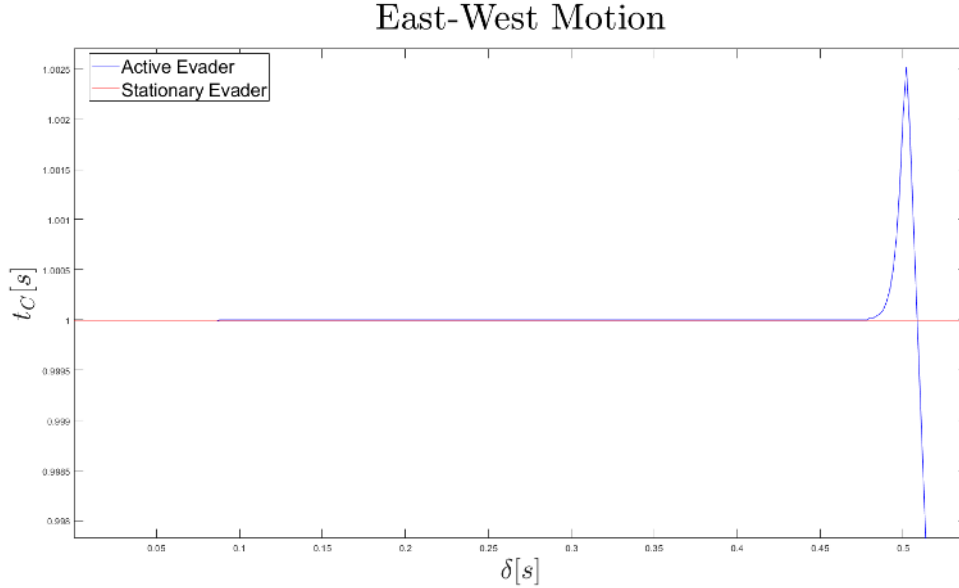capture time to $t_c = 1.003$ seconds, in the best case, when compared to a stationary

118

Figure 79: East-West Oscillation Capture Time t_c vs. δ with Stoppage. $\mu = 0.2$.

Evader.

Under PP, an active Evader can bring about an increase, albeit small, in the time-to-capture. The realized small increases in the time-to-capture is real – we verified it is not an artifact of numerics.

7.8 Conclusion

The two-on-one pursuit-evasion differential game had been solved when the pursuers are faster than the evader, both when point capture is required and also when the pursuers are endowed with capture circles of radius $\ell > 0$. The case where the two pursuers have the same speed as the evader and they are endowed with capture circle of radius $\ell > 0$ has also been addressed. When three pursuers are at work, the pursuit-evasion differential game's complexity increases significantly. In three-on-one pursuit with an initial fully symmetric configuration and where the pursuers employ PP, at first blush it would appear the Evader with less than half the speed of the pursuers, $\mu < \frac{1}{2}$, should remain stationary to prolong its life before being captured.

119

We showed that using an oscillatory motion, the Evader can slightly increase the time-to-capture. If the Evader dithers North-to-South, it is beneficial for the Evader to dither once and return to a position slightly below its initial position at the circumcenter O^*. When the Evader oscillates East-West, he draws all of the pursuers off course. This results in an increase in capture time t_c when the Evader terminates its oscillatory motion at its initial position.

VIII. Thesis Conclusions

The accumulation of the preceding five paper's results are as follows. In Chapters III and IV, the complete solution for the Two-on-One pursuit-evasion differential game where the players have equal speed and simple motion, and the two Pursuers are endowed with capture disks of radii $\ell_1 \geq \ell_2 \geq 0$ was delineated. The solution to the Game of Kind was presented by determining the region in the reduced state space, which is delimited by the tangents of the two capture disks, where isochronous capture is guaranteed. The solution to the Game of Degree was presented by providing the optimal state feedback strategies for the three players, which required the calculation of the aim point I. Additionally, we analyzed the reduced state space in three dimensions, and found the terminal "manifold" to be rank deficient, as it was a curve. Thus, it was explicitly determined, as were the terminal costates.

In games of Pure Pursuit, the equation of the pursuit curve for a Pursuer endowed with a capture range of radius ℓ was derived. For capture to occur, the terminal separation between the Pursuer and Evader must be less than the Pursuer's capture range ℓ, as demonstrated in Chapter V. We also considered the case with two Pursuers employing Pure Pursuit of an equal speed Evader and determined the necessary and sufficient conditions for capture. In Chapter VI, we consider the defense of a stationary Target under attack. We analyze the case where a fast Defender employs Pure Pursuit and determine the conditions for interception of the slow Attacker before he reaches the Target. Then, we determined a "Winning Region" for an Attacker, who's speed is equal to the Defender's, that reaches the Target before interception. Lastly, in Chapter VII, we analyzed the Three-on-One pursuit-evasion game in which the three Pursuers are faster than the Evader and the initial configuration is fully symmetric. It was determined that conventional wisdom for "optimal" play by the Evader was incorrect, as it suggested a stationary Evader lived the longest. We determined

that a dithering Evader outlived a stationary Evader under certain frequencies.

8.1 Future Work

There are numerous paths to diverge upon from this research. The Three-on-One pursuit-evasion game is extremely difficult, and we barely grazed the surface. That research could be continued by considering alternate configurations, variable speed ratios, pursuer capture ranges, minimum turn radii, etc. We could also consider the Two-on-One case in higher dimensional space, that is, analyze the scenario given the Pursuers and Evaders positions have an (x, y, z) component.

Bibliography

1. Rufus Isaacs. *Differential Games : A Mathematical Theory with Applications to Warfare and Pursuit, Control and Optimization.* Dover Publications, 1999.

2. P. Wasz, M. Pachter, and K. Pham. Two-on-one pursuit with a non-zero capture radius. In *27th Mediterranean Conference on Control and Automation (MED) 2019, Akko, Israel*, pages 577–582, July 2019.

3. M. Pachter and P. Wasz. On a two cutters and fugitive ship differential game. *IEEE Control Systems Letters, Oct 2019. Also presented at the 58th IEEE CDC in Nice, France, Dec 11-13, 2019*, 3(4):913–917.

4. Michael Lloyd. Pursuit curves. In *Academic Forum*, volume 24, page 07, 2006.

5. Harold T. Davis and F. Ursell. Introduction to nonlinear differential and integral equations. *Journal of the London Mathematical Society*, s1-39(1):185–186, 1964.

6. J. C. Barton and C. J. Eliezer. On pursuit curves. *The Journal of the Australian Mathematical Society. Series B. Applied Mathematics*, 41(3):358–371, 2000.

7. A. Von Moll, M. Pachter, E. Garcia, D. Casbeer, and D. Milutinovic. Robust policies for a multiple pursuer single evader differential game. *to appear in DGAA*, May 2019.

8. Meir Pachter. Isaacs' Two-on-One Pursuit Evasion Game. *Presented at the 2018 ISDG Symposium in Grenoble, France, To appear in the Annals of the International Society of Dynamic Games.*

9. Meir Pachter, Alexander Von Moll, Eloy Garcia, David W. Casbeer, and Dejan Milutinović. Two-on-one pursuit. *Journal of Guidance, Control, and Dynamics*, 42(7):1638–1644, 2019.

10. M. Pachter, A. Von Moll, and D. Casbeer. On group pursuit. *to appear in AIAA Journal of Information Systems.*

11. B. N. Pshenichnyi. Simple pursuit by several objects. *Cybernetics*, 12:484–485, 1976.

12. Sergey S. Kumkov, Stéphane Le Ménec, and Valerii S. Patsko. Zero-sum pursuit-evasion differential games with many objects: Survey of publications. *Dynamic Games and Applications*, 7(4):609–633, Dec 2017.

13. Seonhyeok Kang, H. Jin Kim, and Min-Jea Tahk. *Aerial Pursuit-Evasion Game Using Nonlinear Model Predictive Guidance.*

14. Kazuhiro Horie and Bruce A. Conway. Optimal fighter pursuit-evasion maneuvers found via two-sided optimization. *Journal of Guidance, Control, and Dynamics*, 29(1):105–112, 2006.

15. J. V. Breakwell and P. Hagedorn. Point capture of two evaders in succession. *Journal of Optimization Theory and Applications*, 27(1):89–97, Jan 1979.

16. Meir Pachter, Eloy Garcia, and David W. Casbeer. Differential game of guarding a target. *Journal of Guidance, Control, and Dynamics*, 40(11):2991–2998, 2017.

17. Mark Vlassakis and Meir Pachter. Two-on-one pursuit when the pursuers have the same speed as the evader. *To be Presented at the International Federation of Automatic Control World Congress, Berlin, Germany*, 2020.

18. B. N. Pshenichnyi. Simple pursuit by several objects. *Cybernetics*, 12:145–146, 1976.

REPORT DOCUMENTATION PAGE

Form Approved
OMB No. 0704–0188

1. REPORT DATE *(DD–MM–YYYY)*	2. REPORT TYPE	3. DATES COVERED *(From — To)*
26–03–2020	Master's Thesis	Sept 2018 — Mar 2020

4. TITLE AND SUBTITLE

An Analytic Study
of Pursuit Strategies

5a. CONTRACT NUMBER

5b. GRANT NUMBER

5c. PROGRAM ELEMENT NUMBER

6. AUTHOR(S)

Vlassakis, Mark E, 2d Lt

5d. PROJECT NUMBER

5e. TASK NUMBER

5f. WORK UNIT NUMBER

7. PERFORMING ORGANIZATION NAME(S) AND ADDRESS(ES)

Air Force Institute of Technology
Graduate School of Engineering and Management (AFIT/EN)
2950 Hobson Way
WPAFB OH 45433-7765

8. PERFORMING ORGANIZATION REPORT NUMBER

AFIT-ENG-MS-20-M-067

9. SPONSORING / MONITORING AGENCY NAME(S) AND ADDRESS(ES)

AFRL/RVBYC
Building 497
Kirtland AFB NM 87117
COMM 505-246-4823
Email: khanh.pham.1@us.af.mil

10. SPONSOR/MONITOR'S ACRONYM(S)

AFRL/RVBYC

11. SPONSOR/MONITOR'S REPORT NUMBER(S)

12. DISTRIBUTION / AVAILABILITY STATEMENT

DISTRIBUTION STATEMENT A:
APPROVED FOR PUBLIC RELEASE; DISTRIBUTION UNLIMITED.

13. SUPPLEMENTARY NOTES

14. ABSTRACT

The two-on-one pursuit-evasion differential game is revisited where the holonomic players have equal speed, and the two pursuers are endowed with a circular capture range $\ell > 0$. Then, the case where the pursuers' capture ranges are unequal, $\ell_1 > \ell_2 \geq 0$, is analyzed. In both cases, the state space region where capture is guaranteed is delineated and the optimal feedback strategies are synthesized. Next, pure pursuit is considered whereupon the terminal separation between a pursuer and an equal-speed evader less than the pursuer's capture range $\ell > 0$. The case with two pursuers employing pure pursuit is considered, and the conditions for capturability are presented. The pure pursuit strategy is applied to a target-defense scenario and conditions are given that determine if capture of the attacker before he reaches the target is possible. Lastly, three-on-one pursuit-evasion is considered where the three pursuers are initially positioned in a fully symmetric configuration. The evader, situated at the circumcenter of the three pursuers, is slower than the pursuers. We analyze collision course and pure pursuit guidance and provide evidence that conventional strategy for "optimal" evasive maneuver is incorrect.

15. SUBJECT TERMS

Pursuit-Evasion, Differential Games, Optimization, Control

16. SECURITY CLASSIFICATION OF:			17. LIMITATION OF ABSTRACT	18. NUMBER OF PAGES	19a. NAME OF RESPONSIBLE PERSON
a. REPORT	b. ABSTRACT	c. THIS PAGE			Dr. Meir Pachter, AFIT/ENG
U	U	U	UU	136	**19b. TELEPHONE NUMBER** *(include area code)* (937) 255-3636, ext 7247; meir.pachter@afit.edu

Standard Form 298 (Rev. 8–98)
Prescribed by ANSI Std. Z39.18